Universidade de Aveiro Departamento de Química
2015

Joana Margarida Mota Gomes

Purificação de IgY usando sistemas aquosos bifásicos constituídos por líquidos iónicos com capacidade tampão

Purification of IgY using aqueous biphasic systems composed of Good's buffers ionic liquids

Universidade de Aveiro Departamento de Química
2015

Joana Margarida Mota Gomes

Purificação de IgY usando sistemas aquosos bifásicos constituídos por líquidos iónicos com capacidade tampão

Purification of IgY using aqueous biphasic systems composed of Good's buffers ionic liquids

Dissertação apresentada à Universidade de Aveiro para cumprimento dos requisitos necessários à obtenção do grau de Mestre em Bioquímica, ramo de Métodos Biomoleculares, realizada sob a orientação científica da Doutora Mara Guadalupe Freire Martins, Investigadora Coordenadora do Departamento de Química, CICECO, da Universidade de Aveiro e coorientação do Professor Doutor Pedro Miguel Dimas Domingues, Professor Auxiliar com Agregação do Departamento de Química da Universidade de Aveiro.

À minha Mãe e ao meu Pai…

o júri

Presidente

Drª. Rita Maria Pinho Ferreira

Professora Auxiliar do Departamento de Química, da Universidade de Aveiro

Drª. Mara Guadalupe Freire Martins

Investigadora Coordenadora do Departamento de Química, CICECO, da Universidade de Aveiro

Dr. Ricardo Simão Vieira-Pires

Investigador Assistente do Grupo de Biotecnologia Estrutural, do Centro de Neurociências e Biologia Celular, da Faculdade de Ciências e Tecnologia da Universidade de Coimbra

Agradecimentos

É com um misto de sentimentos que faço agora uma retrospetiva deste percurso de cinco anos que apesar de longo, passou tão rapidamente. Em primeiro lugar gostava de fazer um agradecimento muito especial à Dr.ª Mara Freire pelo brilhante acompanhamento e por todo o apoio e confiança depositados em mim, durante o desenvolver deste trabalho. Um agradecimento também ao Prof. Dr. Pedro Domingues por todo o apoio prestado, assim como pela disponibilidade.

Agradeço também a todos os elementos do Path e do mini Path, pela boa disposição, motivação e pelos sorrisos. São sem dúvida um grupo de trabalho extraordinário. Mafalda e Ana Paula, um enorme obrigado, foram incansáveis. Agradeço-vos por terem sempre uma palavra reconfortante nos momentos de desespero e por nunca me deixarem desmoralizar. Maria, obrigada pela ajuda no trabalho em muitos momentos de dificuldade, mas acima de tudo, obrigada pelas conversas, confidências, pela amizade e claro, pelas corridas ao domingo de manhã. Vânia, as palavras não são suficientes para te agradecer. És uma amiga para a vida, que já faz parte da família: a minha mana mais velha. É impressionante como parece que te conheço desde sempre. Não preciso de dizer muito mais, sabes bem aquilo que vivemos e partilhamos durante estes meses. Um obrigado muito especial também à Teresa, que com a sua boa disposição tornou os meus dias mais coloridos. A minha família Aveirense: Jé, Titi, Tita, Guida e Sara. Agradeço-vos pela amizade, compreensão e por terem feito destes anos, os melhores cinco da minha vida. Ana, Cláudia e Candy, as melhores amigas que alguém poderia ter. Já lá vão quase dezoito anos de amizade e durante os últimos cinco, nunca faltou uma palavra de apoio e carinho, estivéssemos nós no Porto, em Aveiro, Coimbra, Braga, na Suíça ou em Londres.

Um enorme obrigado ao "meu" André. Obrigada por me pores sempre um sorriso no rosto, por me compreenderes nos momentos de angústia e exaustão e sobretudo, por percorreres este caminho ao meu lado. Foste o melhor de sempre, és o melhor de sempre e eu amo-te.

Por fim, o maior agradecimento de todos, às melhores pessoas que conheço, as que mais admiro e a quem devo tudo aquilo que sou: a minha Mãe e o meu Pai. Obrigada por todas as oportunidades proporcionadas, por todos os abraços, mensagens de bom dia e beijos de boa noite. Amo-vos muito.

Palavras-chave Purificação de anticorpos, imunoglobulina Y, extração líquido-líquido, sistemas aquosos bifásicos, líquidos iónicos.

Resumo

Recentemente, a utilização de anticorpos para imunoterapia passiva tornou-se uma área de investigação atrativa. Tal facto deve-se à diminuição da eficiência dos antibióticos pelo aumento do número de organismos resistentes. Os anticorpos obtidos a partir da gema do ovo de galinhas imunizadas, imunoglobulinas Y (IgY), são uma alternativa viável e promissora aos anticorpos de mamíferos. Estes apresentam inúmeras vantagens, dado que podem ser obtidos em maior quantidade e serem recolhidos por técnicas menos invasivas. Apesar das vantagens apresentadas, as técnicas disponíveis para a extração e purificação de IgY são demoradas, trabalhosas, apresentam baixo rendimento, levam a baixos fatores de pureza, apresentam custos elevados e não são facilmente aplicáveis a nível industrial. Assim, o principal objetivo deste trabalho consistiu no desenvolvimento de uma plataforma de purificação alternativa para a extração e purificação de IgY, utilizando sistemas aquosos bifásicos (SAB) constituídos por líquidos iónicos com capacidade tampão. Neste trabalho foram estudados SAB constituídos por $C_6H_5K_3O_7$ e líquidos iónicos, sendo os últimos sintetizados pela combinação de aniões com capacidade tampão (Good's buffers), com os catiões tetrabutilamónio ($[N_{4444}]^+$) e tetrabutilfosfónio ($[P_{4444}]^+$). Os líquidos iónicos utilizados permitiram o estudo da influência do anião e do catião nos diagramas de fase, ou seja sob a capacidade dos diferentes líquidos iónicos para formar SAB. De seguida, foi testada a capacidade destes sistemas como uma plataforma alternativa para a extração seletiva, e posterior purificação, de IgY. A purificação de IgY não foi conseguida num único passo de extração com os sistemas estudados. No entanto, o estudo do perfil proteico de ambas as fases dos sistemas permitiu concluir que, durante a partição, todas as proteínas migraram para a fase superior e que houve formação de um complexo entre o IL e algumas das proteínas constituintes da fração aquosa proteica da gema do ovo. Os resultados obtidos revelaram que, entre os vários SAB estudados, o mais promissor para a extração de IgY, é aquele constituído por 20.1 (m/m) % $[N_{4444}][CHES]$ + 16.9 (m/m) % $C_6H_5K_3O_7$.

Keywords Antibodies purification, immunoglobulin Y, liquid-liquid extraction, aqueous biphasic systems, ionic liquids.

Abstract The increased inefficiency of antibiotics observed in the past few years, derived from the growing number of drug-resistant organisms and the appearance of individuals with impaired immune system, led to a significant research on antibodies for use in passive immunotherapy. Antibodies obtained from the egg yolk of immunized hens, immunoglobulin Y (IgY), are a promising alternative to mammalian antibodies. They can be obtained in higher titres and by less invasive techniques, thus opening the door for a new kind of more economic biopharmaceuticals. However, the available techniques for the IgY extraction and purification are time-consuming, labor intensive, low yielding, provide low-purification levels, are of high cost and cannot easily be scaled-up for industrial applications. In this work, ABS composed of $C_6H_5K_3O_7$ and ILs synthetized by the combination of anions with buffer capacity (Good's buffers), with the tetrabutylphosphonium ($[P_{4444}]^+$) and tetrabutylammonium ($[N_{4444}]^+$) cations, were investigated. The use of different ILs allowed the study of the cation and anion nature on the phase diagrams behaviour and thus on their ability to form ABS. Further, the ability of these systems as an alternative purification platform for IgY, by a selective extraction, was studied. The complete extraction and purification of IgY was not achieved in a single with the investigated ABS. However, the study of the proteins profile of the coexisting phases allowed to conclude that all proteins migrate for the top phase during the partitioning process, and that a complex between the ILs and the different proteins present in the water-soluble fraction of proteins from egg yolk was formed. Still, the results obtained reveal that the system composed of 20.1 wt % $[N_{4444}]$[CHES] + 16.9 wt % $C_6H_5K_3O_7$ is the most promising ABS for the IgY extraction.

Contents:

List of Tables:

List of Figures:

List of Symbols:

Abs – Absorbance (dimensionless);

Mw – Molecular weight ($g \cdot mol^{-1}$);

R^2 – Correlation coefficient (dimensionless);

wt % – Weight percentage (%);

σ – Standard deviation;

[IL] – Concentration of ionic liquid (wt % or $mol \cdot kg^{-1}$),

$[IL]_{IL}$ – Concentration of ionic liquid in the ionic-liquid-rich phase (wt %);

$[IL]_{Salt}$ – Concentration of ionic liquid in the salt-rich phase (wt %);

[IL]M – Concentration of ionic liquid in the initial mixture (wt %);

$[C_6H_5K_3O_7]$ – Concentration of $C_6H_5K_3O_7$ (wt % or $mol \cdot kg^{-1}$);

[Salt] – Concentration of salt (wt % or $mol \cdot kg^{-1}$);

$[Salt]_M$ – Concentration of salt in the initial mixture (wt %);

$[Salt]_{IL}$ – Concentration of salt in the ionic-liquid-rich phase (wt %);

$[Salt]_{Salt}$ – Concentration of salt in the salt-rich phase (wt %);

[WSPF] – Concentration of the water soluble protein fraction (wt %).

List of Abbreviations:

ABS – Aqueous biphasic system;

AC – Affinity chromatography;

AFC – Antibody forming cells;

Aln – Alanine;

Arg – Arginine;

Asn – Asparagine;

Asp – Aspartate;

B – Bottom phase;

BVC – Bovine rotavirus;

C – Constant region of antibody;

CDR – Complementary-determining region of an antibody;

Cys – Cysteine;

DMSO – Dimethyl sulfoxide;

DTT – Dithiothreitol;

GBs – Good's buffers;

Gln – Glutamine;

Glu – Glutamate;

IgY – Immunoglobulin Y;

IL – Ionic liquid;

IPCRs – Immuno-polymerase chains reactions;

IMAC – Immobilized metal ion binding chromatography;

ELISA – Enzyme-linked immunosorbent assay;

ETEC – Enterotoxigenic *Escherichia Coli*;

Fc – Fragment crystallisable region of antibodies;

FT-IR – Fourier transform infrared spectroscopy;

H – Heavy chain of antibody;

HCIC – Hydrophobic charge induction chromatography;

His – Histidine;

HLA – Human leucocyte antigen;

HPLC - High-performance liquid chromatography;

L – Light chain of antibody;

Leu – Leucine;

MHC – Major histocompatibility complex;

PEG – Polyethylene glycol;

pI – Isoelectric point;

Pro – Proline;

SDS - Sodium dodecyl sulphate

SDS-Page – Sodium dodecyl sulphate polyacrylamide gel electrophoresis;

SE-HPLC – Size-exclusion - High performance liquid chromatography;

Ser – Serine;

T – Top phase;

TAC – Thiophilic affinity chromatography;

TBC – Binodal curve;

TCA – Trichloroacetic acid;

TMS – Tetramethylsilane;

T_H – T-helper cells;

Thr – Threonine;

TL – Tie-line;

TLL – Tie-line length;

Trp – Tryptophan;

Tyr – Tyrosine;

UV – Ultra violet;

V – Variable region of antibody;

Val – Valine;

WSPF - Water soluble protein fraction.

1 - General introduction

1.1 - Scopes and objectives

Biopharmaceuticals, such as recombinant therapeutic proteins, antibodies and nucleic acids, have greatly improved the treatment and diagnosis of some diseases, being already applied in the treatment of anaemia, multiple sclerosis, breast cancer, rheumatoid arthritis and diabetes *(1–3)*. The widespread antimicrobial resistance, the emergence of new pathogens that cannot be treated with the existing antimicrobial drugs, for instance the human immunodeficiency virus (HIV) and *Cryptosporidium parvum*, and the occurrence of many infections in patients with an impaired immune system, in whom antimicrobial drugs are less effective, have made of the implementation of antibiotics and antiviral therapies a challenge *(4–6)*.

Therapeutic proteins have revolutionized the treatment of many diseases and more than 100 genes, and a similar number of modified proteins, are already approved for clinical use in the European Union and in the USA *(7)*. The initial therapeutic proteins approved were recombinant insulins and blood factors *(8)*. Recently, protein engineering has allowed the development and application of new biopharmaceuticals, such as modified insulins, among others *(8)*. Protein engineering entails the controlled alteration of a gene's nucleotide sequence, such that specific pre-determined alterations in the resultant polypeptide's amino acid sequence are introduced *(3,8)*.

Antibodies are the key proteins of organism's specific responses to foreign substances and they are produced when an antigen receptor binds specifically to a B-cell, triggering a mechanism which involves activation, cell division and differentiation *(9–12)*. Because of their versatility, antibody-based therapies can be developed against any existing pathogen, and with high specificity *(4)*. Antibody-based (serum) therapies were first used in the treatment of human infections in the 1890s *(5)*. At that time, antibodies were used to treat a variety of bacterial infections, namely those caused by *Corynebacterium diphtheria, Streptococcus pneumoniae, Neisseria meningitides, Haemophilus influenzae*, group *A streptococcus*, and *Clostridium tetani (5,6)*. However, this methodology was rapidly left due to its immediate side effects, which include fevers, chills and allergic reactions *(4,5)*. Currently, the available techniques for diagnosis and therapy mainly use mammalian monoclonal or polyclonal antibodies *(13,14)*. These practices have however some disadvantages, such as the weakness of the immunogenic response to monoclonal antibodies and the difficulties regarding the production and purification of antibodies from mammalian blood, which is low yielding and laborious *(13)*. Some of these

disadvantages can be overcame by the use of chicken egg antibodies (IgY) instead of the corresponding mammalian immunoglobulins (IgG) *(13,14)*. Nevertheless, the widespread use of IgY is still restricted due to problems associated with these antibodies isolation and purification from the complex egg yolk matrix *(15)*. Moreover, since the demand for biopharmaceuticals is expected to increase in the near future it would be wise to ensure that they will be available on a cost-effective basis *(16)*. Therefore, to ensure the IgY application at a large scale, as alternative antibodies for use in passive immunotherapy, the existing methods should be optimised and/or new techniques should be developed *(15)*.

Aqueous biphasic systems (ABS) offer many advantages, being currently used for proteins extraction and for the downstream processing of biopharmaceuticals and some of them at a large scale *(2)*. The fact that ABS are mostly composed of water makes of them a biocompatible media for biologically active products *(17–20)*. The extraction and purification of biological products using ABS has been reported using combinations of two hydrophilic solutes (two polymers or a polymer and a salt) dissolved in aqueous media *(16,21–24)*. These conventional systems have, however, a restricted polarity difference between the two phases, which have been limiting their success in the selective extraction and purification of IgY *(19)*. Only one work was found for the purification of IgY using micelle-based ABS composed of a phosphate-based salt and Triton X-100 *(20)*.

Ionic liquids (ILs) are salts that are liquid at low temperatures, and in general they remain in the liquid state below the boiling point of water (100 ºC), in contrast to common salts *(19,25)*. ILs have been recently used for chemical syntheses, biocatalytic transformations and analytical separation processes due to their "greener" characteristics, such as a negligible volatility and non-flammability *(26)*. Therefore, they have been considered as potential substitutes of volatile and hazardous organic solvents presently used in a wide range of applications *(19)*. Rogers and his research team *(26)* reported, in 2003, the revolutionary research work on the development of IL-based ABS, by the addition of inorganic salts to aqueous solutions of ILs. The main advantage of using ILs for ABS formation conveys on the ability to design the cation/anion chemical structures and their combinations, allowing thus the tailoring of the polarities and the affinities of the coexisting phases in ABS *(19)*. Due to their tunable physicochemical properties, ILs can cover the whole hydrophilicity–hydrophobicity range and improved and selective extraction can be envisaged *(19,25)*.

Based on the main drawbacks associated with the purification of IgY, and main advantages of ILs as phase-forming components of ABS, the main purpose of this work consists on the development of an alternative platform for the selective extraction and purification of IgY, from egg yolk, using ILs derived from biological buffers (zwitterionic amino acid derivatives). These ILs, which allow the pH adjustment, were evaluated with the objective of preserving the native protein structure and specific activity *(25,27)*. In particular, ILs with anions derived from Good's buffers (GB-ILs) were synthesized and characterized *(28)*. The GB-ILs were then used in the formation of ABS and evaluated for the extraction and purification IgY from the water soluble fraction of proteins egg yolk.

1.2 - Antibodies

Antibodies are glycoproteins, members of the immunoglobulins family, and they encompass one of the principal effects of the immune system *(9,10)*. In the adaptive immune response, soluble proteins and cell-surface receptors bind the pathogen and its products (serum proteins or human cells that became altered in the presence of the pathogen) *(29,30)*. The ability of the immune system to recognize antigens depends on the antibodies generated by B-cells and on the antigen receptors expressed by T-cells; yet, the way in each one of this type of cells recognizes the pathogen is quite different *(12)*. The first sign is delivered by the antigen binding and usually involves a co-receptor, in addition to the antigen-receptor on the B-lymphocyte membrane *(30)*. A B-cell binds to the antigen receptor, comprising the signal 1. The B-cell engulfs the antigen, processes it into peptides in an endosomal compartment, where major histocompatibility complexes (MHC) of Class I, II or III are formed *(30)*. MHC is the genetic loci involved in the rejection of foreign or non-self-tissues, and in humans it is known as the human leucocyte antigen (HLA). The three classes differ considerably in their gene composition, presenting different structural identities *(12)*. Later, the B-cells involve an activated T-helper cell (T_H) specific for the MHC complex *(30)*. T-cell receptors only recognize antigens in association with MHC molecules, on the cell surfaces and, as described, these antigens have often been degraded or processed into fragments, which are recognized by the T-cell receptor *(12)*. The activated T_H cells provide a second set of signals to the B-cells including contact signals or signals delivered by cytokine molecules secreted by the T-cell, which include IL-1, IL-2, IL-4, IL-5, IL-6, IL-10 and IFNγ *(30)*. In the presence

of IL-4 and IL-1 the receptors for IL-2 and other cytokines are expressed. Consequently, IL-2, IL-4 and IL-5 are secreted by T-cells driving to B-cells activation, proliferation and differentiation (Figure 1) *(12)*. An activated B-cell will proliferate and differentiate producing antibody secreting plasma cells or memory B cells *(30)*. Memory B cells are crucial for the secondary immune response. They are capable to produce a faster and more robust antibody-mediated immune response in the case of re-infection *(9,30)*.

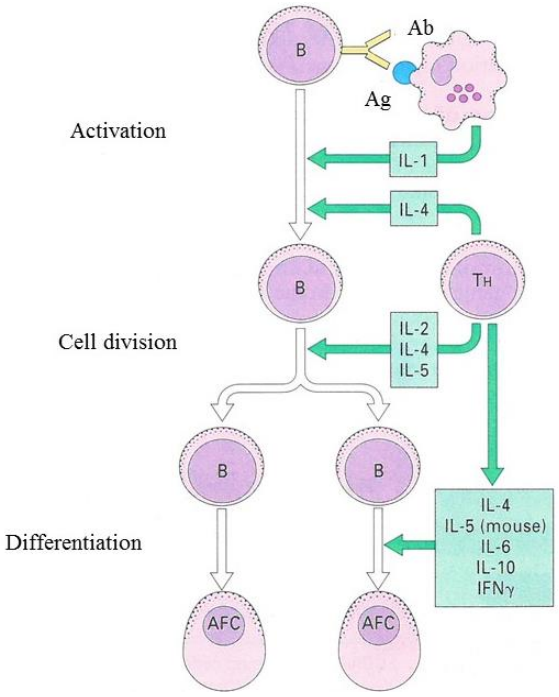

Figure 1 – Stages in B-cell activation and development. Ab – Antibody; Ag – Antigen; AFC – Antibody-forming cells *(12)*.

It is also important to refer that there are a small number of antigens that are capable of activating the B-cells without the T-cell help, referred as T-independent antigens *(12,29,30)*. These have some particular properties since they are large polymeric molecules, they possess the ability, at high concentrations, to activate B-cell clones that are specific for other antigens, and many T-independent B-cells are particularly resistant to degradation *(12)*. However, the mechanism by which T-independent antigens activate the B-cells, without T-cells help, is not fully understood *(12)*.

Antibodies circulate as major components of the plasma in blood and lymph constituting about 20 % of the plasma protein fraction in humans *(10,29)*. The diversity and specificity of the antibody-antigen interaction and the ability to manipulate the characteristics of this interaction, using recombinant technology, has created many uses

for antibodies and antibody fragments in applications such as medicine, passive immunotherapy or diagnosis, biomedical research, experimental biology, among others *(9–11)*. Both monoclonal and polyclonal antibodies can be used for these purposes *(11,16)*. Monoclonal and polyclonal antibodies have many differences regarding their nature and which limit or define their use. Polyclonal antibodies are most frequently produced and they recognize independent antibody binding sites on the antigen *(10,31)*. Hyper-immunised serum is a very good source of polyclonal antibodies, since it contains a mixture of antibodies against multiple epitopes *(10)*. Their production starts with the immunization of the animal with the specific antigen and, throughout this process, the immune response is controlled by the collection of serum titres *(32)*. The desired antigen is generally applied in combination with various adjuvant compounds *(33)*. The serum containing a polyclonal mixture of specific and non-specific antibodies is collected and subjected to purification using techniques such as precipitation and chromatography, followed by digestion with proteases, which minimize the antigenicity against the species-specific Fc region *(32)*. Polyclonal antibodies are also commonly used in immunochemical techniques *(10)*. Moreover, they are also considered more efficient in the treatment of acute illness and medical emergencies, as they can bind and neutralize multiple epitopes on the disease-causing agent *(32)*. On the other hand, monoclonal antibodies are produced by a single B-lymphocyte clone; therefore, all of them are identical *(31)*. Monoclonal antibodies can be produced by specialized cells through hybridoma technology. A hybridoma is produced by the injection of a specific antigen into a mouse, followed by the recovery of the antigen-specific B-cells from the mouse's spleen and the subsequent fusion of this cell with a cancerous immune cell called myeloma cell (myeloma is a cancer B-cell) *(34)*. The fused hybrid cell, hybridoma, can be cloned producing therefore many identical daughter clones and large amounts of the desired antibodies *(34)*. These antibodies present high specificity, since they can only interact with a specific and unique substance *(10,31)*. They can be useful to distinguish subsets of B-cells or T-cells, being helpful on the identification of different types of leukaemia and lymphomas. Monoclonal antibodies are also used to quantify the number of B cells, which is important in immune disorders such as Acquired Immune Deficiency Syndrome (AIDS) *(34)*. The US Food and Drug Administration has already approved 21 monoclonal antibody-based therapeutics to treat several human disorders, including

cancer, transplant rejection, asthma and auto-immune, cardiovascular and infectious diseases *(16,23)*.

1.2.1 - Structure and function of antibodies

Antibodies contain a structural domain composed of four polypeptides similar to many other proteins *(9)*. They are constituted by two identical heavy (H) (~55kDa) chains, each carrying covalently attached oligosaccharide groups; and two identical light (L) (~25kDa) non-glycosylated chains. The resulting molecule is represented by a schematic Y-shaped molecule of ~150kDa *(9,10)*. One heavy and one light chain are joined together by disulphide and non-covalent bonds; two heavy chains are joined together by a disulphide bond *(9,10)* (Figure 2). The disulphide bonds, named *hinge*, have approximately 12 amino acids, essentially Pro, Thr and Ser, and are located in a flexible region of the heavy chain which is exposed to enzymatic or chemical cleavage with papain or pepsin *(9,10)*. This region imparts lateral and rotational movement to the antigen binding site, providing the antibody with the ability to interact with the antigen *(9)*. The four polypeptide chains contain constant (C) and variable (V) regions that are present in the carboxyl and amino terminal portions, respectively. Both heavy and light chains contain only a single V region; the light chains comprise a single C region and heavy chains contain three C regions *(10,29)*. The H and L-chains of antibodies are encoded by two genes, one for the V region and one for the C region. The V region genes do not exist in the germline genome, unlike those from the C region; instead, they are assembled from banks of genomic DNA segments during the development of the cells. The mix-and-much assembly results in a huge diversity of V region genes *(30)*. So, the three V regions in both chains of the antibody constitute the epitope binding site or complementary-determining regions (CDRs). There is a vast array of coding regions and transcription of unique CDRs which are generated by numerous mechanisms like the different combination of heavy and light chains, genetic recombination, imprecise joining during recombination and high somatic mutation rate. In this line, a huge diversity of sequences necessary to bind a diverse spectrum of antigens is created. The antigen-binding specificity is determined by the physical and chemical properties of its CDR *(9)*. The epitope is the antibody binding site in the antigen and is generally composed of carbohydrates or proteins since the surface molecules of pathogens are commonly

glycoproteins, polysaccharides, glycolipids or peptidoglycans *(9,10,29)*. The antigen effector domains are present on the tail of the molecule *(10,29)*.

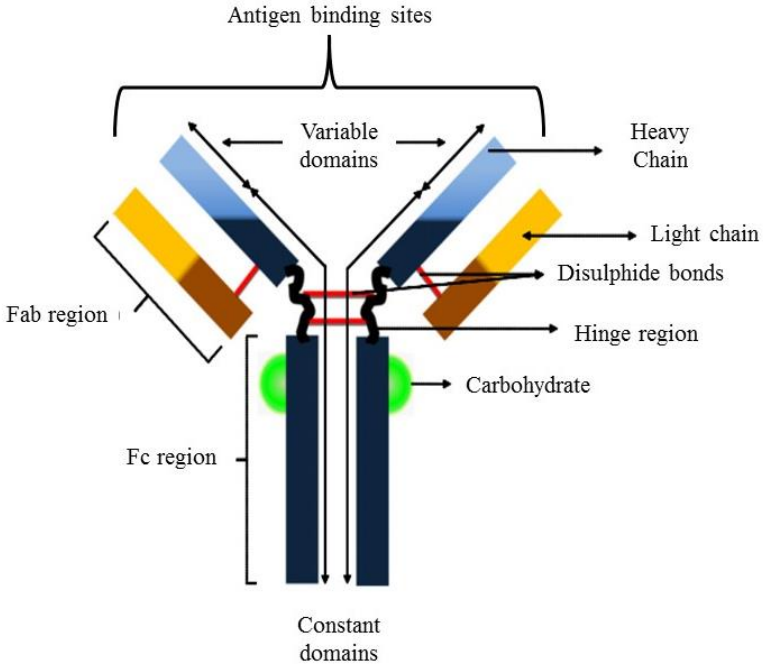

Figure 2 – Schematic representation of an antibody structure *(35)*.

Immunoglobulin molecules are bifunctional; one region of the molecule is responsible for the binding to the antigen while the other mediates the effector functions *(12)*. Each immunoglobulin class has a characteristic type of heavy chain giving rise to diverse immunoglobulin sub-classes; the immunoglobulin sub-class is crucial for the determination of the type and temporal nature of the immune response *(9,12)*. In mammals, there are five immunoglobulin classes: IgG, IgM, IgA, IgD and IgE; and in hens there are three classes: IgY, IgM and IgA. In some mammals, IgG and IgA are subdivided into sub-classes, referred as isotopes, precisely due to polymorphisms in the C regions of the heavy chain *(9)*. In addition, it is important to refer that the carbohydrates content of these glycoproteins vary considerably between the different sub-classes, ranging from 2-3 % for IgG, to 12-14 % for IgM, IgD and IgE, and which significantly influence the immunoglobulins physicochemical properties *(12)*.

The antibodies activity is affected by variations in pH, salt concentration, presence of proteolytic enzymes and other destabilizing factors. However, their structure helps them to resist to severe conditions due to the folding of the immunoglobulin chains into a compact, stable and unique domain named immunoglobulin domain *(29)*. Despite this

stability observed in most antibodies, the antigen binding domain and the effector domain can be separated from each other by proteolytic digestion. Papain is capable of fragmenting all isotypes into Fab (monovalent for antigen binding) and Fc (effector domain) fragments by cleaving the heavy chain above the disulphide bonds that hold them together. This cleavage only occurs under physiological pH. On the other hand, pepsin can cut the Y molecule below this linkage, leading to different Fab and Fc fragments *(9,10)*. These papain and pepsin generated fragments offer insight into structure and function of antibodies because they separate the Fab region from the Fc region, which mediates effector functions and monocyte binding *(12)*. Figure 3 depicts the enzymatic cleavage process of the human IgG.

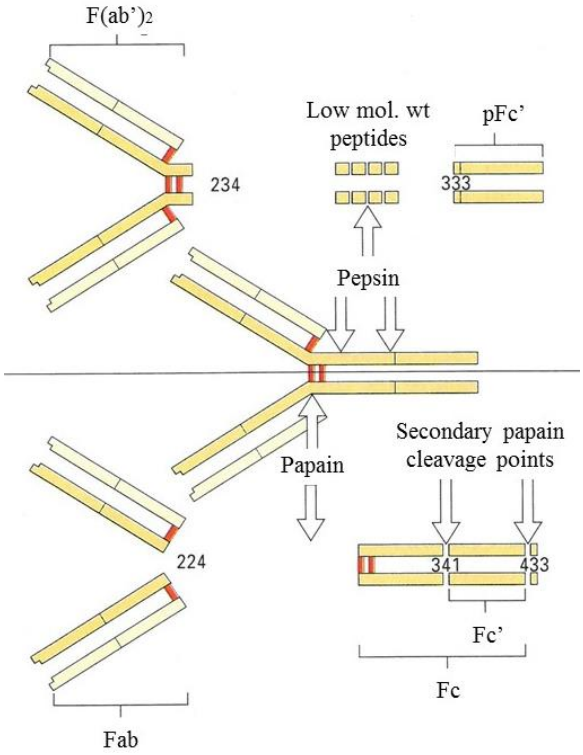

Figure 3 – Schematic representation of the human IgG enzymatic cleavage by pepsin and papain. The human IgG heavy chain is cleaved at positions 234 and 333 to yield the F(ab')2 and the pFc' fragments. Papain cleaves the molecule at the residue 224, in the hinge region, originating two Fab fragments and one Fc fragment. Secondary cleavages give raise do Fc and Fc' fragments *(12)*.

Antibodies are useful tools for passive immunity. Passive immunity represents the process of providing pre-formed antibodies to protect the organism against infections or other diseases *(36)*. The protection provided is immediate and lasts for several weeks to three or four months at most *(36,37)*. The immune system of a neonate is relatively

immature. Therefore, maternal antibodies pass to the descendants in order to confer natural passive immunity, which is essential for the adaptation of the neonate to the extra uterine environment *(38,39)*. The route of transmission of natural passive immunity in mammals is a difficult process since the antibodies are enclosed within the uterus of the mother and because of the diversity of structure of the embryonic membranes *(40)*. Placenta is the most well-known organ involved in exchanges between the maternal and *fetal* circulation. It keeps the two blood streams separated, allowing the exchange of substances of all kind between the *fetus* and the progenitor circulation *(40)*. In humans, maternal antibodies (IgG) are passed from mother to the *fetus* during pregnancy and to the neonate through IgA in the breast milk *(38,41)*. Other mammals obtain their maternal antibodies *via* colostrum which are then transported across the intestinal epithelium of the neonate into circulation *(37,41)*. In chickens, natural passive immunity is transmitted from the mother to the young birds trough the yolk of the egg, while on the ovary *(40)*. On the other hand, acquired passive immunity implies that antigen-specific antibodies are obtained from another source, as presented below in Figure 4 *(37)*. It requires the collection of antigen-specific antibodies from another source (immunized individuals) and their administration on susceptible individuals *(36)*. The first step consists in the injection of the animal with the antigen of interest, which can be done by intravenous, intraperitoneal, subcutaneous or intracutaneous injections *(42)*. Due to the transient nature of the protection provided by passively transferred antibodies, a repeated or continuous administration is necessary and thus large amounts of the specific antibodies are required *(37)*. In this context, chicken eggs are advantageous in passive immunization applications since they are a source of large amounts of antibodies and the recovery of these is carried out though a less-invasive technique *(37)*.

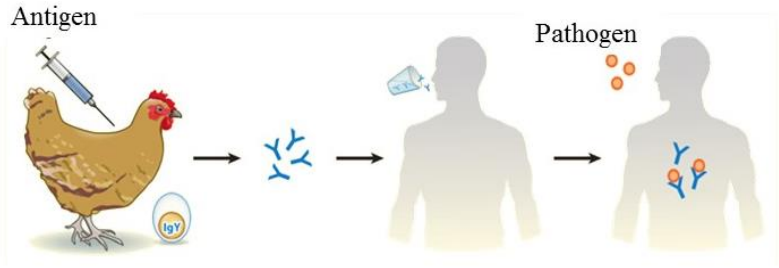

Figure 4 – Passive immunization *(37)*.

1.2.1 – Hen and mammalian antibodies

As referred before, antibodies have numerous applications. In clinical practice, antibodies are widely used in diagnosis or in immunotherapy in order to neutralize pathogens *(33,43)*. Antibody-based immunoassays are the most used type of diagnostic; the first major milestone in antibody-based immunoassays was the development of the binding assay, using radioisotope and later enzyme-labelled immunoassays *(44)*. Besides, these immunoglobulins are also useful in protein science and are frequently employed for detection and determination of various antigens, representing one of the fastest growing technologies for the analysis of biomolecules *(33,43,44)*. In general, these immunoassays were mostly based on polyclonal antibodies. However, in 1975 Kohler and Milstein *(45)* described the use of monoclonal antibodies in immunoassays. The most frequently chosen mammals for polyclonal and monoclonal antibody production are rabbits and mice, respectively *(13)*.

Antibodies are frequently obtained from de blood of animals. However, this practice has numerous disadvantages since some of the steps involved in antibody collecting cause distress to the animals involved. The collection of blood samples by bleeding, which is a prerequisite for antibody preparation, sometimes results in the animal death *(13,33,43)*. On the other hand, these antibodies also have disadvantages related with their production on an industrial scale due to the difficulty in obtaining large quantities of blood *(14)*. More recently, the use of hens instead of mammals for antibodies production has increased *(13,33)*. There are three immunoglobulin classes in hens namely: IgA, IgM and IgY. The molecular characteristics of hen IgA and IgM are similar to mammalian IgA and IgM *(13)*. The structure of IgY, which is the major low molecular weight serum protein in oviparous, is similar to mammalian IgG, containing two light and two heavy chains *(13)*.

The use of chicken egg for antibodies production represents a much more economical and refined source to obtain large quantities of specific antibodies *(13,37,46)*. It enables the reduction of the number of animals used while the collection of blood is replaced by the collection of eggs, being thus less invasive *(13,43,47)*. The IgY concentration in the blood of a chicken is 5-6 mg/mL, whereas in egg yolk it is 10-25 mg/mL *(33)*. *Per* year, an immunized hen produces more than 40g of IgY through eggs, corresponding to the amount of IgG produced from 40 rabbits *(14)*. Due to phylogenetic distance between birds and mammals, mammalian proteins are often more immunogenic in birds than in mammals, resulting in an easier and faster stimulation of antibody synthesis *(13,37)*. IgY

can react with many epitopes of mammalian antigens resulting also in an amplification of the signals and in a different antibody repertoire *(37,48)*. Because of this genetic distance it is further possible to produce antibodies against highly conserved mammalian proteins *(37)*. Chicken egg antibodies neither bind to the mammalian or bacterial Fc receptor, which could mediate an inflammatory response, and do not activate the complement system nor react with the rheumatoid factor, which is an anti-immunoglobulin autoantibody found in many different diseases *(37,47)*. In addition, IgY immunoglobulins do not react with mammalian IgG or IgM and these lack of cross-reactivity is reflected in a great reduction of background and false results in assays using anti-IgG antibodies *(49)*. The above-mentioned advantages have a crucial significance in immunodiagnostics. Currently, IgY are been used as primary antibodies in techniques such as ELISA, Western blotting and immunochemistry and also as secondary antibodies, when combined with peroxidase *(33)*.

Chicken eggs are a preferred antibodies source since these possess properties comparable or in some regards better than those of mammalian antibodies *(33,46)*. In contrast with mammalian serum, egg yolk contains only a single class of antibodies (IgY) that can be isolated from the yolk *(37)*. Nevertheless, there are several disadvantages connected to egg yolk, which have been limiting their widespread use *(11)*. In particular, egg yolk is a fluid emulsion with a dispersive phase rich in lipoproteins and glycoproteins, turning therefore the isolation of IgY difficult to achieve *(33)*.

1.3 - Immunoglobulin Y (IgY)

During the egg formation, IgY is selectively transferred to the yolk *via* a specific receptor present on the surface of the yolk membrane *(33,37)*. IgA and IgM, similar to mammalian IgA and IgM, are secreted in the maturing egg follicle together with other proteins and are deposited into the egg white, as presented in Figure 5 *(33,37)*. The presence of mammalian equivalents of IgE and IgD was proposed, yet not identified or proven in hens *(13)*.

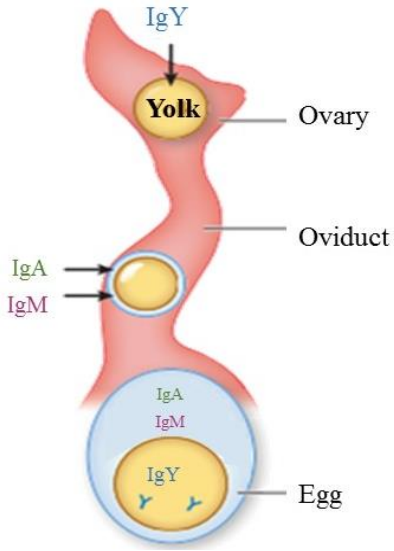

Figure 5 – IgY transfer from the blood to the egg yolk, through specific receptors during the egg formation. IgA and IgM are deposited into the egg white in the oviduct *(37)*.

The overall structure of IgY is similar to mammalian IgG, with two light (L) and two heavy chains. Leslie and Clem *(50)* proved, in 1969, the existence of profound differences between the mammalian and avian IgG, recommending the word IgY for avian IgG. In 1962, Williams *(51)* identified the IgY protein as the predominant and most important ɣ-globulin in a ɣ-levitin fraction of the yolk. Livetins are a fraction of water soluble proteins that constitute 10 % of the egg yolk dry-matter and include α- , β- and ɣ-livetin *(52)*. Among all birds chicken IgY is the most frequently studied, best described and characterized *(13)*.

1.3.1 – Molecular properties of IgY

The general structure of IgY presents two heavy chains (H) with a molecular weight of 67-70 kDa each and two light chains (L) with a molecular weight of 25 KDa each *(13,53)*. Since the heavy chain of IgY has one constant domain longer than that on IgG, it's relative molecular weight increases to 6.4×10^{4} kDa *(33)*. The main difference between the two molecules is the number of constant regions in the heavy chains: IgG has three C regions (Cγ1-Cγ3), while IgY has four (Cv1-Cv4) *(13)*. The heavy chain of IgY does not have a hinge in contrast with the IgG structure, where two of the three constant domains are separated by a hinge which gives considerable flexibility to the molecule (Figure 5) *(43)*. The absence of this hinge region, in IgY, reduces de mobility

of the molecule containing the variable domains (the portion containing the antigen-binding site) and the intra-molecular forces of IgY are thus weaker than those of mammalian IgG *(33,53)*. This affects the cross-linking of a binary complex antigen-antibody, affecting the ability of IgY to form an immunoprecipitate with antigens *(33)*. The regions in IgY near the boundaries of Cv1-Cv2 and Cv2-Cv3, contain proline and glycine residues enabling only a limited flexibility *(13)*. The content of the β-sheet structure in C domains of IgY is lower than in mammalian IgG; as a result, the conformation of IgY is more disordered in comparison to mammalian IgG *(53)*.

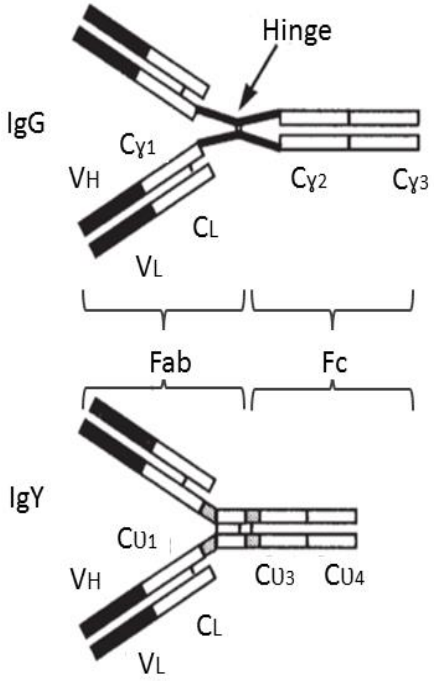

Figure 6 – Structure of IgG and IgY *(43)*.

IgY is more hydrophobic than IgG and its isoelectric point is also lower *(54)*. The IgY isoelectric point ranges between 5.7 and 7.6, whereas that of IgG is in the range between 6.1 and 8.5 *(13,53,54)*. Nevertheless, IgY is more sensitive than rabbit IgG to acid denaturation *(54)*. Shimizu et al. *(55)* reported that the activity of IgY was decreased at pH 3.5 or lower and almost completely lost at pH 3. These results confirmed conformational changes and damage in the Fab portion including the antigen binding site *(53)*. The activity of IgY under alkaline conditions do not change until the pH increase up to 11, being significantly diminished at pH 12 or higher *(55)*. Regarding the IgY proteolysis stability, it largely depends on the nature of the digestion enzymes and on the

pH conditions *(54)*. In 1993, Hatta et al. *(56)* reported that the IgY activity was lost after digestion with pepsine. The same group of researchers demonstrated that at pH 5 or higher pH values, IgY retained its antigen-binding and cell-agglutinating activities, being highly resistant to pepsin digestion *(56)*. However, at pH 4.5 or lower, both activities were lost *(57)*. The SDS-PAGE profiles of IgY after incubation with pepsin showed that at pH 2 IgY was digested to small peptides and no bands corresponding to IgY were detected on the polyacrylamide gel, suggesting the complete hydrolysis of the antibodies *(56)*. At pH 4, IgY digested with pepsin retained is activity at 91 % and 63 % after one hour and four hours of incubation, respectively *(56)*. Regarding the trypsin or chymotrypsin digestion, Shimizu et al. *(57)* and Hatta et al. *(56)* were able to demonstrate that there was a high loss of specific IgY activity during passage through the stomach mostly due to the activities of these pancreatic proteases *(56,57)*. IgY kept is activity at 39 % and 41 % after eight hours of incubation with trypsin or chymotrypsin, respectively *(53)*. The trypsin digestion results in a definitive cleavage of the IgY chains whereas the resulting fragments of the chymotryptic digestion present higher values of activity *(53)*. Concerning the temperature stability, besides being stable at temperatures around the room temperature, IgY is also stable at temperatures ranging between 60 ºC and 70 ºC *(55,57)*. However, the IgY activity decreased by heating at 70 ºC or higher for 15 minutes and it is denatured when exposed to temperatures higher than 75 ºC *(58)*.

1.3.2 – Applications of IgY

Chicken polyclonal antibodies are applied in many different methods for various purposes: as therapeutic reagents, as tools for purification or detection of antigens, in diagnostic and as protective agents of passive immunization *(54,59–61)*. IgY was demonstrated to work in practically all tested immunological methods that were originally developed for mammalian IgG *(61)*. These methods include immunofluorescence, immunoenzyme techniques, immunoelectrophoresis, ELISA, western blotting and immunohistochemistry, among others *(33,49)*. Since it is possible to conjugate IgY with horseradish peroxidase or biotin, the resulting conjugates can be used in common immunochemical procedures *(62,63)*. Besides, IgY was already used for immunodection of *Bortritis*-specific invertase in infected grapes *(64)*. The fact that IgY possesses a lower pI value than mammalian IgG makes it also usable in rocket electrophoresis to quantify immunoglobulins of mammalian sera, namely IgG and IgM *(65)*. The only limitation of

using chicken antibodies for this type of assays consists in the lower ability of IgY to precipitate antigens. However, this can be overcame by using optimized conditions, such as an increase of the ionic strength *(33)*. There is also an increasing interest in the use of IgY in immunodiagnostics and immunotherapy owing to its inherent advantages *(66)*. The relatively inexpensive production of eggs suggests that hen-egg antibodies could be used in cases where a high amount of immunoglobulins is needed to reach the therapeutic effect *(33)*. Passive immunization and prophylaxis are relevant fields and mammalian antibodies have already been applied for these purposes; but, due to their high cost, they were only used to treat emergency cases *(33)*. Hens can be immunized for production of antibodies against various antigens, such as viral and bacterial antigens producing antigen-specific IgY *(37,49,54,66)*. The use of IgY for passive immunization has been an intensively studied research field and its effectiveness has been demonstrated in the prevention and treatment of infectious diseases caused by various pathogens in animal models, especially those of the intestinal tract *(37,49,53)*. Some studies revealed positive results against some pathogens in mice, pigs and calves. Table 1 presents some of these positive results *(53)*.

Table 1 - Effect of passive immunization by enteric pathogen-specific IgY *(53)*.

Pathogen	**Animal specie**	**Effects**	**References**
Salmonella	Mice	Preventing and protecting mice challenged with *S. Enteritidis* or *S. Typhimurium* from experimental salmonellosis	*(67)*
	Calves	Preventing fatal salmonellosis in neonatal calves exposed to *S. Typhimurium* or S. Dublin	*(68,69)*
	Laying hens	Reducing *S. Enteritidis* contaminated eggs rate in experimentally infected hens	*(70,71)*
	Broiler chickens	Reducing caecal colonization and faecal shedding in *S. Enteritidis* challenged chickens	*(72)*
Campylobacter jejuni	Broiler chickens	Inhibiting and Reducing the faecal shedding of *C. jejuni*	*(73)*
Escherichia coli	Pigs	Preventing, protecting and curing piglets infected with *E. coli*-induced enterotoxernia	*(74–76)*
	Calves	Protecting neonatal calves from fatal enteric colibacillosis by K99-piliated ETEC	*(77)*
	Rabbits	Preventing diarrhoea in rabbits challenged with ETEC	*(78)*
Rotavirus	Mice	Preventing murine rotavirus (MRV), human rotavirus (HRV)-induced gastroenteritis and HRV-induced gastroenteritis and protecting mice from bovine rotavirus (BRV)-induced diarrhoea	*(79,80)*
	Calves	Protecting and preventing BRV-induced diarrhoea in neonatal calves	*(81)*

Recently, IgY was also reported to be used as an useful tool in cancer research, diagnosis and therapy *(49)*. Nevertheless, the applications of IgY are still limited mainly due to the prior extraction and purification steps that are difficult to accomplish. To overcome these obstacles, the existing methods should be optimised or new techniques should be established *(15)*.

1.4 – Purification of antibodies

The production and applications of both monoclonal and polyclonal antibodies have been receiving considerable attention in the last few decades, emerging as one of the fastest growing fields of biotechnology *(21,82)*. For diagnosis, antibodies are the ideal biological recognition reagents, and thus, are useful in a range of analytical platforms, namely western blotting (immunoblotting), immunohistochemistry, immunocytochemistry, immunoprecipitation, enzyme linked immunosorbant assay (ELISA), antibody microarrays, antibody-imaging, radioimmunoassays, flow cytometric analysis, immuno-polymerase chain reactions (IPCRs) and real-time IPCRs *(9,83–85)*. In addition, they are also used as a useful tool in immunoaffinity chromatography *(35)*. Antibodies are generally isolated from plasma, serum, ascites fluids, cell culture medium, egg yolk, plan extracts or bacterial yeast cultures. All of these sources have different proteins in addition to antibodies and most of the above-mentioned applications demand homogeneous antibody preparations. Hence, an efficient purification of antibodies becomes imperative *(35)*. The purification of antibodies can be achieved by a range of methodologies based on the specific physical and chemical properties of these molecules, such as size, solubility, charge, hydrophobicity and binding affinity *(21,35,86)*.

Affinity chromatography is the most widely employed method for antibody purification and it was first introduced in 1968 by Cuetrecasas and co-workers *(87)*. This technique relies on a reversible interaction between the antibody and its specific antigen. The specificity of binding is exploited for the selective absorption of the target protein from a complex matrix, and it can be eluted by using competitive analogues, denaturing agents or other factors, such as pH, ionic strength and polarity *(35,87)*. The successful application of this technique depends on a number of favorable characteristics regarding the chromatographic matrix and the ligands used *(35,87)*. The matrix should be uniform, microporous, hydrophilic, chemically and mechanically stable, selective, exhibit minimum non-specific absorption and it should provide a large scale area for the ligand attachment *(35)*. The ligand, which also plays a major role in the specificity and stability of the system, must have affinity to the target antibody, specificity, immobilization feasibility, stability in harsh washing and elution conditions, and retention of the target binding capacity after its attachment to the matrix *(35)*. Bispecific ligands, such as bacterially derived receptor, antigens and lectins, have been suggested for this purpose. The most commonly used ligands for purification of full length antibodies are

staphylococcal protein A and streptococcal protein G *(21,35,82,86)*. Protein A is a component of the cell surface of *Staphylococcus aureus* and it is composed of five Ig-binding domains (E, D, B and C) *(35,88)*. It interacts with antibodies through two distinct binding events: the typical binding site on the Fc portion of human IgG1, IgG2, and IgG4, and the alternate binding site found on the Fab portion of human IgG, IgM, IgA, and IgE *(88)*. Protein G is isolated from *Streptococcus* and it binds strongly to the Fc region on the IgG *(35)*. Due to the protein A superior stability and binding capacity, when compared to protein G, it is often preferred for industrial-level purifications of IgG *(35,86)*. Besides, protein G binds to albumin, α_2- macroglobulin and kinogen, along with IgG, leading to a reduced purification efficiency *(89)*. Despite the popularity of these ligands, they have some disadvantages, including high manufacturing and processing costs, instability, potential for the ligand to leak from the column, storage, are labor-intensive, and difficulty in sterilization steps. Besides, the majority of biospecific ligands are produced in bacteria from which there is an attendant risk of contaminants, such as viruses, pyrogens and DNA *(35)*. Other chromatographic techniques have been applied for antibodies purification, namely hydrophobic charge induction chromatography (HCIC), thiophilic affinity chromatography (TAC) and immobilized metal affinity chromatography (IMAC). HCIC is based on the hydrophobic interactions between the ligand and the target and it is achieved under physiological conditions *(35,90)*. The desorption step is then based on electrostatic charge repulsions and it is accomplished by reducing the pH of the mobile phase. Under acidic conditions both, the ligand and the target molecule have positive charge and the binding is disrupted *(35,90)*. This technique has already been successfully applied in the capture and purification of IgG *(90)*. TAC is another method used for antibodies purification; it uses sulfur-containing ligands attached to a matrix which binds antibodies in the presence of high concentrations of salts that induce the exposition of the hydrophobic regions of proteins *(35)*. Thiophilic gels are the most commonly used absorbents, based on a reaction between divinylsulfone and 2-mercaptoethanol. The structure of the immobilized ligand can be written as agarose-$CH_2CH_2SO_2CH_2CH_2SCH_2CH_2OH$. As the aforementioned technique, thiophilic chromatography as already been used as a method for purification of IgG from different species *(91,92)*. In IMAC, the capacity of biomolecules with exposed His, Cys, Ser, Glu, Asp and Trp residues is exploited for the design of ligands, which are attached to a covalently linked chelating compound and a spacer group *(35)*. This technique is reported

to be used in the purification of antibodies from different species and classes namely the IgG from human plasma *(93)*.

Despite all these encouraging results, these techniques are laborious and of high cost. These methods usually involve more than one step of purification to remove the remaining host cell proteins, DNA, possible leached Protein A and IgG aggregates *(21)*. In order to provide an adequate level of viral clearance, a viral inactivation step (low pH hold) and a viral filtration step are sometimes needed *(21,94)*. Furthermore, in each step, some quantity of the target molecule can be lost, resulting in low yields *(94)*. In order to ensure that downstream costs do not cancel out the expected upstream gain, the development of effective and economical purification methods is a crucial demand *(82)*. Recently, the use of ABS has been suggested as an interesting alternative to the traditional purification schemes, since clarification, concentration and purification can be combined in only one operation, while using a water-rich biocompatible environment, as discussed below *(21,82)*.

1.4.1 – IgY extraction and purification

Nowadays, there is an increasing interest in chicken egg yolk for the production of polyclonal antibodies *(13,95)*. Chicken egg yolk is an interesting source of IgY, a specific antibody with potential applications in many fields *(33)*. Despite all the advantages IgY is commercially produced only in small quantities and with high production costs, which are mainly due to the several steps required for IgY purification *(96)*. In addition, IgY do not bind to protein-A or protein-G, which are the most widely used affinity ligands for the purification of IgG from biological fluids, as mentioned before *(97)*. Egg contains approximately 50 % of water and its dry weight is made up of 2/3 of lipids and 1/3 of proteins. The proteins are divided into four fractions: lipovitellin, phosvitin, low-density lipoproteins and livetins (the IgY is a subclass of livetins) *(20)*.

IgY purification schemes involve extraction of the water-soluble fraction followed by several purification steps *(96)*. The purification of IgY usually proceeds in two stages: i) separation of the water-soluble fraction containing IgY from the lipidic fraction, which is mainly composed of lipids and lipoproteins; and ii) isolation of IgY from other water soluble proteins *(15,33,98)*. The first step is usually carried out by a simple water dilution method *(96)*. However, many techniques have been developed and tested to remove the lipophilic yolk components from the crude IgY extract *(98)*. Polyethylene glycol (PEG),

dextran sulphate, algina, caprylic acid and other organic solvents were investigated by a simple dilution of the yolk, or by a freezing-thawing approach of the diluted yolk, in order to form lipid aggregates large enough to be removed by centrifugation and filtration *(98)*. Some methods, such as ultracentrifugation, hydrophobic or affinity chromatography were also investigated as a first purification step *(47,98)*. For a large scale production, the limiting step is usually the separation of the water soluble proteins from the lipids and other hydrophobic substances *(20,47,98)*. The second stage comprises the recovery of the pure IgY fraction from the WSPF of the yolk *(98)*. Many methods have been described for such a purpose, with most of them involving most of them involving salt precipitation or chromatographic techniques *(99)*.

Jenesenius et al. *(100)* introduced a new method based on the water dilution of egg yolk as a simplification of the dextran sulphate precipitation method. After freezing and thawing, at low ionic strength and at a pH 7 or lower, the yolk lipids aggregate and can be removed by centrifugation. The freeze and thaw step was additionally substituted by water dilution, at pH 6 and pH 7, by Kwan and co-workers *(101)*. The lowering of the pH values and increasing of the dilution ratio strongly contributed to a higher lipids removal *(15,101)*. The study of the aqueous dilution method was performed in detail by Akita and Nakai, in 1992 *(102)*. Their results showed that with pH values below 5.0, the recovery of IgY decreased from 93 to 75 %, while a pH increase up to 6.6 caused even a more dramatic loss (55 %). So, the optimum pH values were established between 5-5.2, corresponding to the maximal IgY's recoveries *(102)*. Polson et al. *(103)* were the first to introduce the extraction of IgY from egg yolk using PEG as a precipitation agent for the lipidic fraction. This method was rejected later, mainly due to the fact that it is time consuming and the yields obtained were very low *(15)*. Several studies were carried out using cadmium sulphate, zinc sulphate and ammonium sulphate for inducing the IgY precipitation *(99,104)*. The results obtained by Gazin Bizanova et al. *(99)*, in 2003, revealed that IgY preparations purified with ammonium sulphate contain a higher total amount of proteins than those purified by the other two salts. However, regarding the purity of IgY, the results were not satisfactory *(99)*. In 1981, Jensenius et al. *(105)*, made use of the interaction between the anionic polysaccharide dextran sulphate with egg yolk lipoproteins to obtain the IgY fraction. Nevertheless, dextran sulphate is very expensive, making the method unviable in a large scale. Natural gums, like xanthan and carrageenan, were also tested and seemed to be able to remove most of the lipids, while maintaining

an acceptable protein recovery *(106)*. Recently, Chang and co-workers *(107)*, used λ-carregeenan, alginate, pectin and Na-carboxymethyl cellulose to recover IgY from adequately diluted yolks in a single step process. The optimum isolation conditions were determined at pH 5 and the best IgY recovery was performed using pectin (20.87 % purity) *(15,107)*. With the goal of developing a new and pioneering affinity purification technique, Verdorliva et al. *(97)*, studied the TG19318 ability to capture IgY directly from the water soluble extract. Protein A Mimetic TG19318 is a new synthetic ligand which binds specifically and selectively to the constant portion of immunoglobulins *(97)*. The results showed a yield value of 10.2 % and a purity > 90 % *(97)*. Several commercial kits are also available for IgY purification. Two of the most used kits are Thermo Pierce's Eggcellent™ and Promega's EGGstract®. They are based on a dilipidation step followed by a protein purification/precipitation step. However, in spite of both kits are able to produce reasonably pure IgY (70-90 %) they are particularly expensive given the yield of IgY produced *(47)*. It should be pointed that, in most of the above mentioned studies sodium dodecyl sulfate polyacrylamide gel electrophoresis (SDS-PAGE) was used to confirm the presence of IgY at the different steps of the isolation process *(20,46,102,108)*. The stained gels revealed the decreasing number of proteins in the mixture at each purification step while evaluating the purity of IgY by the two major protein bands corresponding to the reduced heavy and light chains of IgY *(20,46)*.

A previous study has proposed the use of ABS, instead of the previously referred techniques, for IgY extraction and purification *(20)*. ABS could be used to separate IgY into one phase and lipoproteins into another, and as the primary purification step. Then, IgY can be extracted from the IgY-rich-phase by affinity chromatography, or the IgY-fraction can be extracted by selective precipitation or T-gel chromatography in a secondary purification step *(20)*.

1.5 – Extraction and purification of biomolecules using aqueous biphasic systems (ABS)

The extraction and purification of biomolecules generally encompasses four stages namely recovery, isolation, purification and polishing *(94)*. The use of liquid-liquid extraction techniques as the first downstream purification step allows the separation and concentration of the target proteins simultaneously *(16)*. Liquid-liquid extraction using

ABS is a powerful non-chromatographic technique that has been suggested as an attractive alternative as a primary stage unit operation in the downstream processing of biological products, such as cells, virus, RNA, plasmids, nucleic acids and proteins *(16,22,94)*. These systems are formed when two mutually incompatible hydrophilic solutes, usually two polymers or a polymer and a salt, are dissolved in water above a certain concentration *(94,109)*. The process of aqueous two phase partition of biomolecules was firstly introduced by Albertson *(110)*, based on ABS formed by PEG, potassium phosphate (K_2HPO_4) and water, and PEG, dextran and water *(110,111)*. This discovery was the boost to the use of these systems as an important separation technique in the downstream processing of biomolecules *(2,94)*. ABS have many advantages since they provide a suitable environment (water-rich) to maintain the proteins integrity and biological activity *(16,94)*. ABS are also a fast separation technique with weak denaturation effects and do not use volatile and hazardous organic compounds *(23,94)*. Liquid-liquid extraction in ABS is also a relatively inexpensive technique, is easily operated and scaledup, it presents high resolution capacity and allows clarification, separation, purification and concentration in just one step *(22,94,109)*.

The partitioning of a target compound in ABS depends on a number of parameters, which include the physicochemical properties of the system, the nature and structure of target solute and the interactions between the last and the phase-forming components of ABS *(2)*. The properties of the system comprise the pH value, ionic strength, and type of the phase-forming components, while the nature of the target solute includes its charge, molecular weight, hydrophobicity and conformational characteristics *(2,94)*.

Benavides and Rito-Palomares *(112,113)* suggested the division of the ABS process into four main stages: initial physicochemical characterization of the feedstock, selection of the adequate ABS, selection of the system parameters and evaluation of the influence of the process parameters upon product recovery/purity. Once the product of interest is characterized, the phase-forming components of the ABS must be selected *(2)*. When the partition of the molecules is not one-sided it is possible to increase the process yield and selectivity by the addition of neutral salts or affinity ligands for the target protein *(2,23)*. In polymer-polymer systems, the addition of an electrolyte and its partitioning through the phases may alter the partition of the target molecule. The more hydrophilic phase is rich in ions such as Li^+, Na^+, NH_4^+, Ca^{2+}, Mg^{2+}, F^-, SO_4^{2-}, CO_3^{2-},PO_4^{3-} and CH_3COO^-; on the other hand, more hydrophobic phases are rich in ions such as K^+, Rb^+, Cs^+, Cl^-, Br^-,

I^-, SCN^-, NO_3^- and ClO_4^- *(2)*. In polymer-salt systems, the addition of neutral salts, such as NaCl, may increase the hydrophobicity difference between the phases due to the decrease of the amount of bounded water, resulting in an exposure of the hydrophobic domains on the protein surface, which will promote hydrophobic interactions with the polymer phase *(2)*. The addition of selective ligands is mainly used in polymer-polymer ABS and it can make the extraction in ABS more predictable and selective, improving the partitioning of the target molecule *(2)*. PEG is frequently used for derivatization mainly because of its terminal hydroxyl groups which can be functionalized. A large variety of functionalized groups can be covalently attached to PEG and have been largely investigated to increase the affinity between the polymer and the target protein *(2,23)*.

ABS have unique phase diagrams under a particular set of conditions, namely pH and temperature. They can provide information related with the concentration of the phase components required to form two phases, the concentration of the phase components in the top and bottom phases, and the ratio of the phase volumes. A typical ABS diagram has a binodal curve (TBC), which divides a region of components concentrations that form two immiscible aqueous phases from those that form one phase. Usually, the region which allows the formation of two immiscible phases is the one above the binodal curve (Figure 7) *(94)*. The three global mixtures, X, Y and Z, differ in their initial compositions and volume ratios, but all have the same composition at the top phase (T_{IL},T_{salt}) and at the bottom phase (B_{IL},B_{salt}). This similarity is mainly due to the fact that they are lying on the same tie-line (TL), whose end points are determined by the equilibrium phase composition. The length of the tie-line (TLL) has the same units as the component concentrations and defines the difference on the compositions among the phases *(94)*.

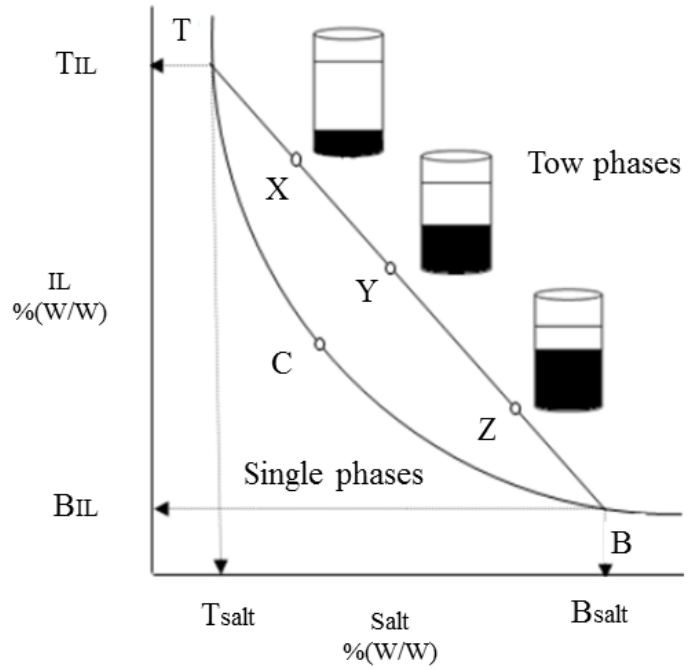

Figure 7 – ABS phase diagram binodal curve. TCB = binodal curve; C=critical point; TB = tie-line; T=composition of the top phase; B = composition of the bottom phase; X, Y and Z = mixture compositions at the biphasic region *(94)*.

Nowadays, ABS are extensively used as an alternative to the existing chromatographic techniques to purify biopharmaceuticals, such as monoclonal antibodies, growth factors and hormones *(94)*. The use of ABS-based extractions in the downstream processing of monoclonal antibodies was reported in 1996, by Zijlstra and co-workers *(114)*, who have used a functionalised PEG/Dextran system to recover IgG from hybridoma cell supernatants. Meanwhile, another research team used polymer-salt based ABS to recover IgG from hybridoma cell supernatants *(115)*. In 2007, Rosa et al. *(116)* proved the viability of using ABS for the purification of human antibodies from a protein mixture containing albumin and myoglobin. They achieved a recovery yield of 101 % and a purity of 99 % using an ABS composed of 8 wt% of PEG, 10 wt% of a buffer composed of K_2HPO_4 and NaH_2PO_4 and 15 wt % of NaCl *(116)*. The same research team also optimized the method of purifying IgG from Chinese Hamster Ovary (CHO) using an ABS constituted by 12 wt % of PEG, 10 wt % of a buffer composed of K_2HPO_4 and NaH_2PO_4 and 15 wt % of NaCl at pH 6, with a recovery of 88 % *(16)*. Table 2 shows some of the developed ABS and their successful application in biopharmaceuticals purification.

Table 2 – Aqueous two-phase extraction/purification of biopharmaceuticals *(2)*.

Biopharmaceutical	Production source	ABS	Recovery yield (%)	Purity (%)	References
Monoclonal Antibody (human IgG)	Chinese hamster ovary cells	PEG/ K_2HPO_4	88	-	*(16,21,24,82 ,117)*
		PEG/ NaH_2PO_4	96	95	
		PEG/dextran			
		PEG-$(COOH)_2$/dextran	82	96	
		EOPO/dextran	85	88	
		PEG/ HOC(COONa)$(CH_2COONa)_2 \cdot 2H_2O$	97	76	
Human Interleukin-18 binding protein (IL-18BP)	Chinese hamster ovary cells	PEG/ $(Na_2)SO_4$	98	92	*(118)*
Human monoclonal anti-human immunodeficiency virus (HIV) 2F5	Transgenic tobacco extract	PEG/ K_2HPO_4	95	-	*(119)*
		PEG/ NaH_2PO_4			
Human growth hormone (hGH)	Escherichia col	EOPO/starch	70	-	*(120)*
Human growth hormone antagonist	E. coli	PEG/ $(NH_4)_2SO_4$	83	-	*(121)*
Human insulin-like growth factor I (IGF-I)	E. coli	PEG/Na_2SO_4	70	97	*(122)*
Monoclonal antibody (immunoglobulin G)	Hybridoma cells	PEG/KH_2PO_4	90	-	*(82,123)*
		PEG/K_2HPO_4	99	96	
		PEG/ HOC(COONa)$(CH_2COONa)_2 \cdot 2H_2O$			
Hepatitis B surface antigen (HBsAg)	Yeast cells	PEG/ $(NH_4)_2SO_4$	89	-	*(124)*

1.5.1– ABS using ionic liquids (ILs)

In 2003 Rogers and co-workers *(26)* proposed a novel approach to create ABS with the use of ionic liquids (ILs). ILs are a new class of purely ionic salt-like materials that are liquid at low temperatures *(19,125,126)*. Their low melting temperatures are due to the large size of their ions which leads to a diffuse charge. As a result, they present reduced electrostatic forces that make difficult the formation of a regular crystalline

structure, and therefore, they can be liquid at or near room temperature *(19)*. The focal interest in ILs is due to their generally unique combination of physicochemical properties, such as a negligible vapor pressure, null flammability, high ionic conductivity, as well as high thermal and electrochemical stabilities. The fact that ILs present non-flammability and negligible volatility contributes to their epithet as "green solvents". Nevertheless, the main advantage of using ILs in ABS relays on their tailored solvation/extraction ability *(19,126,127)*. The ability to tailor the polarities of the ILs in ABS formation by the proper manipulation of cation/anion design and their combination is the major benefit of IL-based ABS given the difficulty of overcoming the limited polarity range of polymer-based ABS. In polymer-based ABS the difference of polarities between the phases is restricted, which have been preventing a vast use of these systems for extraction and purification purposes. Due to their tunability, ILs can cover the whole hydrophilicity-hydrophobicity range *(19)*. The use of ILs in conventional systems provide tailored and optimized extractions by a proper choice of the IL. Moreover, IL-based ABS are substantially less viscous than typically polymer-based ABS and usually display faster phase separation rates *(19,128)*. Therefore, these encouraging properties have led to the research on ILs as alternative phase-forming components of ABS *(126)*. The most studied ILs are the nitrogen-based and their general cation chemical structures are presented below (Figure 8).

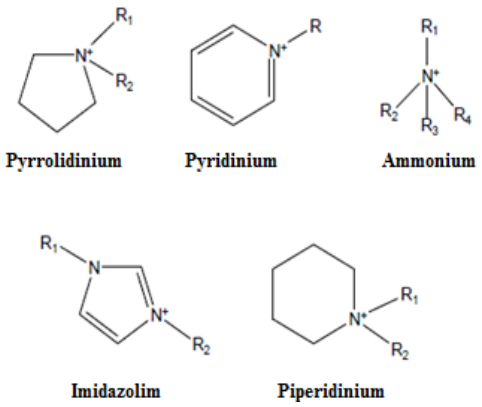

Figure 8 - Chemical structures of the nitrogen-based cations of ILs

In the past decade, the extraction of biomolecules using IL-based ABS has been extensively investigated *(126,127,129–132)*. However, few reports are found concerning the extraction of proteins and enzymes *(133)*. Proteins are either insoluble or their solubility is very low in hydrophobic ILs and the inactivation of enzymes is a recurrent scenario in pure ILs *(133,134)*. ABS composed of ILs and salts were suggested as a good

alternative for solving these problems since a large amount of water is introduced *(134)*. The extraction of proteins by means of IL-based ABS was firstly achieved by Du et al. *(133)* using a ABS formed by 1-butyl-3-methylimidazolium chloride ([C_4mim]Cl) + K_2HPO_4. Later on, several authors employed IL-based ABS for the extraction of other proteins and enzymes, such as bovine serum albumin, trypsin, lysozyme, myoglobin, cytochrome c, γ-globulins, hemoglobin, peroxidase, ovalbumin and horseradish peroxidase *(17,26,133–135)*.

The stability of proteins is strongly affected by the proton activity of the solution, and, consequently by its pH *(25,136)*. It has been accepted that salt ions exert their effects indirectly by affecting the protein structure, enzyme activity and protein crystallization *(25)*. Recent results revealed that, in some cases, there is a direct interaction between the protein and the salt ions *(137)*. However, adding a buffer into aqueous IL solutions, will not provide an adequate pH control since the ILs acidity or basicity could swamp the buffer effect. The pH can be however adjusted to optimum values by the addition of proper ILs with buffer capacity *(25)*. Good and co-workers *(138)* have described five new biological buffers, namely 3-chloro-2-hydroxypropanesulfonic acid, N-[1,3-dihydroxy-2-(hydroxymethyl)-2-propanyl]glycine (Tricine), [N-bis(hydroxyethyl)amino]-2-hydroxy propane sulfonic acid, 3-{[1,3-dihydroxy-2-(hydroxymethyl)-2-propanyl]amino}-1-propanesulfonic acid (TAPS), N-hydroxyethyl piperazine-N'-2-hydroxy propane sulfonic acid and piperazine-N,N'-bis(2 hydroxy propane sulfonic acid)dehydrate. Good's buffers (GBs), which are zwitterionic amino acid derivatives, can be used as anion or cation radicals of ILs still covering the physiological pH range (6 to 10), leading thus to the creation of a new class of ILs: Good's buffers ionic liquids (GB-ILs) *(138)*. Either GBs or IL-derived GBs have demonstrated to be enhanced protein structure stabilizers *(25)*.

This type of GB-ILs was also used in this work, and these were already shown to be able to maintain the protein structure while leading to high extraction efficiencies when employed as phase-forming components of ABS (bovine serum albumin was used as a model protein) *(25,136)*. Moreover, in a recent study by Taha et al. *(139)*, the same GBs anions were combined with the cholinium cations, and these were employed to create ABS with a polymer (PEG 400) and further applied in the extraction and purification of IgY. Extraction efficiencies of the water-soluble fraction of proteins, ranging between 79

and 94 % were achieved in a single step, while the IgY purification was still far from being completely achieved *(139)*.

In the current work, GB-ILs with anions derived from Tricine, 2-{[1,3-dihydroxy-2-(hydroxymethyl)-2-propanyl]amino}ethanesulfonic acid (TES), N-cyclohexyl-2-aminoethanesulfonic acid (CHES), N-cyclohexyl-2-aminoethanesulfonic acid (HEPES), and 2-(N-morpholino)ethanesulfonic acid (MES) combined with tetrabutylammonium ($[N_{4444}]^+$) and tetrabutylphosphonium ($[P_{4444}]^+$) cations were investigated. The synthetized GB-ILs were at first combined with $C_6H_5K_3O_7$ for the ABS formation, their phase diagrams were ascertained and the extraction experiments were performed, aiming the development of an alternative platform for the selective extraction and purification of the IgY from the egg yolk.

2. Purification of IgY using Good's buffers ionic liquids (GB-ILs) + $C_6H_5K_3O_7$ ABS

2.1. Experimental section

2.1.1. Chemicals

Fresh eggs were periodically provided from Dr. Ricardo Pires from Biocant, located in Cantanhede, Portugal.

The material required for the ILs synthesis, namely the buffers CHES (purity > 99 wt %), HEPES (purity > 99.5 wt %), MES (purity > 99 wt %), Tricine (purity > 99 wt %), and TES (purity > 99 wt %), as well as the hydroxide-based compounds, $[P_{4444}][OH]$ (40 wt % in H_2O) and $[N_{4444}][OH]$ (40 wt % in H_2O) were purchased from Sigma–Aldrich.

The material requires to perform the SDS-PAGE analysis comprises: tris(hydroxymethyl)aminomethane, PA from Pronalab; sodium dodecyl sulfate, SDS (> 98.5 wt % pure) andglycerol, 99.5 wt % pure, from Sigma-Aldrich; bromophenol blue and acid acetic, 99.8 wt % pure, from Merck; dithiothreitol, DTT (99 wt % pure), from Acros; and methanol, HPLC grade, from Fisher Scientific. The Amersham ECLGel Box, the Amersham ECL Running Buffer (10X), the Amersham ECL Gel 4-20 %, 10 wells, and the Full-Range Rainbow Molecular Weight Marker were acquired from GE Healthcare. The Coomassie Brilliant Blue G-250 was purchased from Sigma-Aldrich.

Citrate tribasic monohydrate ($C_6H_5K_3O_7 \cdot H_2O$, purity ≥ 99 wt %), sodium phosphate monobasic (NaH_2PO_4, purity: 99 – 100.5 %), sodium phosphate dibasic heptahydrate ($Na_2HPO_4 \cdot 7H_2O$, purity: 98.2 – 102.0 %) and sodium chloride (NaCl) were obtained from Sigma–Aldrich. The mixture composed of dimethyl sulfoxide-d_6 (DMSO D6) and 0.03 % v/v tetramethylsilane (TMS), purity > 99.8 wt % was purchased from Euriso-top.

The water employed was double distilled, passed through a reverse osmosis system and treated with a Milli-Q plus 185 water purification apparatus.

2.2. Experimental procedure

2.2.1. Synthesis and characterization of the GB-ILs

The GB-ILs were synthesized *via* neutralization of the base with the proper acid. An excess of an equimolar aqueous solution (1:1.05) of buffer was added drop-wise to the tetrabutylphosphonium or tetrabutylammonium hydroxide solutions. By way of example, the CHES buffer was added dropwise into an aqueous solution of tetrabutylphosphonium hydroxide. The mixture was stirred continuously for at least 24h at room temperature (≈ 25 ± 1) °C. The anion source (1.05 equivalents of acid) was added to an aqueous solution

of [P_{4444}][OH] (1 equivalent, 40 wt % in water) and the mixture was stirred at room temperature for at least 24h to produce the ionic liquid and water as by-product. The mixture was evaporated at 50-60 ºC under reduced pressure giving rise to a viscous liquid. A mixture of acetonitrile and methanol (1:1, v:v) was added drop-wise to the viscous liquid and then stirred for at least 1h at room temperature. The mixture was filtered to remove any excess buffer. The solvent mixture was evaporated and the GB-IL product was dried in vacuum (10 Pa) for 4 days at 50-60 ºC *(25)*. The water content in each GB-IL was measured by Karl–Fischer (KF) titration, using a KF coulometer (Metrohm Ltd., model 831). The chemical structures of the GB-ILs were confirmed by ^{1}H and ^{13}C NMR spectroscopy (Bruker AMX 300) operating at 300.13 and 75.47 MHz, respectively. Chemical shifts are expressed in δ (ppm) using TMS as internal reference and D_2O as deuterated solvent. The synthesized ILs synthetized in this work showed high purity level without signs of decomposition.

2.2.2. Phase diagrams and tie-lines

The binodal curve of each ABS was determined through the cloud point titration method at (25 ± 1) °C and atmospheric pressure. This procedure was already validated in previous reports, although it was validated in this work with the phase diagram of the ABS formed by [C_4mim]Cl + K_3PO_4 + water. The results obtained in this work are in close agreement with literature data *(140)* and are shown in Appendix A – Figure A. 1. In summary, an aqueous salt solution was added drop-wise to the IL solution until the detection of a cloudy biphasic solution, followed by the drop-wise addition of water until the detection of a monophasic region, characterized by a clear and limpid solution. The drop wise addition was carried out under constant stirring. The ternary systems composition were determined by weight of all the components added within an uncertain of ± 10^{-4} g. In particular, for the systems composed of [N_{4444}][HEPES], [N_{4444}][MES], [N_{4444}][TES] + $C_6H_5K_3O_7$ + water, the turbidimetric method was used *(141)*. Various mixtures at the biphasic region were initially prepared, and then ultra-pure water was added until the detection of a clear and limpid solution (monophasic region), under constant stirring. Each mixture correspond to one point of the binodal curve. The mixture compositions were gravimetrically determined within ± 10^{-4} g and at (25 ± 1) °C.

The TLs were determined by a gravimetric method originally described by Merchuk et al. *(142)*. A previous selected mixture, at the biphasic region, was gravimetrically

prepared and then vigorously stirred. The mixture was then submitted to centrifugation for 15 min, at 5000 rpm, at controlled temperature (25 ± 1) ºC. After centrifugation the mixture was left in the equilibrium for more 10 min at (25 ± 1) °C, in order to guarantee the equilibrium of the coexisting phases. Then, each phase was separated and the top and bottom phases were weighted. Finally, each individual TL was determined by the application of the lever-arm rule. The experimental binodal curves were fitted using Equation 1 *(142)*,

$$[\mathrm{IL}] = \mathrm{Aexp}[(\mathrm{B}[\mathrm{Salt}]^{0,5}) - (\mathrm{C}[\mathrm{Salt}]^{3})] \quad (1)$$

where [IL] and [Salt] are the IL and salt weight fractions percentages, respectively, and A, B and C are fitted constants obtained by least-squares regression.

For the determination of the TLs the following system of four equations (Equations 2 to 5) was used to estimate the concentration of IL and salt at each phase ($[\mathrm{IL}]_{\mathrm{IL}}$, $[\mathrm{IL}]_{\mathrm{Salt}}$, $[\mathrm{Salt}]_{\mathrm{Salt}}$ and $[\mathrm{Salt}]_{\mathrm{IL}}$),

$$[\mathrm{IL}]_{\mathrm{IL}} = \mathrm{Aexp}\left[\left(\mathrm{B}[\mathrm{Salt}]_{\mathrm{Salt}}^{0.5}\right) - \left(\mathrm{C}[\mathrm{Salt}]_{\mathrm{Salt}}^{3}\right)\right] \quad (2)$$

$$[\mathrm{IL}]_{\mathrm{Salt}} = \mathrm{Aexp}\left[\left(\mathrm{B}[\mathrm{Salt}]_{\mathrm{Salt}}^{0.5}\right) - \left(\mathrm{C}[\mathrm{Salt}]_{\mathrm{Salt}}^{3}\right)\right] \quad (3)$$

$$[\mathrm{IL}]_{\mathrm{IL}} = \frac{[\mathrm{IL}]_{\mathrm{M}}}{\alpha} - \left(\frac{1-\alpha}{\alpha}\right)[\mathrm{IL}]_{\mathrm{Salt}} \quad (4)$$

$$[\mathrm{Salt}]_{\mathrm{IL}} = \frac{[\mathrm{Salt}]_{\mathrm{M}}}{\alpha} - \left(\frac{1-\alpha}{\alpha}\right)[\mathrm{Salt}]_{\mathrm{Salt}} \quad (5)$$

where the subscripts Salt and IL designate the Salt- and IL-rich phases, respectively, and M is the initial mixture composition. The parameter α is the ratio between the weight of the top phase and the total weight of the mixture. The solution of the described system provides the concentration of the IL and salt in the top and bottom phases.

In order to calculate each the tie-line length (TLL) Equation 6 was applied,

$$\mathrm{TLL} = \sqrt{([\mathrm{salt}]_{\mathrm{IL}} - [\mathrm{salt}]_{\mathrm{salt}})^2 + ([\mathrm{IL}]_{\mathrm{IL}} - [\mathrm{IL}]_{\mathrm{salt}})^2} \quad (6)$$

The correlation parameters of Equation 1 were determined using the software Sigmaplot.v11.0, while the compositions of the top and bottom phases, were determined using the software Matlab R2013a.

All the calculations considering the mass fraction or molality of the citrate-based salt were carried out discounting the complexed water.

2.2.4. Purification of IgY using GB-ILs + $C_6H_5K_3O_7$ ABS

The water soluble protein fraction (WSPF) of egg yolk was prepared from fresh eggs, following a protocol described in literature *(143)*, and then applied in the subsequent purification step. The ternary mixtures compositions were chosen based on the phase diagrams determined for each GB-IL + $C_6H_5K_3O_7$ + water system. A ternary mixture was prepared, within the biphasic region, using a common composition of IL (20 wt %) and variable concentrations of salt (from 13.5 to 30 wt %) to achieve a similar TLL (with values within $39.6 \geq TLL \leq 44.3$ for systems composed of $[P_{4444}][GB]$ and values within $39.1 \geq TLL \leq 58.1$ for those composed of $[N_{4444}][GB]$).

Each mixture was vigorously stirred and left to equilibrate for at least 3 h, at (25 ± 1) °C, to achieve a complete IgY partitioning and other contaminant proteins between the two phases.

In all the ternary mixtures evaluated, the IL-rich aqueous phase is the top phase, while the bottom phase is mainly composed of salt and water.

The extraction yield of IgY was defined by the ratio between the mass of IgY in the top phase and the total mass of IgY initially added to the system by the application of Equation 7,

$$\text{Yield}_{IgY} = \frac{m_{IgY\ (top\ phase)}}{m_{\ IgY\ (WSPF)}} \qquad (7)$$

2.2.3. pH measurements

The pH values of both the IL-rich and $C_6H_5K_3O_7$-rich aqueous phases were measured at (25 ± 1) ºC using a METTLER TOLEDO SevenMulti pH meter within an uncertainty of ± 0.02.

2.2.5. Size-exclusion HPLC (SE-HPLC)

After a careful separation of the phases, the SE-HPLC technique was used with the aim of quantifying the amount of each protein in each phase. A calibration curve was specially determined for this purpose (Appendix B - Figure B. 1). The IgY used to prepare the calibration curve was purified using the commercial kit EggsPure IgY. A phosphate buffer solution (1000 mL) was prepared using 47 mL of a Solution A (27.8 g NaH_2PO_4), 203 mL of a Solution B (53.65 g $Na_2HPO_4 \cdot 7H_2O$) and 35 g of NaCl. Each phase was diluted at a 1:9 (v:v) ratio in the phosphate buffer solution before injection. A Chromaster HPLC (VWR Hitachi) was used for IgY quantification. The SE-HPLC was performed on an analytical column Shodex Protein KW- 802.5 (8 mm x 300 mm). A 100 mM phosphate buffer + NaCl 0.3 M was run isocratically with a flow rate of 0.5 $mL.min^{-1}$. The column oven and autosampler temperatures were kept at 25 ºC and at 10 ºC, respectively. The injection volume was 25 µL. The wavelength was set at 280 nm using a DAD detector. The obtained chromatograms were treated and analyzed using the OriginPro8 software.

2.2.6. Sodium dodecyl sulphate polyacrylamide gel electrophoresis (SDS-PAGE)

The proteins profiles of the obtained aqueous rich phases, as well as the quantification of IgY in each phase, were determined by SDS-PAGE. All samples were diluted so that the amount of protein in each gel lane was about 0.5 µg. This amount was predicted taking into account the HPLC quantification of the total amount of proteins in each phase. Samples of the bottom and top phases of each ABS were diluted in the order of 1:1 (v:v) in a dissociation sample buffer constituted by 2.5 mL of 0.5 M Tris-HCl pH 6.8, 4.0 mL of 10 % (w:v) SDS solution, 2.0 mL of glycerol, 2.0 mg of bromophenol blue and 310 mg of dithiothreitol (DTT). This overall solution was heated at 95 ºC for 5 min, to reduce the disulphide linkages and denature the proteins. This step overcomes some forms of the tertiary protein folding and breaks up the quaternary proteins structure. Electrophoresis was run on polyacrylamide gels (stacking: 4 % and resolving: 20 %) with a running buffer consisting of 250 mM Tris HCl, 1.92 M glycine, and 1 % SDS. The gels were stained with a solution of Coomassie Brilliant Blue G-250 0.1 % (w:v), methanol 50 % (v:v), acetic acid 7 % (v:v) and water 42.9 % (v:v), in an orbital shaker at a moderate speed overnight at room temperature. The distaining of the gel was done using a solution containing acetic acid 7 % (v:v), methanol 20 % (v:v) and water 73 % (v:v) in an orbital

shaker at a moderate speed until removing all the excess of dye. SDS-PAGE molecular weight standards, marker molecular weight full-range (VWR), were used as protein standards.

A calibration curve by SDS-PAGE was also established for the IgY quantification (Appendix C - Figure C. 2). The IgY used to prepared the calibration curve was purified using the commercial kit EggsPure IgY. The scanning of the SDS-PAGE electrophoresis gels was done using the GenoSmart2 image capturing system and the quantification was achieved through the evaluation of the IgY light chain band intensity, using the GenoSoft software, both from VWR.

2.2.7 – Molecular docking

The molecular docking between IgY-Fc and the GB-IL cations was performed using the Auto-dock Tools vina 1.5.4 program *(144)*. The crystal structure of IgY-Fc (2W59) was used in the docking *(145)*. The natural bond orbital (NBO) charges for the GB cations in water phase were used. The center of the grid in the x, y, z axes was (-17.141 × -8.262 × 16.727) Å and the grid dimension was (78 × 70 × 84) Å.

2.2.8 – Fourier transform infrared spectroscopy (FT-IR)

The FT-IR spectra were recorded using a Perkin Elmer Spectrum Bx spectrophotometer, with a resolution of 4 cm^{-1} and 32 scans. The FTIR analysis was performed using the WSPF sample, as well as the aqueous samples from the IL-rich phase of each one of the studied ABS, containing proteins from the WSPF. The spectra were obtained in the wavelength range from 1700 to 1500 cm^{-1}, in a room under controlled humidity (35 %) and temperature (23 ºC). The PeakFit Version 4.05 was used for the spectra evaluation.

2.3. Results and discussion

2.3.1. Characterization of the synthetized GB-ILs

The NMR chaterization data of each GB-IL are presented below:

[P_{4444}][CHES]: From CHES buffer (47.2 mmol), this compound was obtained as a translucent viscous liquid. Water content < 0.05 wt %. ^{1}H NMR (300 MHz, D_2O/TSP):

2.76 (m, 2H), 2.50-2.52 (*m*, 1*H*), 2.02 (m, 8H), 1.37-1.45 (m, 16H,), 0.94 (m, 10H), 0.92 (t, 12H).

[P_{4444}][HEPES]: From HEPES buffer (44.3 mmol), this compound was obtained as a white viscous liquid. Water content < 0.05 wt %. ^{1}H NMR (300 MHz, D_2O/TSP): 3.59 (t,4H), 2.97 (t, 2H), 2.94 (t, 2H), 2.36 (t, 8H), 2.18 (m, 8H), 1.35-1.52 (m, 16H), 0.92 (t, 12H).

[P_{4444}][MES]: From MES buffer (48.5 mmol), this compound was obtained as a white solid. Water content < 0.05 wt %. ^{1}H NMR (300 MHz, D_2O/TSP): 3.63 (t, 4H), 2.99 (t, 2H), , 2.72 (t, 2H), 2.50 (t, 4H), 2.02 (m, 8H), 1.27-1.42 (m, 16H), 0.92 (t,12H).

[P_{4444}][TES]: From TES buffer (45.1 mmol), this compound was obtained as a white solid. Water content < 0.05 wt %. ^{1}H NMR (300 MHz, D_2O/TSP): 3.31 (s, 6H), 2.81 (s, 2H), 2.50 (m, 8H), 1.35-1.49 (m,16H), 0.92 (t, 12H).

[P_{4444}][Tricine]: From Tricine buffer (50.3 mmol), this comppound was obtained as a white solid. Water content < 0.05 wt %. ^{1}H NMR (300 MHz, D_2O/TSP): 3.34 (s, 6H), 3.18 (s, 2H), 2.00 (m, 8H), 1.27-1.44 (m, 16H), 0.77 (t. 12H).

[N_{4444}][CHES]: From CHES buffer (47.2 mmol), this compound was obtained as a translucent viscous liquid. Water content < 0.05 wt %. ^{1}H NMR (300 MHz, D_2O/TSP): 2.75 (m, 2H), 2.49-2.51 (*m*, 1*H*), 2.3 (m, 8H), 1.27-1.37 (m, 16H,), 0.94 (t, 12H).

[N_{4444}][HEPES]: From HEPES buffer (44.3 mmol), this compound was obtained as a yellow solid. Water content < 0.05 wt %.^{1}H NMR (300 MHz, D_2O/TSP): 3.34 (s,6H), 3.17 (t, 8H), 2.51 (t, 2H), 2.34 (2H, t), 1.31 (quin, 8H), 1.30 (sext,8 H) 0.94 (t,12 H).

[N_{4444}][MES]: From MES buffer (48.5 mmol), this compound was obtained as a white solid. Water content < 0.05 wt %. ^{1}H NMR (300 MHz, D_2O/TSP): 3.34 (t, 4H), 3.17 (t, 8H); 2.51 (t, 2H,), 2.49 (t,2H,), 2.32 (t, 4H), 1.55 (quin 8H), 1.31 (sext, 8H), 0.94 (t,12H).

[N_{4444}][TES]: From TES buffer (45.1 mmol), this compound was obtained as a white solid. Water content < 0.05 wt %. ^{1}H NMR (300 MHz, D_2O/TSP): 3.34 (s,6H), 3.27 (t, 8H), 2.86 (t, 2H), 2.51 (2H, t), 1.55 (quin, 8H), 1.30 (sext,8 H) 0.91 (t,12 H).

[N_{4444}][Tricine]: From Tricine buffer (50.3 mmol), this comppound was obtained as a white solid. Water content < 0.05 wt %. ^{1}H NMR (300 MHz, D_2O/TSP): 3.53 (s, 6H) 3.27 (s, 2H), 3.21 (t, 8H), 1.65 (quin, 8*H*), 1.37 (sext, 8*H*), 0.93 (t,12H).

The chemical structures and synthetic pathways of the synthesized GB-ILs are displayed in Figure 9 for the [P_{4444}][GB] ILs and in Figure 10 for the [N_{4444}][GB] ILs.

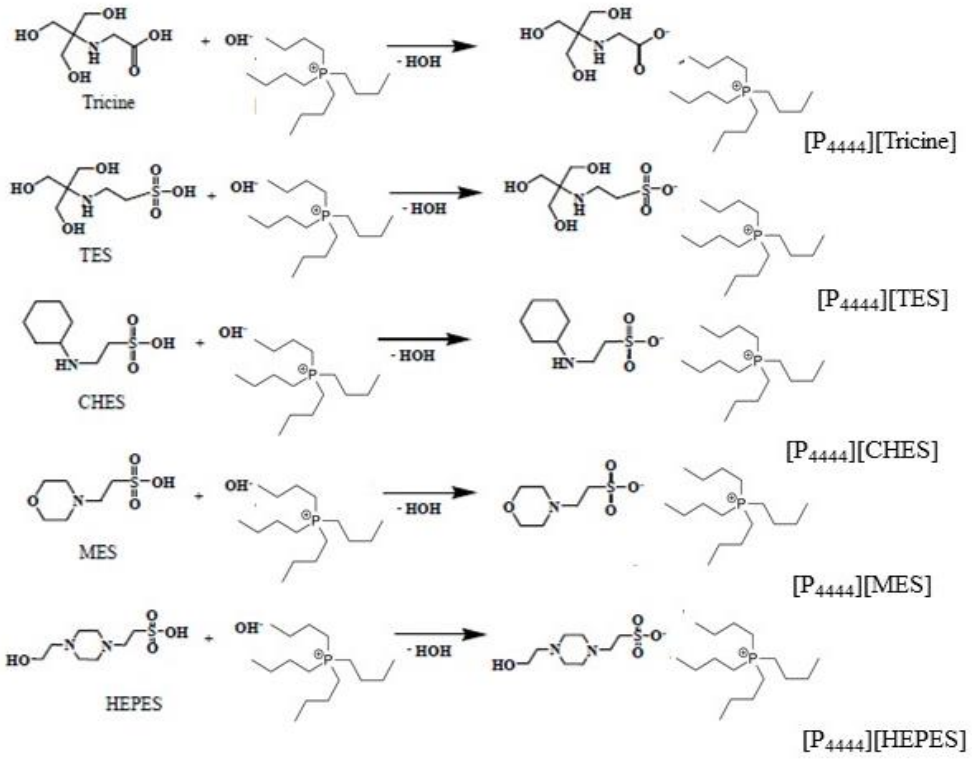

Figure 9 - The synthetic pathway for [P_{4444}][GB].

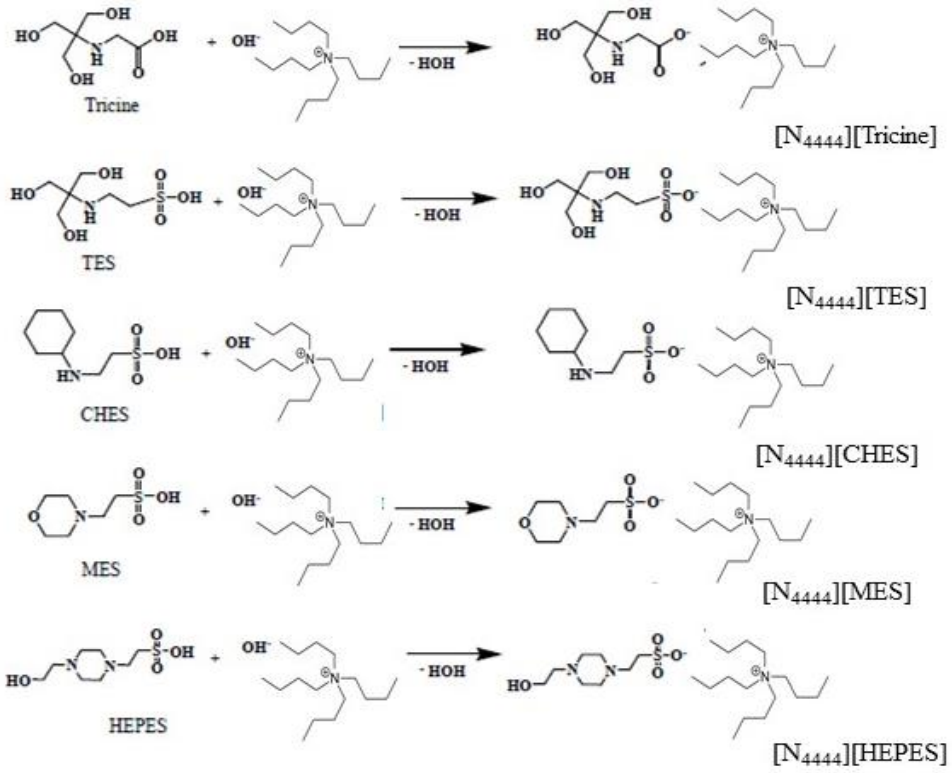

Figure 10 - The synthetic pathway for [N_{4444}][GB].

2.3.2. Phase diagrams and tie-lines (TLs)

The phase diagrams for the systems composed of $C_6H_5K_3O_7$, water, and the $[P_{4444}][GB]$ and $[N_{4444}][GB]$ ILs are illustrated in Figure 11 and Figure 12, respectively. The obtained results for the diagrams of the ABS containing the $[N_{4444}][GB]$ ILs are in close agreement with literature data and are presented in Appendix D *(25)*. The experimental data are shown in molality units in order to avoid differences that could result from different molecular weights, which allow a better understanding of the impact of the ILs molecular weight and structure on the phase diagrams behaviour. The detailed experimental data corresponding to the ternary phase diagrams are presented in Appendix E. For all studied ABS, the bottom phase is mostly composed of salt and water while the top phase corresponds to the IL-rich phase. This is an useful advantage considering the IL recovery, which may follow thereafter *(146)*. In the presented phase diagrams, the biphasic region is located above the solubility curve. Below the solubility curve, the concentration of each component is not sufficient to induce liquid-liquid demixing thus falling within the monophasic regime. Considering the representations in Figure 11 and Figure 12, the closer the axis is the binodal curve, the larger the biphasic area and the stronger the demixing ability of the IL, *i.e*. the easier the IL is salted-out by the salt.

Regarding the phosphonium-based ILs, the IL anion ability to form an ABS, for instance at 1.0 $mol \cdot kg^{-1}$ of $C_6H_5K_3O_7$, follows the order: $[P_{4444}][CHES] > [P_{4444}][MES] \approx [P_{4444}][HEPES] > [P_{4444}][TES] \approx [P_{4444}][Tricine]$ (Figure 11). For ammonium-based ILs, the order keeps almost the same: $[N_{4444}][CHES] > [N_{4444}][MES] \approx [N_{4444}][HEPES] > [N_{4444}][TES] \approx [N_{4444}][Tricine]$ (Figure 12). The formation of an ABS depends on the type of salt and IL, as well as on their concentrations, temperature and other features, such as the pH of the medium. The salting-out effect of the salt over the IL, in aqueous media, strongly affects the ABS formation. The salt ions dissolved in an aqueous solution are surrounded by a layer of water molecules, a process known as hydration *(147)*. When an salt is added to an aqueous solution of IL the two solutes will compete for the solvent molecules. The competition is usually won by the salt ions and, consequently, it occurs a migration of solvent molecules away from the ions of the IL towards those of the salt, which decreases the hydration and therefore the solubility of the IL in water – a process known as salting-out.

Accordingly to the Hofmeister series, which provides a qualitative ranking of salt anions and cations based on their effectiveness as protein precipitants, $C_6H_5K_3O_7$ is a salt

with a strong salting-out capacity since it is composed of a trivalent charged anion *(148)*. This organic salt anion has a strong affinity to water and thus there is an exclusion of the IL from the aqueous media, promoting the separation of the phase rich in IL from the rest of the solution. Since the set of ILs presented in Figure 11 and Figure 12 share the same IL cation, it is possible to evaluate the effect of the IL-anion on the ABS formation; the temperature (25 ºC) and pressure (1 bar) were also fixed in all experiments. Anions, when compared to cations, have a higher aptitude for hydration since they are more polarized and have a more diffuse valence electronic configuration *(147)*. Consequently, anions with lower hydrogen bond basicity values present lower ability to create hydration complexes, being more easily salted-out by salts. No hydrogen-bond basicity values have been reported for GB-ILs anions. However, some conclusions can be drawn using use of the water-octanol partition coefficients (K_{ow}) of each GB-IL. The higher the value of log(K_{ow}) the higher is the affinity of a given anion for the octanol-rich phase. As greater it is the affinity of a compound for the octanol-rich phase, the lower it is its polarity. As a result anions with higher log(K_{ow}) values are more easily separated into two phases and their phase diagrams are located near the binodal origin. The K_{ow} value of each buffer strongly reflects their affinity for water molecules. The values of log(K_{ow}) are as follow: CHES: -0.59; MES: -2.48; HEPES: -3.11; TES: -4.48; Tricine: -5.25 *(149)*. Therefore, these values are in close agreement with the trends depicted in Figure 11 and Figure 12. The phase diagrams for the ILs composed of the anions with higher log(K_{ow}) ($[CHES]^-$, $[HEPES]^-$ and $[MES]^-$) are nearest the bimodal. On the other hand, the phase diagrams for the ILs composed of the anions with lower log(K_{ow}) ($[TES]^-$ and $[Tricine]^-$) are those that are more distant from the axes origin.

The presence of –OH groups on the ILs chemical structures also increases their hydrogen bonding capacity with water, which turns more difficult the salting-out process by the citrate-based salt. The phase diagrams of ILs composed $[Tricine]^-$ and $[TES]^-$, which are anions composed of more than one –OH group, are those that are more distant from the axes origin. This means that these systems need more salt for two-phase formation. Then, $[HEPES]^-$, with only one –OH group is followed by $[MES]^-$ and $[CHES]^-$, with no –OH groups. Nevertheless, the presence of –OH groups and the ILs affinity for water is further reflected on the K_{ow} values.

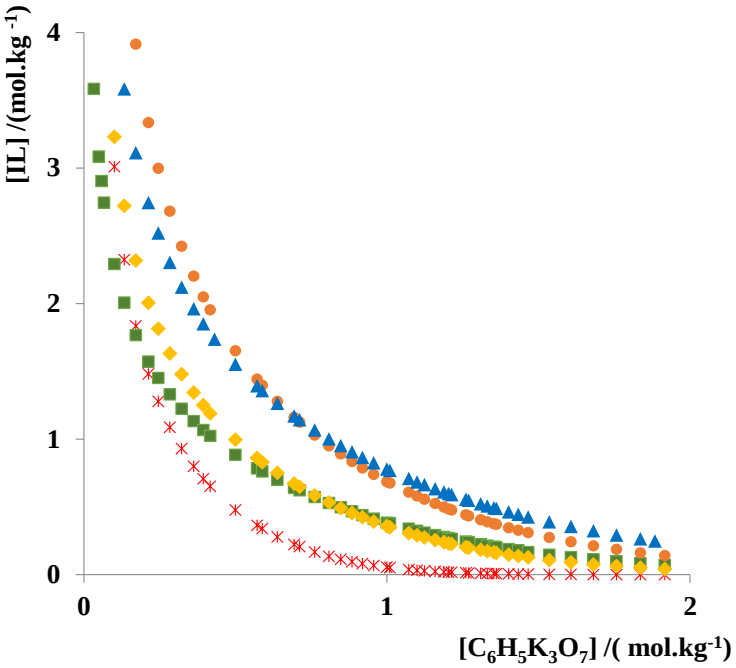

Figure 11 - Ternary phase diagrams for systems composed of IL + $C_6H_5K_3O_7$ + water at (25 ± 1) °C and atmospheric pressure in mol.kg^{-1}: (×) [P_{4444}][CHES], (■) [P_{4444}][HEPES], (♦) [P_{4444}][MES], (●) [P_{4444}][TES] and (▲) [P_{4444}][Tricine].

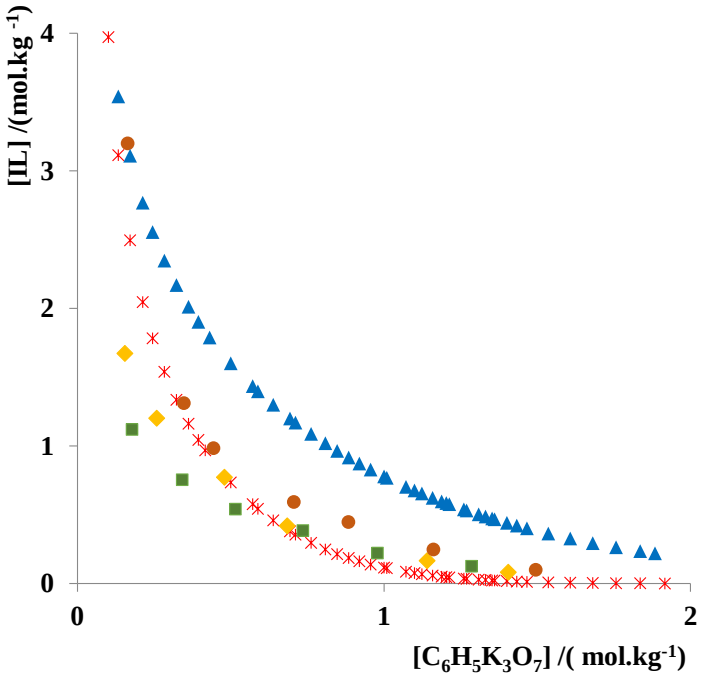

Figure 12 - Ternary phase diagrams for systems composed of IL + $C_6H_5K_3O_7$ + water at (25 ± 1) °C and atmospheric pressure in mol.kg^{-1}: (×) [N_{4444}][CHES], (■) [N_{4444}][HEPES], (♦) [N_{4444}][MES], (●) [N_{4444}][TES] and (▲) [N_{4444}][Tricine].

The effect of the IL cation is presented in Figure 13. Both cations, $[P_{4444}]^+$ and $[N_{4444}]^+$, reveal a high ability to form ABS in presence of $C_6H_5K_3O_7$ aqueous solutions. However, the obtained results are not conclusive regarding the systems composed of $[Tricine]^-$ and $[HEPES]^-$ anions. In these systems, no meaningful differences were observed concerning their capability to form ABS in presence of $C_6H_5K_3O_7$. Although both types of compounds are composed of four alkyl chains with the same size, the $[P_{4444}]^+$ ability to form the two-phase systems is higher than that displayed by $[N_{4444}]^+$, for all the other remaining systems. It suggests that there are some contributions derived from the central atom at the cation core, which influence the ABS formation. Analogous results were reported for ABS composed of more conventional ILs such as: $[P_{4444}]Cl$ and $[N_{4444}]Cl$ combined with Na_2CO_3 and $C_6H_5K_3O_7$ *(146,150)*. In general, due to their highly shielded charges, located mostly on the heteroatom that is surrounded by four alkyl chains and no aromatic character which is responsible for their low affinity for water molecules, both cations are known for their strong ability in ABS formation with salts. The lower the affinity for water and/or hydrophobic nature of the IL, discussed above, more effective is the IL in promoting the phase separation *(146,151)*.

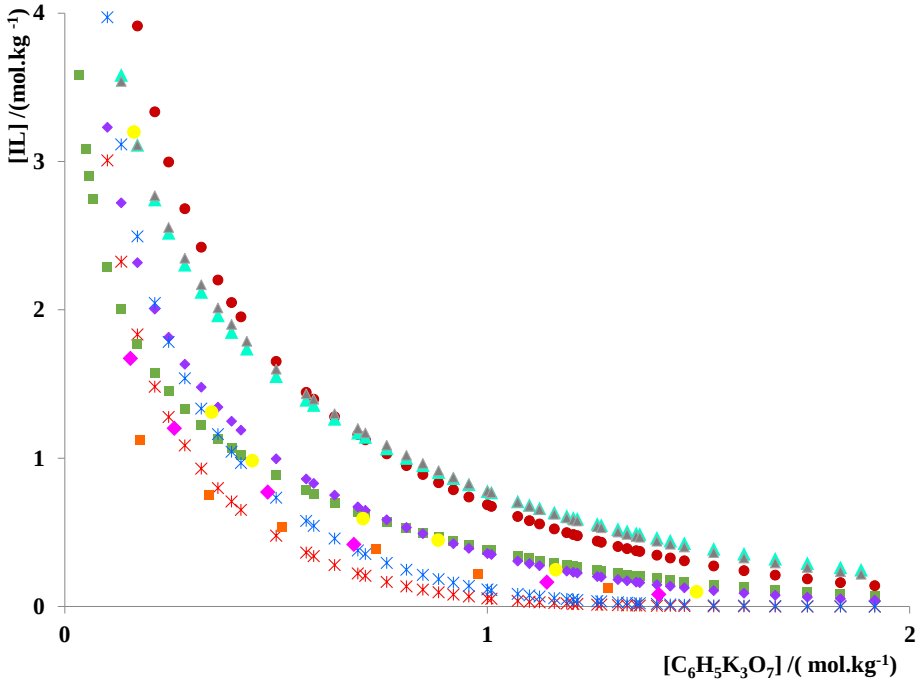

Figure 13 - Evaluation of the cation nature in the ternary phase diagrams composed of IL + $C_6H_5K_3O_7$ + water at (25 ± 1) °C and atmospheric pressure in $mol.kg^{-1}$: (×) $[P_{4444}][CHES]$, (■) $[P_{4444}][HEPES]$, (♦) $[P_{4444}][MES]$, (●) $[P_{4444}][TES]$ and (▲) $[P_{4444}][Tricine]$, (×) $[N_{4444}][CHES]$, (■) $[N_{4444}][HEPES]$, (♦) $[N_{4444}][MES]$, (●) $[N_{4444}][TES]$ and (▲) $[N_{4444}][Tricine]$.

The experimental binodal data for the studied systems were fitted by the empirical relationship described by Equation 1. The regression parameters *A*, *B* and *C*, which were estimated by the least-squares regression method, are provided in Table 3, along with their corresponding standard deviations (σ). Overall, good correlation coefficients were obtained, indicating that these fittings can be used to predict data in a given region of the phase diagram where no experimental results are available.

Table 3 – Correlation parameters used to describe the experimental bimodal data by Equation 1, respective standard deviations (σ) and correlation coefficients (R^2).

GB-IL	$A \pm \sigma$	$B \pm \sigma$	$10^5 (C \pm \sigma)$	R^2
$[P_{4444}][CHES]$	126.0 ± 2.0	- 0.44 ± 0.01	13.78 ± 0.06	0.999
$[P_{4444}][HEPES]$	82.3 ± 0.6	- 0.25 ± 0.01	3.25 ± 0.08	0.999
$[P_{4444}][MES]$	97.6 ± 1.5	- 0.29 ± 0.01	4.34 ± 0.10	0.998
$[P_{4444}][TES]$	109.8 ± 22.5	- 0.23 ± 0.06	2.86 ± 0.44	0.981
$[P_{4444}][Tricine]$	94.8 ±1.9	- 0.22 ± 0.01	1.89 ± 2.95	0.999
$[N_{4444}][CHES]$	120.1 ± 4.7	- 0.36 ± 0.02	1.12 ± 0.47	0.998
$[N_{4444}][HEPES]$	67.3 ± 4.7	- 0.23 ± 0.02	1.85 ± 0.21	0.999
$[N_{4444}][MES]$	80.1 ± 8.3	- 0.25 ± 0.04	2.95 ± 0.50	0.997
$[N_{4444}][TES]$	160.7 ± 16.0	- 0.37 ± 0.03	1.25 ± 0.32	0.996
$[N_{4444}][Tricine]$	90.4 ± 1.6	- 0.21 ± 0.01	2.27 ± 0.01	0.999

The experimental data for the TLs and their respective length (TLL) are reported in Table 4. In Appendix F are reported the TLs for each ABS combined with the respective phase diagrams. In general, the total composition of the system does not usually have a significant effect upon the slope of the TLs *(152)*. This implies that the TLs are generally parallel to each other, as presented in the example shown in Figure 14, allowing the knowledge of the phase compositions for any given system.

Table 4 – Data for the tie-lines (TLs) and respective tie-line lengths (TLL) at (25 ± 1) °C. Initial mixture compositions are represented as $[Salt]_M$ and $[IL]_M$, whereas $[Salt]_{Salt}$ and $[IL]_{Salt}$ represent the composition of IL and salt at the IL-rich phase, respectively, and vice-versa.

Weight fraction composition / wt %							
IL	**$[IL]_{IL}$**	**$[Salt]_{IL}$**	**$[IL]_{M}$**	**$[Salt]_{M}$**	**$[IL]_{Salt}$**	**$[Salt]_{Salt}$**	**TLL**
$[P_{4444}][CHES]$	58.4181	2.9915	21.5658	15.7489	3.7167	21.9278	57.8863
	53.3384	3.7161	21.6769	13.3839	10.9762	16.6513	44.2931
$[P_{4444}][HEPES]$	39.9933	7.8974	20.4424	22.2288	6.4838	32.4838	41.5868
	47.0802	7.8974	19.6265	23.3039	6.4526	32.4838	48.1599
$[P_{4444}][MES]$	45.4549	6.4378	20.0039	22.5176	4.8522	31.7285	48.6869
	41.0494	8.6166	19.8486	21.4342	7.1823	29.0920	39.5755
$[P_{4444}][TES]$	53.3864	9.3191	20.1175	28.7076	7.0057	36.3489	53.6822
	44.6798	13.2572	20.2998	27.9458	7.9131	35.4086	42.9241
$[P_{4444}][Tricine]$	44.8550	10.7267	19.9908	30.0090	6.7839	40.2462	48.1748
	42.6900	11.9573	20.4195	28.0210	13.2939	33.1607	36.2452
$[N_{4444}][CHES]$	68.0848	2.7169	19.9442	24.2430	0.2290	33.4421	72.6707
	64.8733	2.8843	20.4611	20.7988	1.3093	28.5241	68.5404
$[N_{4444}][HEPES]$	62.0163	0.1252	19.8522	29.5671	4.6970	40.1495	69.9103
	40.6380	4.7148	19.7431	24.1009	7.3500	35.5992	45.4085
$[N_{4444}][MES]$	52.7680	2.7461	20.1521	24.8860	4.9861	35.1807	57.7504
	61.8115	1.0649	19.8977	29.7056	1.7287	42.1209	72.7705
$[N_{4444}][TES]$	37.3675	14.7886	18.9075	28.3520	11.7925	33.5797	31.7362
	74.3040	4.3640	20.6716	34.6771	5.0115	43.5282	79.5946
$[N_{4444}][Tricine]$	68.7572	1.7395	30.1636	29.9058	0.9659	51.2148	83.9253
	54.8910	5.6872	28.0005	23.3887	9.3062	35.6949	54.5750

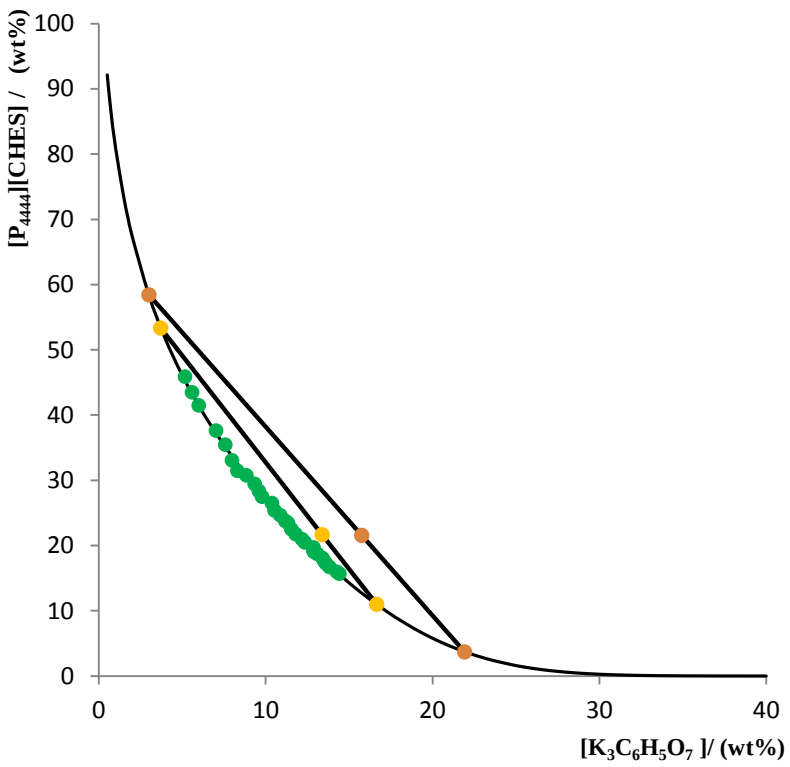

Figure 14 – Phase diagrams for the ternary systems composed of $C_6H_5K_3O_7$ + $[P_{4444}][CHES]$ + water at (25 ± 1) °C and atmospheric pressure: binodal data (●), TL1 data (●), TL2 data (●), adjusted binodal data using Equation 1 (-).

2.3.3. Purification of IgY using GB-ILs + $C_6H_5K_3O_7$ ABS

Initially, the extraction and purification of IgY was tested using a ternary mixture with a selected mixture point composed of 30 wt % of GB-IL and 30 wt % of $C_6H_5K_3O_7$. In Figure 15 it is presented the macroscopic appearance of a ternary mixture with the selected point. It should be highlighted that the organic salt, $C_6H_5K_3O_7$, was chosen to perform the extraction and purification experiments of IgY due to its biodegradable and non-toxic nature *(150)*.

The mixture compositions firstly used were not appropriated for the extraction and purification of IgY since a large amount of precipitated proteins was found - Figure 15. Moreover, in some situations, it was not evident the formation of ABS. The visible turbidity in Figure 15 suggests that some proteins present in the WSPF such as IgY, γ-, α- and β-livetin are being precipitated.

Figure 15 - ABS composed of 30 wt % $[P_{4444}][CHES]$ + 30 wt % $C_6H_5K_3O_7$ + WSPF.

After these experiments, a fixed tie-line length (TLL) of ≈ (40 ± 5) was tested while decreasing the IL composition to 20 wt % in all the experiments, with the exception of the system composed of GB-IL $[N_{4444}][Tricine]$ since at this composition a monophasic systems will be formed. For this IL, the mixture point evaluated was 25 wt % $[P_{4444}][Tricine]$ + 30 wt % $C_6H_5K_3O_7$. The main goal was to reduce the concentrations of the phase-forming components to avoid the protein's precipitation while still assuring the formation of ABS. The implementation of a fixed TLL also allows avoiding differences in the compositions of the coexisting phases amongst the ten IL-based ABS studied. In Figure 16 and Figure 17 it is presented the macroscopic appearance of the ternary mixtures with the compositions described in Table 5. By visual inspection, it was possible to observe a significant amount of precipitated protein in the systems composed of $[P_{4444}][HEPES]$, $[N_{4444}][HEPES]$ and $[N_{4444}][TES]$.

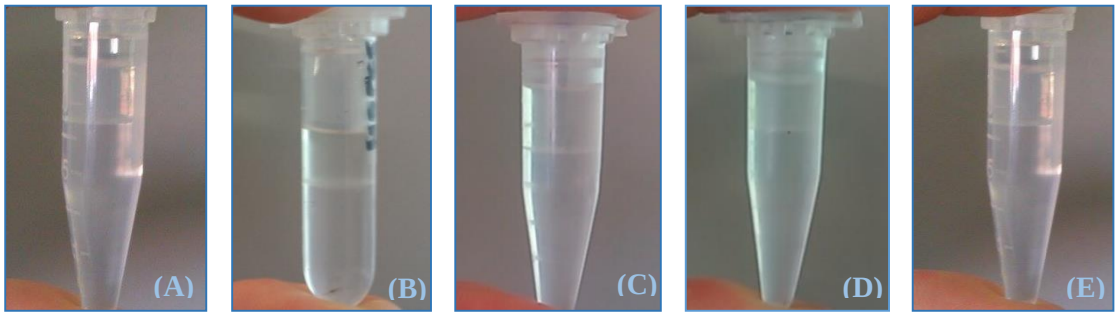

Figure 16 – ABS formed by $[P_{4444}][GB]$ + $C_6H_5K_3O_7$ + WSPF: (A) 21.6 wt % $[P_{4444}][CHES]$ + 13.4 wt % $C_6H_5K_3O_7$, (B) 20.4 wt % $[P_{4444}][HEPES]$ + 22.2 wt % $C_6H_5K_3O_7$, (C) 19.8 wt % $[P_{4444}][MES]$ + 21.4 wt % $C_6H_5K_3O_7$, (D) 20.3 wt % $[P_{4444}][TES]$ + 27.9 wt % $C_6H_5K_3O_7$, (E) 20.0 wt % $[P_{4444}][Tricine]$ + 29.0 wt % $C_6H_5K_3O_7$.

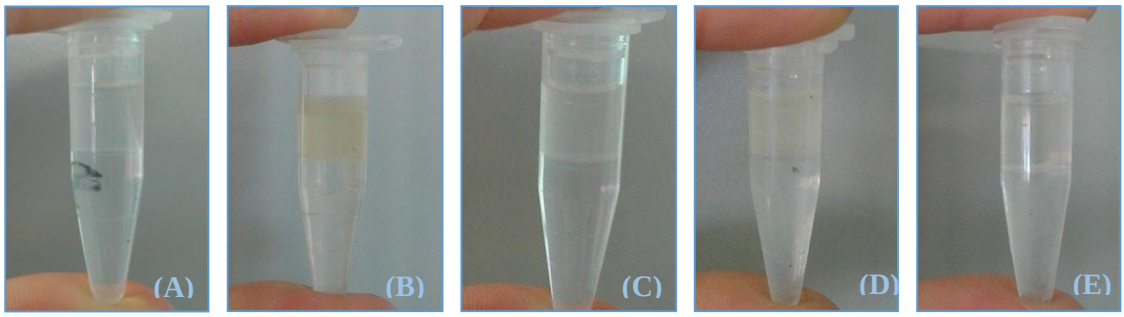

Figure 17 - ABS formed by $[N_{4444}][GB]$ + $C_6H_5K_3O_7$ + WSPF: (A) 20.1 wt % $[N_{4444}][CHES]$ + 16.9 wt % $C_6H_5K_3O_7$, (B) 20.0 wt % $[N_{4444}][HEPES]$ + 22.9 wt % $C_6H_5K_3O_7$, (C) 20.2 wt % $[N_{4444}][MES]$ + 21.9 wt % $C_6H_5K_3O_7$, (D) 20.1 wt % $[N_{4444}][TES]$ + 28.2 wt % $C_6H_5K_3O_7$, (E) 24.8 wt % $[N_{4444}][Tricine]$ + 30.1 wt % $C_6H_5K_3O_7$.

Table 5 – Mixture composition for the ABS composed of GB-ILs and salt for the purification of IgY from the WSPF and respective TLL.

ABS	**[GB-IL] / (wt %)**	**[$C_6H_5K_3O_7$] / (wt %)**	**[WSPF] / (wt %)**	(≈) **TLL**
$[P_{4444}][CHES]$	21.6	13.4	65.0	44.3
$[P_{4444}][HEPES]$	20.4	22.2	57.4	41.6
$[P_{4444}][MES]$	19.8	21.4	58.8	39.6
$[P_{4444}][TES]$	20.3	27.9	51.8	42.9
$[P_{4444}][Tricine]$	20.0	29.0	51.0	41.6
$[N_{4444}][CHES]$	20.1	16.9	63.0	39.1
$[N_{4444}][HEPES]$	20.0	22.9	57.1	42.3
$[N_{4444}][MES]$	20.2	21.9	57.9	40.5
$[N_{4444}][TES]$	20.1	28.2	51.7	43.9
$[N_{4444}][Tricine]$	24.8	30.1	45.1	69.8

In all the studied systems no proteins were detected at the salt-rich phase, which is supported by the results presented in the HPLC chromatograms, as well as in the SDS-PAGE gels, both discussed below. This occurrence can be a direct result of the strong salting-out ability of $C_6H_5K_3O_7$, which leads to the exclusion of all the proteins of the WSPF from the salt-rich phase to the IL-rich phase. Even though the $C_6H_5K_3O_7$ –rich phase is more hydrated, comparatively to the GB-IL-rich phase, proteins revealed a higher affinity for the GB-IL-aqueous phases. As mentioned, the interaction of the proteins with

the IL phase-forming components seems to be quite complex phenomenon and as will be discussed below. Particularly, the partitioning in ABS is a process whereby the exposed groups of the proteins come into contact with the phase components, being therefore a surface-dependent phenomenon *(153)*. It is known that a protein interacts with the surrounding molecules within a phase through different kinds of interactions namely hydrogen-bonding, electrostatic interactions, π···π interactions between the aromatic groups and dispersive-type interactions between the aliphatic groups. The effect of these interactions is expected to be different in the two phases and the proteins will partition preferentially into one phase, being, in that specific case, the IL-rich phase

Good's buffers are zwitterionic amino acids, either *N*-substituted taurine or glycine derivatives, with two protonation sites namely at the carboxylic/sulfonic group (pK_{a1}) and at the amino group (pK_{a2}) *(139)*. These are responsible for their buffering ability near the physiological pH region. All the extractions performed in this work were carried out in a buffered alkaline medium. The pH values of both phases in each ABS are presented in Table 6. The GB-ILs used in the current work were already used as anions in the development of ILs that allowed the control of the pH, hence acting as protein stabilizers, namely BSA *(25)*. Though the GB-IL-based systems studied allowed to maintain the pH values of each phase within 7.8 - 10.9, some precipitation and/or denaturation was observed in some systems, namely in those composed of $[P_{4444}]$[HEPES], $[N_{4444}]$[HEPES] and $[N_{4444}]$[TES].

Table 6 – pH values of the coexisting phases of the ABS composed of GB-ILs + $C_6H_5K_3O_7$.

IL	**pH (IL-rich phase)**	**pH (salt-rich phase)**
$[P_{4444}]$[CHES]	10.8	10.4
$[P_{4444}]$[HEPES]	9.2	9.1
$[P_{4444}]$[MES]	8.0	7.8
$[P_{4444}]$[TES]	8.8	8.4
$[P_{4444}]$[Tricine]	10.2	10.2
$[N_{4444}]$[CHES]	10.9	10.5
$[N_{4444}]$[HEPES]	9.9	9.5
$[N_{4444}]$[MES]	7.9	7.7
$[N_{4444}]$[TES]	9.4	9.2
$[N_{4444}]$[Tricine]	9.9	9.5

The SDS-PAGE of the ten GB-IL-based systems was also carried out to identify the major proteins in the WSPF and to determine the IgY amount in the IL-rich phase, after the extraction. The protein profiles obtained from the WSPF, as well as of the coexisting phases of the ABS composed of $[P_{4444}][GB]$ or $[N_{4444}][GB]$ + $C_6H_5K_3O_7$ + WSPF are presented in Figure 18 and Figure 19, respectively.

The commercial pure IgY, under reducing conditions, presents two major bands at 65 kDa and 25 kDa which correspond to the two heavy chains and the two light chains, respectively. The SDS-PAGE of the salt-rich phase, *i.e.*, the bottom phase samples, did not show any bands. Therefore, there systems seem to be good alternatives for extraction but they do not allow any purification since no selective extractions were attained. In the SDS-PAGE of the IL-rich phases of the systems composed of $[P_{4444}][HEPES]$, $[P_{4444}][Tricine]$, $[N_{4444}][HEPES]$ and $[N_{4444}][TES]$, in addition to the β–livetin fraction, only a band around 65 kDa is detectable. It should be noted that, by a visual inspection of the ABS, three of the stated systems shown a significant amount of precipitated protein, namely those composed of $[P_{4444}][HEPES]$, $[N_{4444}][HEPES]$ and $[N_{4444}][TES]$. However, as the visible precipitate may correspond to other contaminant proteins rather than the IgY, the SDS-PAGE of both phases of these systems was also carried out. The SDS-PAGE analysis of the precipitate was further attempted. However, due to problems regarding the precipitate solubilization this step was not successfully accomplished.

The light chain band of IgY allows a better and unambiguous evaluation of the presence of IgY, due to the fact that the heavy chain band can induce some error since it has a similar molecular weight to the other unidentified contaminant proteins present in the WSPF, which also appear around 65 kDa. Taking this phenomenon into account, the light chain band was used to determine the amount of IgY at the IL-rich phase through the establishment of a previous calibration curve. The quantification results are presented in Table 7. The gels used for the IgY quantification and the respective calibration curve are reported in Appendix C, in Figure C. 1 and Figure C. 2, respectively. Overall, the ABS composed of the $[N_{4444}][GB]$ ILs provided the best results, providing extraction yields in the range of 31.18 to 37.18 %. Among those, the ABS that allowed the extraction of a higher amount of IgY (7.38 g/L), also combined with the best yield (37.18 %), was the ABS featuring the $[CHES]^-$ anion. As demonstrated above, among all the $[N_{4444}][GB]$ ILs studied, the IL $[N_{4444}][CHES]$ is the most hydrophobic. This inherent hydrophobicity rises the opportunity for dispersive-type interactions of the proteins present in the water

soluble fraction with these more hydrophobic ILs. For the ABS composed of $[P_{4444}][HEPES]$, $[P_{4444}][Tricine]$, $[N_{4444}][HEPES]$ and $[N_{4444}][TES]$ the quantification was not accomplished. The SDS-PAGE gels of the stated ABS did not show any band corresponding to the IgY light chain band, as depict in Figure 18 and Figure 19. This is thought to be the result of IgY precipitation.

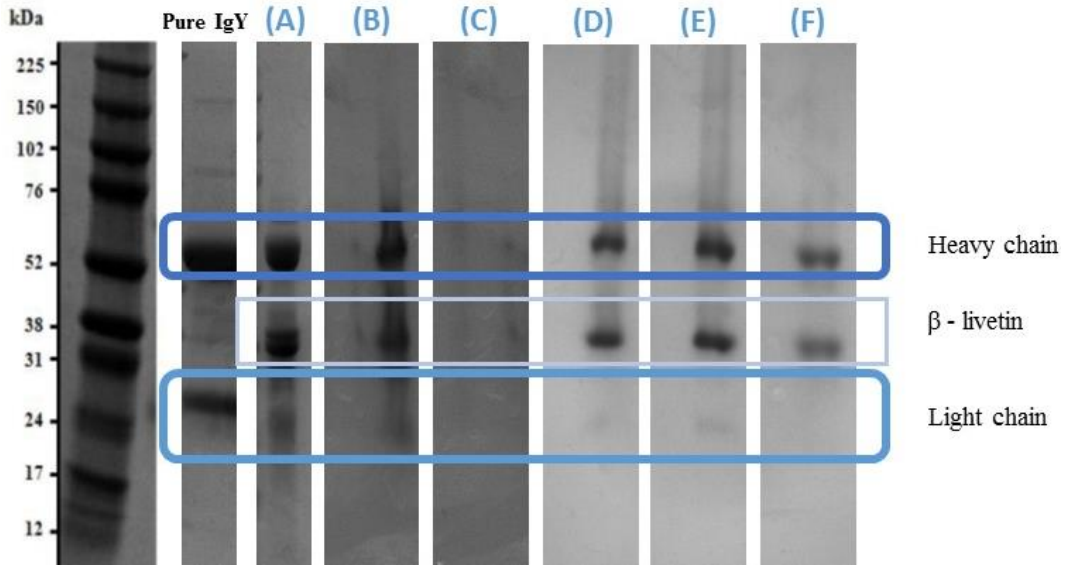

Figure 18 - SDS-PAGE of a gel loaded with samples of bottom and top phases from systems composed of $[P_{4444}][GB]$ + $C_6H_5K_3O_7$ stained with Coomassie blue:

Lane 1 (Std): Standard molecular weights.

Lane 2 (Pure IgY): Pure IgY, purified using the commercial kit EggsPure IgY.

Lane 3 (A): WSPF.

Lane 4 (B): Bottom and top phases, respectively, of the ABS composed of 21.6 wt % $[P_{4444}][CHES]$ 13.4 wt % $C_6H_5K_3O_7$.

Lane 5 (C): Bottom and top phases, respectively, of the ABS composed of 20.4 wt % $[P_{4444}][HEPES]$ + 22.2 wt % $C_6H_5K_3O_7$.

Lane 6 (D): Bottom and top phases, respectively, of the ABS composed of 19.8 wt % $[P_{4444}][MES]$ + 21.4 wt % $C_6H_5K_3O_7$.

Lane 7 (E): Bottom and top phases, respectively, of the ABS composed of 20.3 wt % $[P_{4444}][TES]$ + 27.9 wt % $C_6H_5K_3O_7$.

Lane 8 (F): Bottom and top phases, respectively, of the ABS composed of 20.0 wt % $[P_{4444}][Tricine]$ + 29.0 wt % $C_6H_5K_3O_7$.

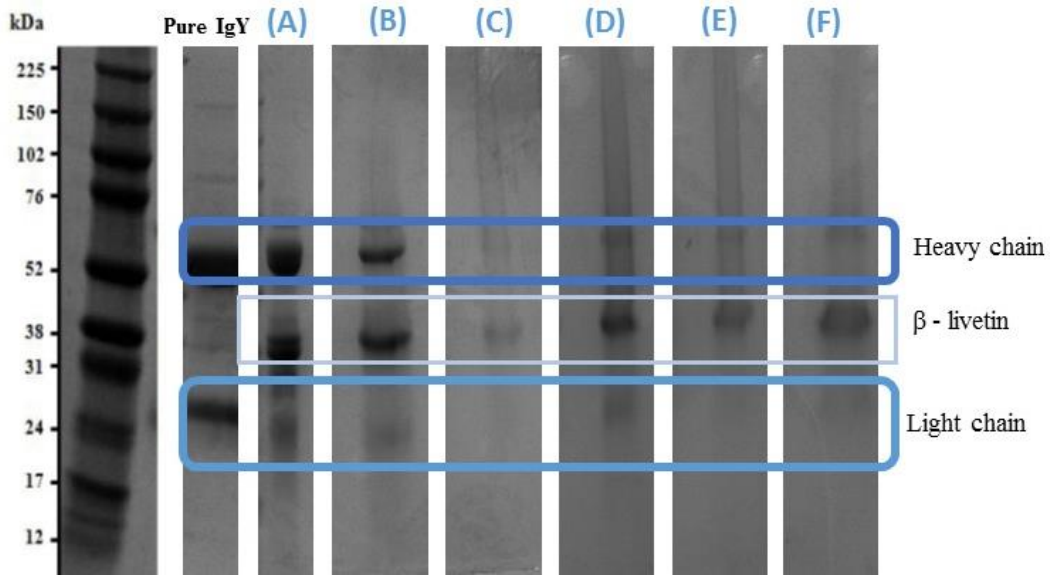

Figure 19 – SDS-PAGE of a gel loaded with samples of bottom and top phases from systems composed of $[N_{4444}][GB]$ + $C_6H_5K_3O_7$ stained with Coomassie blue:

Lane 1 (Std): Standard molecular weights.

Lane 2 (Pure IgY): Pure IgY, purified using the commercial kit EggsPure IgY.

Lane 3 (A): WSPF.

Lane 4 (B): Bottom and top phases, respectively, of the ABS composed of 20.1 wt % $[N_{4444}][CHES]$ + 16.9 wt % $C_6H_5K_3O_7$.

Lane 5 (C): Bottom and top phases, respectively, of the ABS composed of 20.0 wt % $[N_{4444}][HEPES]$ + 22.9 wt % $C_6H_5K_3O_7$.

Lane 6 (D): Bottom and top phases, respectively, of the ABS composed of 20.2 wt % $[N_{4444}][MES]$ + 21.9 wt % $C_6H_5K_3O_7$.

Lane 7 (E): Bottom and top phases, respectively, of the ABS composed of 20.1 wt % $[N_{4444}][TES]$ + 28.2 wt % $C_6H_5K_3O_7$.

Lane 8 (F): Bottom and top phases, respectively, of the ABS composed of 24.8 wt % $[N_{4444}][Tricine]$ + 30.1 wt % $C_6H_5K_3O_7$.

Table 7 – Concentration and recovery yield of IgY in the IL-rich phase.

GB-IL	[IgY] / (g/L)	Yield (%)
$[P_{4444}][CHES]$	4.45	12.44
$[P_{4444}][MES]$	0.14	13.71
$[P_{4444}][TES]$	0.19	16.10
$[N_{4444}][CHES]$	7.38	37.18
$[N_{4444}][MES]$	4.46	31.18
$[N_{4444}][Tricine]$	2.84	31.35

The results obtained by HPLC were similar in all the studied systems. Figure 20 depicts the HPLC chromatograms of the top and bottom phases of the ABS composed of $[N_{4444}][Tricine]$ + $C_6H_5K_3O_7$ + WSPF. The chromatograms corresponding to all the extractions carried out in this work are presented in Appendix G in Table G. 1 and Table G. 2, for the $[P_{4444}][GB]$ ILs and $[N_{4444}][GB]$ ILs, respectively. The HPLC allowed the separation of some proteins which are originally present in the WSPF: IgY, with 15 min of retention time, and other non-identified contaminant proteins (≈17-18 min). As mentioned, no proteins were found in the chromatograms corresponding to the bottom phases, agreeing with the results discussed before and attained by SDS-PAGE. Regarding the top phase samples, it was expected the presence of a peak at 15 min of retention time, corresponding to IgY. Instead, it was detected a new peak, at a lower retention time (≈12 min), which is thought to be an IL-protein complex resulting from the high interaction of each IL with IgY. The peaks after 20 min belong mostly to the IL and salt present in the system, as confirmed by the HPLC chromatograms of the IL-based ABS for which no IgY or WSPF was added.

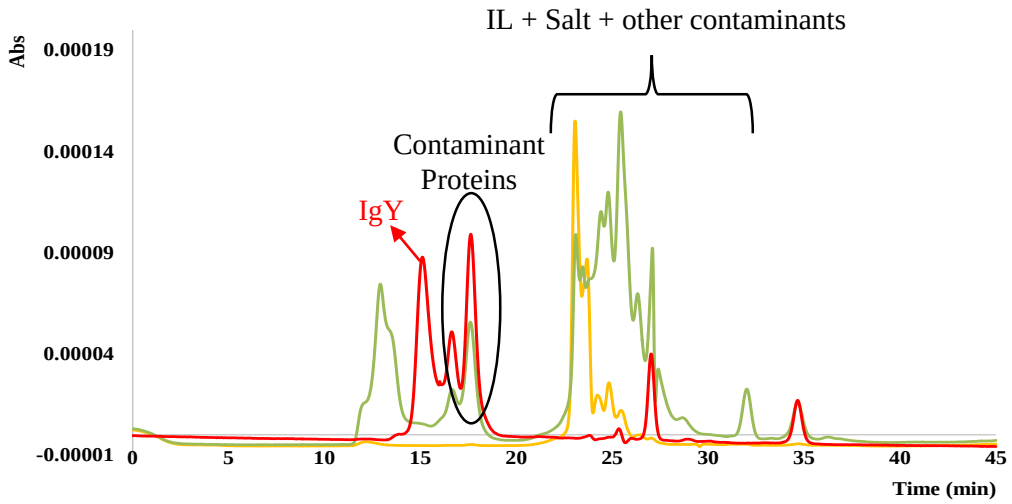

Figure 20 – SE-HPLC chromatogram of a system composed of 24.8 wt % $[N_{4444}][Tricine]$ + 30.1 wt % $C_6H_5K_3O_7$ + 45.1 wt % WSPF: bottom phase (–), top phase (–) and initial WSPF (–).

Aiming the confirmation of the phenomenon that occurs between the IgY and the ILs, an additional SE-HPLC study was performed using mixtures composed of pure IgY + GB-ILs or salt. In Figure 21 and Figure 22 are presented the chromatograms corresponding to the pure IgY sample, as well as the chromatograms of mixtures composed of pure IgY plus 40.0 wt % $[N_{4444}][CHES]$ and 8.1 wt % $C_6H_5K_3O_7$. By the inspection of these chromatograms it is possible to conclude that the IL interferes with the IgY in aqueous solution, while the salt has no significant effect under its retention time. Similar results were obtained for all GB-ILs. Several studies were then developed in order to understand this particular type of interaction. In addition, some techniques were further tested aiming the recovery of the proteins from the WSPF of egg yolk, from the IL-rich phase. These studies are reported and discussed in Chapter 3.

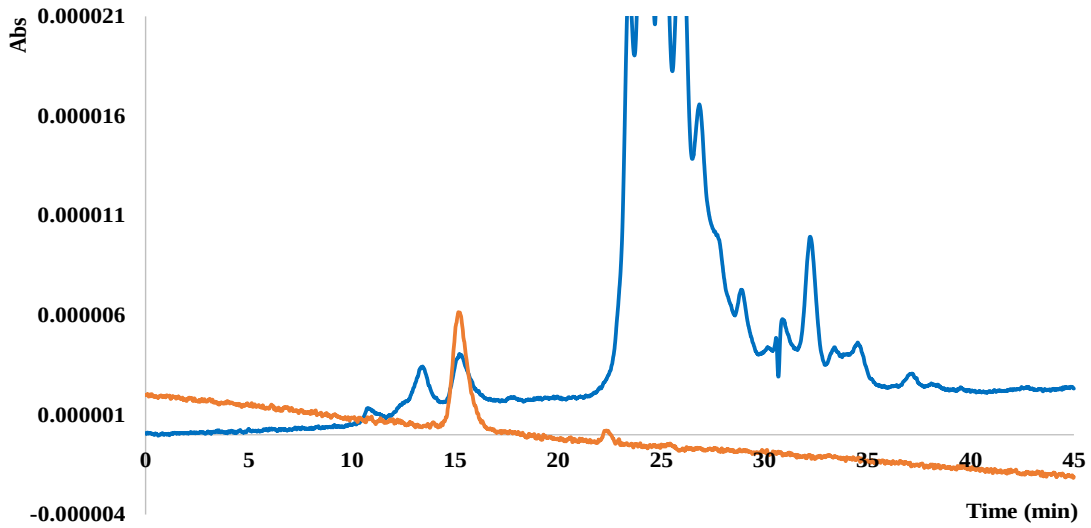

Figure 21 - SE-HPLC chromatogram of the pure IgY solution (–) and of a mixture composed of $[N_{4444}][CHES]$ + pure IgY (–)

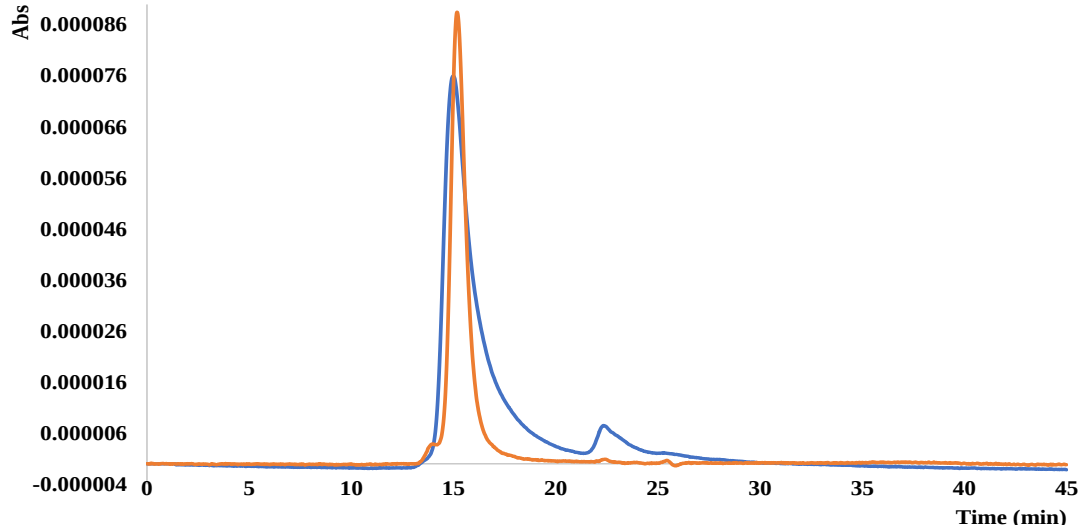

Figure 22 - SE-HPLC chromatogram of the pure IgY solution (–) and of a mixture composed of $C_6H_5K_3O_7$ + pure IgY(–)

A molecular docking study was then performed in order to further investigate the binding sites of the ILs $[P_{4444}][GB]$ and $[N_{4444}][GB]$ ions with IgY, aiming to obtain more information regarding the affinity and stability of IgY in the IL-rich aqueous phases. Molecular docking is a computational procedure that allows to predict noncovalent binding of macromolecules, such as proteins, with the aim of predicting the bond conformations and the binding affinity *(144)*. The crystal structure of the fragment crystallisable region of IgY *i.e.*, the Fc region or tail, was used to identify the hydrogen-bonding interaction and binding sites between the IL ions and the protein. The interaction

sites of IgY with the $[P_{4444}]^+$ and $[N_{4444}]^+$ cations were identified and the hydrogen-bonding results are displayed in Figure 23 *(144)*. Binding free energies of -4.0 kcal mol^{-1} were obtained for both cations. The residues found next to the $[P_{4444}]^+$ cation are Arg485, Glu551, Asn449, Trp423,Ser445, Pro484, Pro359, Arg448, Tyr447, Asp486, Pro356, Thr450, and Val446 (Figure 24 (B)), and those found nearby $[N_{4444}]^+$ are: Arg485, Pro484, Pro357, Val446, Thr450, Arg448, Pro359, Glu551, Pro356, Ser445, Asn449, Asp486, Leu362, Trp423, Tyr447, and Gly451) (Figure 24 (C)). The similarities obtained from these results suggest that both IL cations establish similar interaction with IgY – an expected result since both cations are similar with a central atom and four butyl chains. Taha et. al *(139)* already studied the interaction of IgY with some of the anions used in the current work namely $[MES]^-$, $[TES]^-$, $[Tricine]^-$ and $[HEPES]^-$. They have found that the binding free energies of the anions $[MES]^-$, $[TES]^-$, $[Tricine]^-$ and $[HEPES]^-$ with IgY are -4.1, -4.4, 4.4 and -4.1 kcal mol^{-1}, respectively. The residues located next to $[MES]^-$, $[TES]^-$ and $[Tricine]^-$ are Gln563, Gln565, Thr561, His464, Pro460 and Ala462. On the other hand, $[HEPES]^-$ is located next to Asn449, Tyr447 and Arg485. The molecular docking results of the IL anions are displayed in Figure 24. Through these results it is demonstrated that the partitioning of IgY is dominated by hydrogen-bonding and van der Waals interactions *(139)*. However, the GB anions $[Tricine]^-$, $[TES]^-$, $[MES]^-$, and $[HEPES]^-$, respectively form 9, 5, 5 and 4 hydrogen bonds with Gln565 and Gln563, while no information is available for $[CHES]^-$, which was the anion that promoted the best extraction results (lower losses of IgY) with both cations.

The ABS composed of the ILs with the anion $[HEPES]^-$, which is the one that is located near to the different residues of IgY and it is the anion that forms the lowest number of hydrogen bonds, did not allow the IgY extraction, when combined with any of the cations. The computational results regarding the other anions, namely $[Tricine]^-$, $[TES]^-$ and $[MES]^-$, which interact with the IgY molecule in the same residues, did not allow a full understanding of the partitioning behaviour. Different cations, combined with the same anions, promoted different results. It is important to highlight that the top phase of the system also has a small amount of $C_6H_5K_3O_7$ in its composition, which is a salt with a strong salting-out capacity, and therefore also strongly influences the partitioning behaviour of IgY. In summary, the partitioning phenomenon of IgY in the studied ABS is not fully understood. Though, it is possible to assure that the ILs used in the ABS composition are not suitable for IgY extraction.

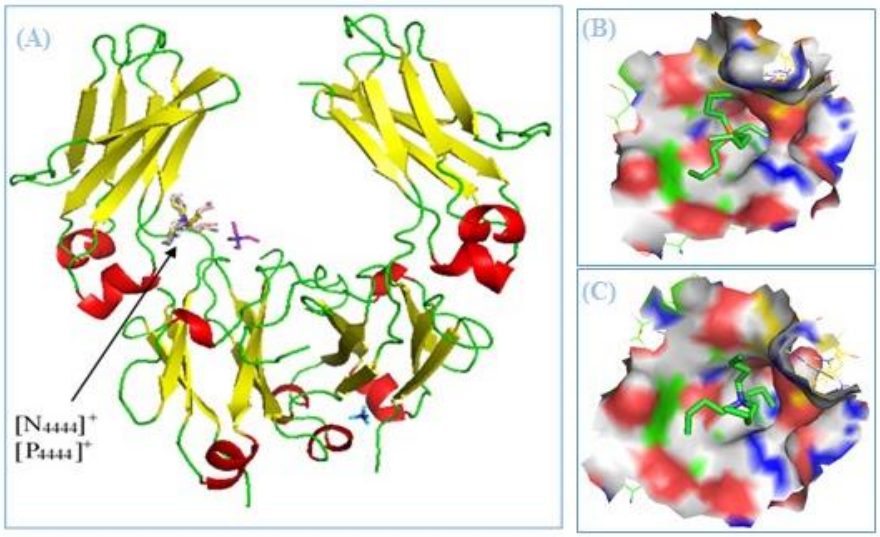

Figure 23 – Molecular docking of IgY with IL cations (A): (B) $[P_{4444}]^+$, (C) $[N_{4444}]^+$.

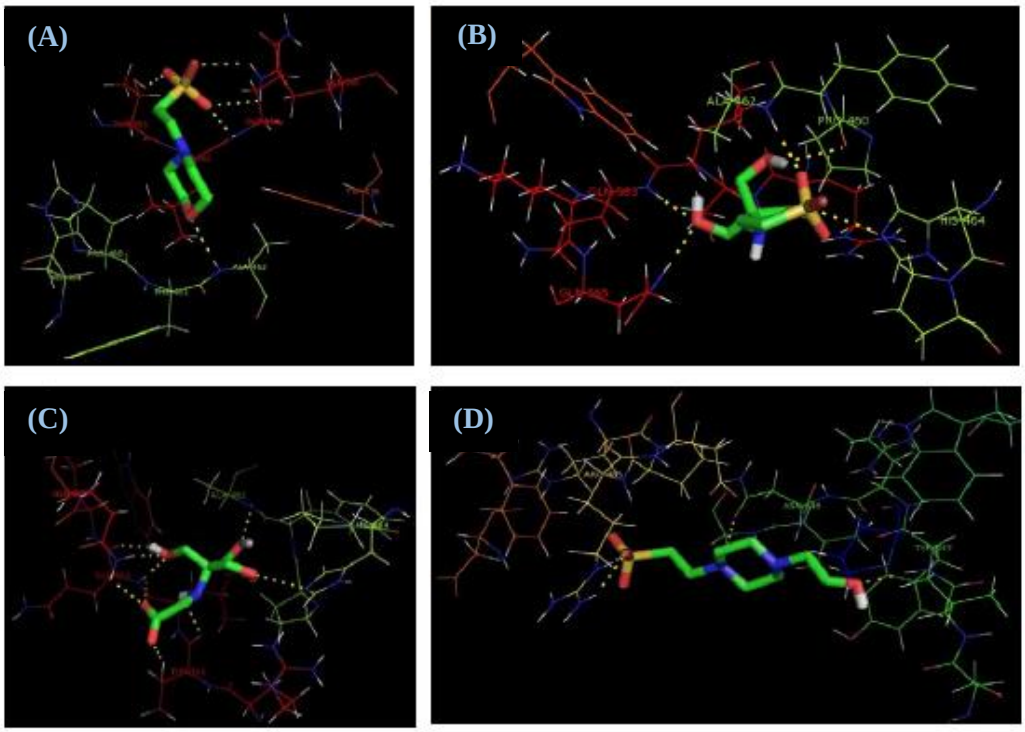

Figure 24 - Molecular docking of IgY-Fc with the IL anions; (A) $[MES]^-$, (A) $[TES]^-$, (C) $[Tricine]^-$, (D) $[HEPES]^-$ *(139).*

An additional study was performed in order to evaluate the proteins structure in the WSPF and further extraction by FT-IR (Fourier transform-infrared spectroscopy). The FT-IR spectra are selective in what concerns the absorption band frequency positions, widths and intensities in response to proteins structural changes, providing thus

information for identifying the structure of proteins based on energy absorption bands of specific functional groups or chemical bonds *(154–156)*. The most distinct FT-IR bands for proteins are the amide I bonds signature, ranging from 1700 to 1600 cm^{-1} and thus, in this work, the FT-IR spectra were obtained in that wavelength range *(154,157)*. The primary components of the amide I band are mainly generated by C=O stretching vibrations, the band is influenced by hydrogen-bonding, and thus, information about conformational changes are provided *(157,158)*. The secondary structure elements were resolved using a second-derivative procedure *(158,159)*. To reveal differences in the proportions of the secondary structure of proteins the total area of all peaks from each spectrum was defined to be 100 % and the individual peak areas were expressed as proportions (%) of the corresponding secondary structure elements. Table 8 presents the assignment of the principal amide I frequencies to the protein secondary structure as previously described in the literature *(156)*.

Table 8 – Frequencies (cm^{-1}) and assignments of IR bands of Amide I component frequencies to Protein Secondary Structure in H_2O (According to second derivatives) *(156)*.

Wavenumber (cm^{-1})	**Assignment**
1680-1696	β–turn
1655-1675	
1650-1657	α–helix
1640-1651	Random coil
1626-1640	Parallel β-sheet
1612-1642	Antiparallel β–sheet
1670-1690	(weak)

In Table 9 and Table 10 are presented the proportions of each secondary structure elements for the samples of the initial WSPF and the coexisting phases of the systems composed of $[P_{4444}][GB] + C_6H_5K_3O_7$ + WSPF and $[N_{4444}][GB] + C_6H_5K_3O_7$ + WSPF, respectively. In all the studied samples, it is possible to notice major alterations regarding the proportions (%) of the secondary structure elements after the extraction, which suggests alterations in the proteins secondary structure or protein aggregation. In general, it is observed an increase in the random coil and α–helix proportions, when comparing the top phase of the ABS samples with the initial WSPF. As is known, the secondary

structure of a peptide defines the spatial orientation of its backbone and the presence of specific hydrogen bonds *(156)*. Thus, the systems composed of $[P_{4444}]$[CHES] and $[N_{4444}]$[CHES], corresponding to the more hydrophobic IL-rich phases, contribute to a better maintenance of the protein secondary structure, while reducing the hydrogen bonds between the proteins and the IL. In contrast, systems composed of more hydrophilic GB-ILs, such as $[P_{4444}]$[Tricine] and $[N_{4444}]$[Tricine] revealed more significant changes regarding the proteins secondary structure. Their hydrophilicity will increase their hydrogen-bonding with the H_2O molecules in solution, which will dehydrate the WSPF proteins, leading to their denaturation. These results are in close agreement with the literature data since it was found that proteins, such as enzymes, are more stable in more hydrophobic ILs than in more hydrophilic ILs *(160)*. Also, these results agree with the ones discussed before regarding the protein precipitation and with the ones attained by SDS-PAGE. The ABS featuring the most hydrophobic ILs ($[P_{4444}]$[CHES] and $[N_{4444}]$[CHES]) were the ones that allowed the best extraction results, promoting less IgY losses by precipitation.

Concerning the β–turn, it is possible to observe an increase in its proportions in systems composed of more hydrophilic GB-ILs. Even though many factors remain unanswered about what factors determine the β–turn formation, it is known that this secondary structure element is prevalent in globular proteins, and may also be possible sites for nucleation in protein folding *(161)*. Its increase in the most hydrophilic systems may be a result of a higher protein folding, due to a decrease in proteins solubilisation. On the other hand, α–helix is a favoured structure in nonpolar solvents. Nevertheless, its proportions does not differ greatly between the different studied ABS. There is however, a major increase in the α–helix proportions between the WSPF and the ABS top phase samples. This is probably due to the fact that, in the WSPF, the proteins are in a more hydrated medium when compared with the IL-rich phase of the systems. In proteins or protein complexes, β–sheet are stabilized by hydrogen bonds between protein chains, oriented either in a parallel or in an antiparallel fashion *(156)*. Once again, as expected, there narrowest differences in this element proportions are seen in the systems composed of more hydrophobic GB-ILs. In the ABS composed of more hydrophobic ILs, the hydrogen bond is not favoured. Instead, more hydrophilic systems present, in general, a major reduction the β–sheet proportions.

Table 9 – Proportions (%) of the secondary structure elements of the WSPF and from the top phase of the ABS composed of $[P_{4444}][GB] + C_6H_5K_3O_7$ + WSPF.

	Amide I components (%)					
	WSPF	**$[P_{4444}][CHES]$**	**$[P_{4444}][HEPES]$**	**$[P_{4444}][MES]$**	**$[P_{4444}][TES]$**	**$[P_{4444}][Tricine]$**
β-turn	28.27	29.46	20.36	33.99	26.02	36.59
α-helix	7.00	12.74	13.26	13.55	11.85	14.16
Random coil	17.38	38.82	40.25	27.43	22.17	40.69
Parallel β-sheet	27.98	27.30	26.16	31.91	34.82	29.73
Antiparallel β-sheet	43.63	43.34	41.92	38.23	46.50	32.77

Table 10 - Proportions (%) of the secondary structure elements of the WSPF and from the top phase of the ABS composed of $[N_{4444}][GB] + C_6H_5K_3O_7$ + WSPF.

	Amide I components (%)					
	WSPF	**$[N_{4444}][CHES]$**	**$[N_{4444}][HEPES]$**	**$[N_{4444}][MES]$**	**$[N_{4444}][TES]$**	**$[N_{4444}][Tricine]$**
β-turn	28.27	28.54	30.41	27.76	34.24	39.63
α-helix	7.00	10.26	13.26	13.18	13.19	12.82
Random coil	17.38	31.91	40.25	40.96	39.07	25.08
Parallel β-sheet	27.98	20.40	20.62	22.10	18.47	22.99
Antiparallel β-sheet	43.63	45.70	41.92	44.77	36.89	24.57

In Figure 25 and Figure 26 are depicted the FT-IR experimental data spectrum, plus the spectrum after deconvolution of the top phase belonging to the ABS composed of $[N_{4444}][CHES] + C_6H_5K_3O_7$ + WSPF, and the second derivative FT-IR spectrum of the same sample, respectively. Regarding the peaks shifts and the secondary structure elements proportions, presented and discussed above, no significant variations are seen in the β – turn wavelength range, between the WSPF and the top phase samples. However, after the extraction, perturbations in the secondary structure occurred, resulting in changes in the α–helix proportion changes and in a peak dislocation. The WSPF sample exhibited an amide I band maximum at 1650 cm^{-1}, while the sample from the top phase of the ABS showed an absorbance maximum at 1656 cm^{-1}. Regarding the other secondary structure elements, no major changes were observed.

In the Appendix H are depicted all the spectra obtained for the ABS composed of $[P_{4444}][GB]$ and $[N_{4444}][GB]$, in Figure H. 1 and Figure H. 2, respectively. In Table H. 1 and Table H. 2 it is presented an overall comparison of the second derivative peak values

obtained in this work, together with the data found in the literature *(157,158,162)*. Since no consistency was found between different authors *(155–159,162)*, we selected three papers taking into account the similarity in the experimental conditions *(157,158,162)*. Generally, major alterations were seen regarding the α–helix wavenumber range in all systems. The ABS top phases featuring $[P_{4444}]$[HEPES] and $[N_{4444}]$[HEPES] in their composition revealed major changes in the β–turn and β–sheet peaks shifts. These significant alterations, in terms of the secondary structure peak shifts, indicate significant changes regarding the WSPF proteins stability after the extraction. The results obtained for these two systems are in close agreement with the SDS-PAGE electrophoresis results, since no quantification was accomplished, which may be due to the significant changes regarding the proteins secondary structure.

The obtained results corroborate the possible formation of protein aggregates after being extracted into the IL-rich phase. However, the systems composed of $[P_{4444}]$[CHES] and $[N_{4444}]$[CHES], which have more hydrophobic IL-rich phases, reveal to contribute to a better maintenance of the protein secondary structures. These results are in close agreement with the literature data, where proteins are more stable in more hydrophobic ILs than in hydrophilic ones *(163,164)*. Still, no conclusive and insightful differences were observed between the systems that provided the best extraction results when compared with others, which did not allow the IgY extraction. It is important to bring up that there are some complications which indicate that there is no simple correlation between the IR spectra and the secondary structural components *(158)*. Some minor structures can interfere with the band assignments indicated above, such as the β–turn band at approximately 1665 cm^{-1} is near the characteristic IR band representing the 3_{10}-helices, vibrations of some amino acid side chains might make small contributions to the intensity of characteristic protein amide bands and, in addition, the experimental procedure might also bring some errors.

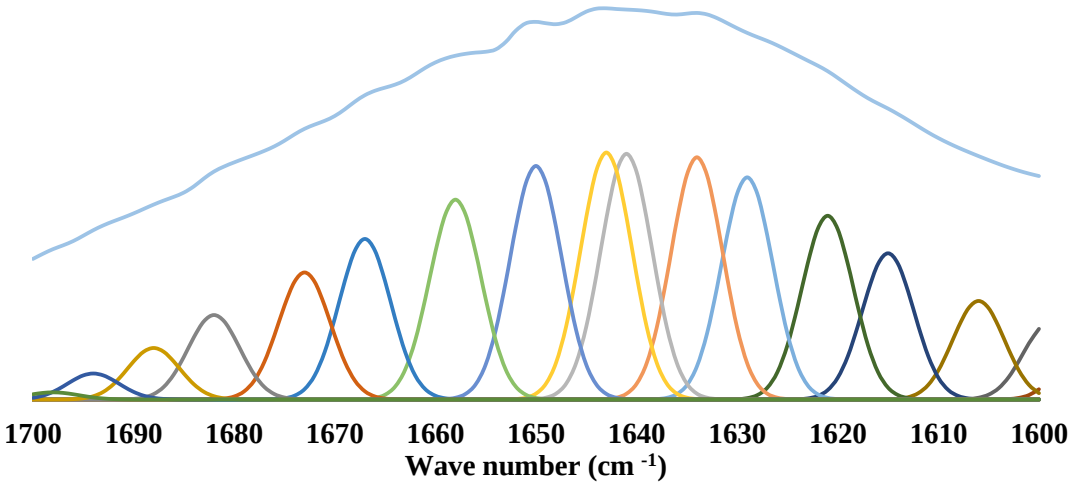

Figure 25 - FT-IR experimental data spectra of a top phase sample of an ABS composed of 20.1 wt % [N_{4444}][CHES] + 16.9 wt % $C_6H_5K_3O_7$ + 63.0 wt % WSPF (−) and the resultant deconvolution spectra (∧∧ / \/ \/ \ ).

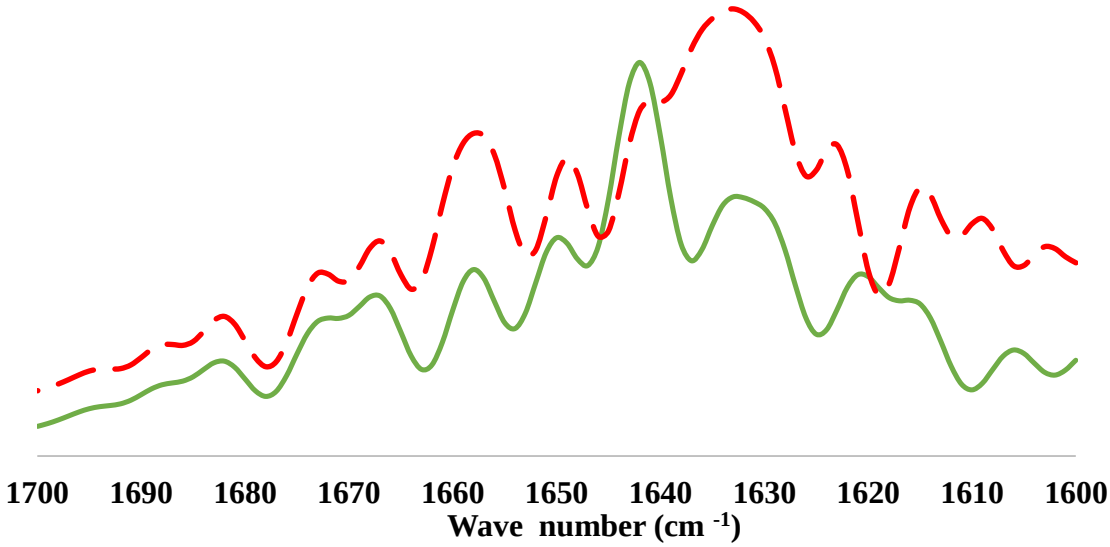

Figure 26 – FT-IR spectra of a top phase sample of an ABS composed of 20.1 wt % [N_{4444}][CHES] + 16.9 wt % $C_6K_3H_5O_7$ + 63.0 wt % WSPF (−) and WSPF (- · -).

2.4 – Conclusions

In this work it was evaluated the capacity of GB-IL-based ABS, combined with the biodegradable salt $C_6H_5K_3O_7$, for the extraction and purification of antibodies from the WSPF of egg yolk. In this chapter, the synthesis and characterization of the GB-ILs was described, together with the determination of the phase diagrams for each ABS, and the

respective TLs and TLLs. The diversity of GB-ILs investigated allowed to study the influence of the IL cation and anion on the ABS formation. Overall, an increase in the hydrophobicity of the IL promotes the ABS formation, following the same behaviour of other more conventional ILs and salts ABS. According to the results obtained, the ability of the studied systems to form ABS follows the trend: $[P_{4444}][CHES] > [P_{4444}][MES] \approx [P_{4444}][HEPES] > [P_{4444}][TES] \approx [P_{4444}][Tricine]$, for the phosphonium-based ILs and $[N_{4444}][CHES] > [N_{4444}][MES] \approx [N_{4444}][HEPES] > [N_{4444}][TES] \approx [N_{4444}][Tricine]$, for ammonium-based ILs.

The extraction and purification of the IgY with the investigated systems was not successfully achieved. Despite the already proved efficiency of GB-ILs in the separation and extraction of proteins, which are sensitive to the pH of the medium, the studied ABS probably induced the formation of an IL-IgY complex or induced the precipitation of the proteins of the WSPF of egg yolk, as a result of the diverse type of interactions of the proteins of the water soluble fraction of egg yolk with cations of long alkyl side chains. This fact made it impossible to perform an efficient extraction and purification of IgY from the other proteins from the WSPF. However, the ABS composed of 20.1 wt % $[N_{4444}][CHES]$ + 16.9 wt % $C_6H_5K_3O_7$ provided the best results, being the most promising amongst the ten studied ABS. Regarding the IgY quantification, obtained through the analysis of the intensity of the bands from the SDS-PAGE stained gels, this system allowed the extraction of 7.38 g/L of IgY and a recovery yield of 37.18 %, which represents the best yield value among all the studied ABS. When compared with the other systems, this ABS also provided a greater protein stability as confirmed by the study of the secondary structure elements proportion analysis and the second derivative FT-IR spectrum peaks.

3. Recovery of the proteins in the IL-rich phase for further analysis

3.1 - Introduction

Taking into account the possible precipitation of IgY, when using the investigated ABS, and as evidenced by the vanishing of the IgY peak from the HPLC chromatograms, after a careful phases separation, some techniques were applied in order to recover the proteins from the IL-rich phase of the ABS.

Protein precipitation is commonly accomplished by altering the solvent conditions and taking advantage of the changes in solubility of the protein of interest relative to those of many of the other components in solution *(165)*. Different protein precipitation techniques (by the addition of organic solvents, acids and salts) act through different modes *(166)*. In general, the proteins three-dimensional structure is maintained through some interactions such as hydrogen bonds, hydrophobic and ionic interactions *(160)*. Protein's solubility is the result of polar interactions with the aqueous solvent, ionic interactions with the salts and repulsive electrostatic forces between like charged molecules *(166,167)*. Taking this into account, a small change in the microenvironment of proteins can disrupt these interactions, causing their denaturation which leads to protein unfolding and inactivation *(160)*.

As referred, precipitants exert specific effects on proteins *(166)*. Organic solvent precipitants, such as acetone, methanol and ethanol, lower the dielectric constant of a protein solution, increasing the attraction between charged molecules which facilitates electrostatic protein interactions *(166,167)*. Additionally, through their polar groups, these solvents interact with polar groups on the proteins, in competition with water *(167)*. Thus, the hydrophobic interactions between proteins are minimized and electrostatic interactions become predominant, leading to protein aggregation *(166,168)*. Acidic reagents form insoluble salts with the positively charged amino groups of the protein molecules at pH values below their p*I*. Proteins are precipitated as the salt ions become hydrated and the available water molecules decrease, drawing the water away from the protein hydrophobic surface regions which results in aggregation of protein molecules via protein-protein hydrophobic interactions *(166)*.

Dialysis and ultrafiltration exploit equivalent separation mechanisms, since both techniques employ a semipermeable barrier or membrane to separate the sample containing the desire solute, from a sample-free solution *(168)*. Dialysis, which is the most popular method employed for removal of low-molecular-weight solutes from large protein molecules, is a size-based separation of molecules by selective diffusion through

a semipermeable membrane *(168)*. This technique has the advantage of allowing the buffer exchange under benign or physiological conditions with minimum risk of impacting the target protein. The dialysis membrane usually possesses a specific pore size (molecular weight cut-off) which permits the free passage of molecules smaller than this in both directions. On the other hand, ultrafiltration is a pressure driving membrane-based process *(169)*. Ultrafiltration membranes can operate at a wide temperature range, from 2 to 26 ºC, which are mechanically stronger than those used in dialysis, since ultrafiltration works by conventional mass transfer driven by pressure differences applied across the membrane *(168)*.

In this work, two different protein precipitation techniques, acetone and trichloroacetic acid (TCA) precipitation, plus ultrafiltration and dialysis, were tested. These protocols were developed in order to isolate the IgY from the IL and the other top phase components. These compounds are present in the IL-rich aqueous phase and are responsible for the suspected target protein agglomeration and/or denaturation.

3.2 – Experimental section

3.2.1 – Chemicals

Acetone (C_3H_6O, 100 % purity) was obtained from VWR Normapur. Analytical TCA was aquire from Prolabo. Sodium dodecylsufate (SDS, 99 % purity) was purchased from Alfa Aesar.

3.3 – Experimental procedure

3.3.1 – Acetone precipitation

After a careful separation of the phases of the ABS, an acetone precipitation procedure was applied to all samples. First, 400 µL of acetone, previously stored at -20 ºC, was added to 100 µL of each sample. The mixture was then incubated for 1 h, at -20 ºC. After the incubation, the mixture was centrifuged at 14 000 g, at 4 ºC, for 30 min. The supernatant was gently discarded and the acetone excess was evaporated at room temperature (25 ± 1) °C. The resultant pellet was solubilized in a 100 mM phosphate buffer + NaCl 0.3 M, pH 7.00 and its protein profile was investigated by SE-HPLC.

3.3.2 – Trichloroacetic acid (TCA) precipitation

For the TCA precipitation method, two solutions were initially prepared: a 100 % (w:v) TCA solution (solution 1), by dissolving 2.2 g of TCA in 1 mL of H_2O, and a 10 % (v/v) solution (solution 2) by adding 0.1 mL of 100 % (w:v) TCA solution to 0.9 mL of H_2O. These solutions were kept in ice cold. After, 0.11 volumes of solution 1 were added to the protein sample and the mixture was stored for 10 min, at -20 ºC. After, 500 µL of the ice-cold solution 2 were added to the sample and it was incubated at -20 ºC, for 30 min. The supernatant was carefully removed, the pellet was washed with 500 µL of acetone and left to dry at room temperature. The resulting pellet was ressuspended in a 100 mM phosphate buffer + NaCl 0.3 M, pH 7.00 and it protein profile was studied by SE-HPLC.

3.3.3 – Dialysis

A dialysis procedure was tested with the IL-rich phase of each ABS, after the partition experiments. Initially, 200 µL of each IL-rich phase sample were added inside a dialysis cellulose membrane, acquired from Sigma-Aldrich, with a molecular weight cut-off of 14.0 kDa. A 100 mM phosphate buffer + NaCl 0.3 M, pH 7.00 (dialysate) was added on the opposite side of the membrane. The experiment was performed during 3h, at room temperature (≈ 25 ± 1) °C and the dialysate was replaced in every 1h. The same procedure was developed using a 4 % (w:v) and 6 % (w:v) SDS solution within the dialysis membrane.

3.3.4 – Ultrafiltration

The ultrafiltration protocol was applied in samples of both bottom and top phases of each ABS. In order to carry out the ultrafiltration procedure, Amicon Ultra-0.5 mL centrifugal Filters, from Merck Millipore, were used. Each device is supplied with two microcentrifuge tubes. During the experiment, one tube is used to collect the filtrate and the other one is used to recover the precipitated sample (Figure 27). First, 200 µL of each sample were added to the Amicon Ultra-0.5 mL device and then centrifuged at 14 000 g, for 10 min, at room temperature (≈ 25 ± 1) °C. The precipitated sample was solubilized in 200 µL of a 100 mM phosphate buffer + NaCl 0.3 M, pH 7.00.

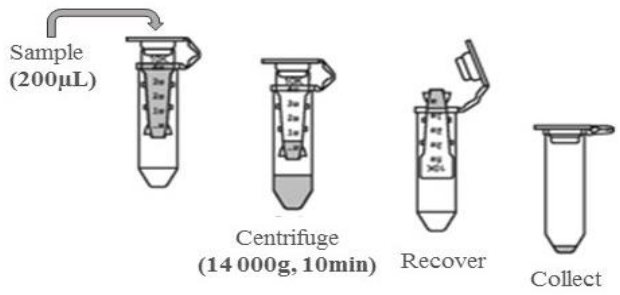

Figure 27 – Schematic representation of the ultrafiltration procedure.

The described protocol was also executed using a 1 % (w:v) and 10 % (w:v) SDS solutions (aiming at increasing the proteins solubility). After a first ultrafiltration step, similar to the one described above, the pellet was washed with a 1 % (v:v) SDS solution and centrifuged at 14 000 g, for 10 min, at room temperature (≈ 25 ± 1) °C. The pellet was then washed with a 10 % (w:v) SDS solution and centrifuged at 14 000 g, for 10 min, at (≈ 25 ± 1) °C. The precipitated sample was solubilized in 200 µL of a 100 mM phosphate buffer + NaCl 0.3 M pH 7.00, and its protein profile was investigated by SE-HPLC.

3.4. Results and discussion

The acetone precipitation procedure was applied in samples of each phase, of each ABS. The results obtained from these experiments were not satisfactory due to the inability of dissolving the resultant pellet in the 100 mM phosphate buffer + NaCl 0.3 M, pH 7.00 solution, impeding the study of its protein profile by HPLC.

The TCA precipitation procedure was then tested using a WSPF sample. The HPLC chromatogram obtained is displayed in Figure 28. The obtained pellet was successfully resuspended in the 100 mM phosphate buffer + NaCl 0.3 M, pH 7, allowing its protein profile analysis by HPLC. By the analysis of the chromatogram, it is possible to confirm the occurrence of some protein loss or denaturation, and in particular for IgY, that is completely lost and does not appear.

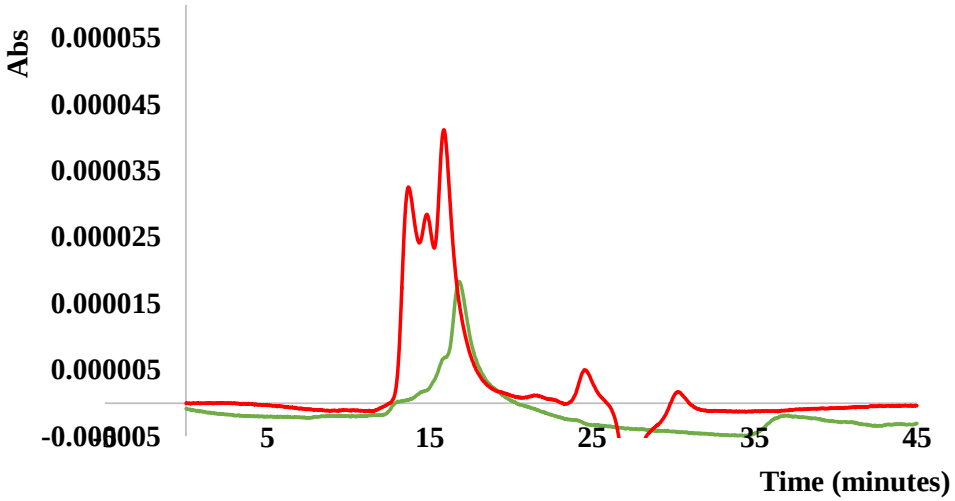

Figure 28 – Chromatogram of an original WSPF sample (–) and a sample of the WSPF after being exposed to the TCA precipitation procedure (–).

After, and with the aim of preserving the IgY molecule in the interior of the dialysis cellulose membrane, while allowing the repulsion of the IL for the exterior dialysate solution, the dialysis method was tested. Figure 29 depicts the macroscopic appearance of the dialysis procedure during the experiment. By visual inspection, it can be seen the formation of a precipitate within the dialysis membrane. Further, the dilution of this precipitate in a 100 mM phosphate buffer + NaCl 0.3 M pH 7, was also attempted, although with no success. The proteins denaturation/precipitation has made impossible the resuspension in a buffer aqueous solution.

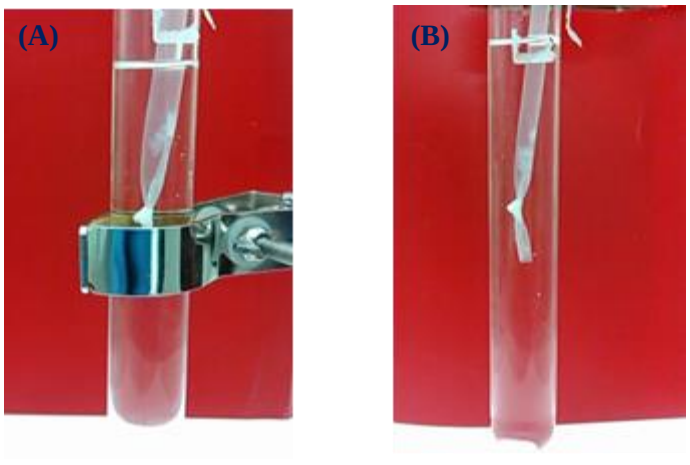

Figure 29 – Dialysis of a top phase sample, corresponding to an ABS composed of wt % $[N_{4444}][HEPES]$ + 22.9 wt % $C_6H_5K_3O_7$ + 57.1 wt % WSPF, using a solution of phosphate buffer pH 7.0 (A) 60 min (B) 120 min.

Taking into account the difficulties regarding the pellet solubilization, additional experiments were carried out using solutions of SDS. SDS has a typical surfactant structure, having a polar group, *i.e.*, a hydrophilic head, and a hydrocarbon hydrophobic chain. Because of its amphiphilic nature, SDS is able to solubilize hydrophobic compounds in solution. As reported, at low concentrations detergents bind weakly to the exposed hydrophobic regions of proteins preventing aggregation *(168)*. These compounds can also successfully promote the refolding of unfolded proteins without aggregation *(168,170)*. The aim of using a SDS solution in some of the traditional protein precipitation experiments stated above was to induce the proteins solubilization, aiming the pellet ressuspension and a further protein profile analysis.

The macroscopic appearance of the dialysis procedure, using a 4 % (w:v) and 6 % (w:v) SDS solution within the dialysis membrane is displayed in Figure 30. As previously, it is noticeable the formation of a precipitate in the dialysis membrane. The attempt of diluting these precipitated protein in the 100 mM phosphate buffer + NaCl 0.3 M, pH 7 was still not successfully accomplished.

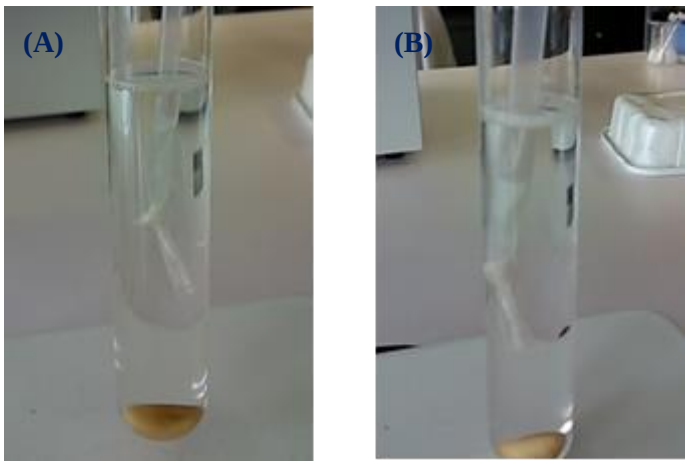

Figure 30 – Dialysis of a top phase sample, belonging to an ABS composed of 20.1 wt % $[N_{4444}][TES]$ + 28.2 wt % $C_6H_5K_3O_7$ + 51.7 wt % WSPF, in a solution of phosphate buffer pH 7.0 (A) combined with a 4 (w/v) % SDS solution (60 min), (B) combined with a 6 (w/v) % SDS solution (120 min).

The next procedure tested was the ultrafiltration method. The results obtained from these tests were also not satisfactory, since again the same problems on the pellet solubilization in the 100 mM phosphate buffer + NaCl 0.3 M, pH 7, were found. As before, the resuspension of the pellet in the adequate buffer, after the proteins

precipitation was not successfully accomplished so that no SE-HPLC experiments could be conducted. The ultrafiltration procedure was also executed using two distinct SDS solutions. The solubilization of the pellet was accomplished with success when using a 10 % (w:v) SDS solution. The results obtained are presented in Figure 31. Taking into account the results presented in the chromatogram, it is possible to notice the interference of the SDS with the protein profile analysis. As reported, to permit the HPLC analysis, the concentration of SDS in the sample must be reduced to below 0.01 % *(171)*. However, the complete solubilization of the pellet was not achieved with this concentration and no additional studies were performed.

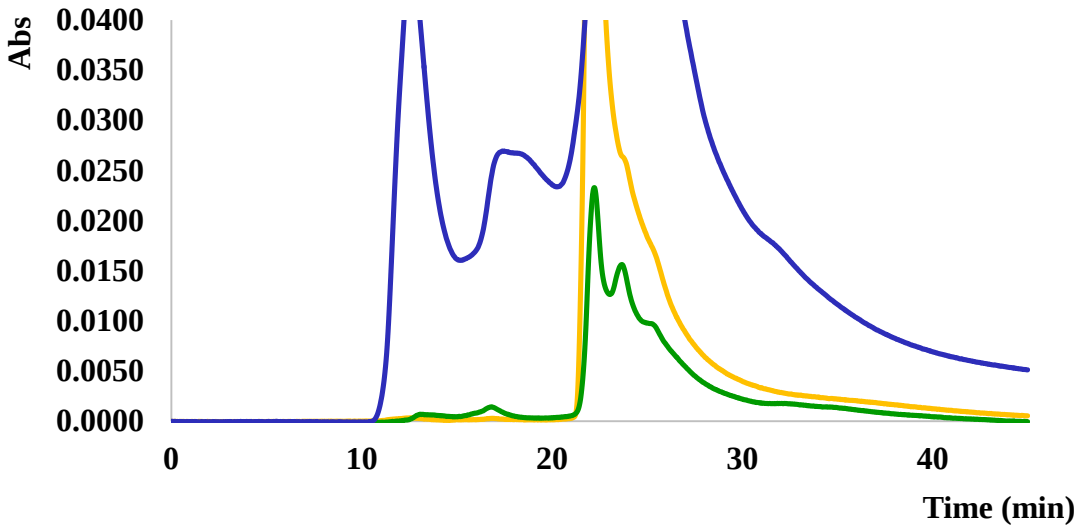

Figure 31 – Chromatogram of the bottom phase (–), top phase (–) and top phase after ultrafiltration using a 10 % (w:v) SDS solution (–) of a system composed of 20.0 wt % $[P_{4444}][Tricine]$ + 29.0 wt % $C_6H_5K_3O_7$ + 51 wt % WSPF.

3.5 – Conclusions

In this chapter we tested the ability of two different protein precipitation techniques, acetone and TCA precipitation, plus ultrafiltration and dialysis, to recover the IgY from the IL-rich phase aiming at analysing the proteins profile by HPLC. Acetone precipitation, ultracentrifugation and dialysis were tested; however, no successful results were obtained. The failure of these procedures was mainly due to difficulties regarding the pellet solubilization in an adequate phosphate buffer which prevented the further study on the proteins profiles by HPLC. Regarding the TCA precipitation technique, in spite of the facility concerning the pellet solubilization, it led to proteins losses and denaturation. Moreover, a surfactant (SDS) was also used with the aim of solubilizing the proteins pellet

and thus to allow the proteins profile study. Despite of the satisfactory results concerning the proteins solubilization, this compound revealed to major interfere with the protein profile analysis by HPLC, when used above at high concentrations (still required to dissolve the pellet).

4 - Final remarks

4.1 – Conclusions and future work

The main purpose of this work consisted on the development of an alternative platform for the selective extraction and purification of the IgY, from egg yolk, using ABS composed of biocompatible and self-buffering ILs, the GB-ILs.

The GB-ILs investigated, namely $[P_{4444}][CHES]$, $[P_{4444}][MES]$, $[P_{4444}][HEPES]$, $[P_{4444}][TES]$, $[P_{4444}][Tricine]$, $[N_{4444}][CHES]$, $[N_{4444}][MES]$, $[N_{4444}][HEPES]$, $[N_{4444}][TES]$ and $[N_{4444}][Tricine]$ were at first combined with $C_6H_5K_3O_7$, a biodegradable salt, for the ABS formation. Their phase diagrams were ascertained and then the extraction experiments, using the WSPF from egg yolk, were performed. However, with these systems the extraction and purification of the IgY was not successfully achieved. In all the studied systems, no proteins were detected at the salt-rich phase and all proteins belonging to the WSPF revealed to have preference for the IL-rich phase. The systems composed of $[P_{4444}][HEPES]$, $[N_{4444}][HEPES]$ and $[N_{4444}][TES]$ shown a significant visible turbidity, suggesting that some proteins present in the WSPF precipitated. The SDS-PAGE results of these systems did not reveal any band matching the IgY light chain (25 kDa). Only β–livetin band (38 kDa) was detected, and a band around 65 kDa, which can correspond to the IgY heavy chain and/or correspond to other contaminant proteins. Regarding the IgY quantification, which was carried out through the analysis of the intensity of the IgY light chain band, favourable results were obtained with the ABS composed of 20.1 wt % $[N_{4444}][CHES]$ + 16.9 wt % $C_6H_5K_3O_7$. This system was found to be also the most promising concerning the stability of the proteins of the WSPF of egg yolk at the GB-IL-rich phase.

Finally, four techniques were applied with the aim of isolating the proteins present at the IL-rich phase so that their profile could be evaluated by SE-HPLC. Acetone and TCA precipitations, dialysis and ultrafiltration techniques were applied at this stage. In three of the experiments, acetone, dialysis and ultrafiltration, the precipitated proteins were not able to be resuspended in an aqueous buffer medium. SDS was further employed to facilitate the proteins dissolution. However, some major drawbacks were found, namely the failure in the proteins solubilisation and the need of higher concentrated SDS solutions, which interferes with the protein profile evaluation by HPLC.

Based on the results gathered in this work, the next step is to implement a successful method that could allow the complete extraction and purification of IgY from egg yolk. Nevertheless, the ABS investigated in this work are not promising alternatives and other

phase-forming components should be evaluated in the future. Moreover, it will be of high importance to identify the two major WSPF contaminant proteins by techniques such as MS/MS. Additional investigations on the protein stability and activity, such as Circular dichroism, should also be carried out to better understand the effects of the phase-forming components through the IgY stability. Moreover, after the IgY complete purification, the recycling nature of the ABS should be used aiming at decreasing the cost involved. The systems used in this work could be an adequate strategy for future investigation due to their benign and biocompatible character and since they already proved to maintain the integrity of other proteins. However, they do not seem adequate candidates for purifying IgY and other ABS composed of GB-ILs with different cations and combined with polymers, and as previously investigated *(139)*, should be studied in detail.

5 - References

(1) Deignan, T., Kelly, J., Alwan, A., and O'Farrelly, C. (2000) Comparative Analysis of Methods of Purification of Egg Yolk Immunoglobulin. *Food Agric. Immunol. 12*, 77–85.
(2) Rosa, P. A. J., Ferreira, I. F., Azevedo, A. M., and Aires-Barros, M. R. (2010) Aqueous two-phase systems: A viable platform in the manufacturing of biopharmaceuticals. *J. Chromatogr. A 1217*, 2296–305.
(3) Walsh, G. (2005) Biopharmaceuticals: Recent approvals and likely directions. *Trends Biotechnol. 23*, 553–558.
(4) Casadevall, A. (1996) Antibody-Based Therapies for Emerging Infectious Diseases. *Emerg. Infect. Dis. 2*, 200–208.
(5) Casadevall, A., and Scharff, M. D. (1995) Return to the past: the case for antibody-based therapies in infectious diseases. *Clin. Infect. Dis. 21*, 150–161.
(6) Casadevall, A., and Scharff, M. D. (1994) Serum therapy revisited: Animal models of infection and development of passive antibody therapy. *Antimicrob. Agents Chemother. 38*, 1695–1702.
(7) Dimitrov, D. (2012) Therapeutic proteins. *Methods Mol. Biol. 899*, 1–26.
(8) Horiguchi, T., and Takeshita, K. (2003) Neuropsychological developmental change in a case with Noonan syndrome: longitudinal assessment. *Brain Dev. 25*, 291–293.
(9) Lipman, N. S., Jackson, L. R., Trudel, L. J., and Weis-Garcia, F. (2005) Monoclonal Versus Polyclonal Antibodies: Distinguishing Characteristics, Applications, and Information Resources. *ILAR J. 46*, 258–268.
(10) Biosciences, A. (2002) Antibody purification handbook. *Ed. AC*.
(11) Leenaars, M., and Hendriksen, C. F. M. (2005) Critical Steps in the Production of Molyclonal and Polyclonal Antibodies: Evaluation and Recommendations. *ILAR J. 46*, 269–279.
(12) Roitt, I., Brostoff, J., and Male, D. (1998) Immunology 4rd edtion. Mosby.
(13) Michael, A., Meenatchisundaram, S., Parameswari, G., Subbraj, T., Selvakumaran, R., and Ramalingam, S. (2010) Chicken egg yolk antibodies (IgY) as an alternative to mammalian antibodies A. *Indian J. Sci. Technol. 3*, 468–474.
(14) Kovacs-Nolan, J., and Mine, Y. (2004) Avian egg antibodies: basic and potential applications. *Avian Poult. Biol. Rev. 15*, 25–46.
(15) Meulenaer, B. De, and Huyghebaert, A. (2001) Isolation and Purification of Chicken Egg Yolk Immunoglobulins : A Review. *Food Agric. Immunol. 13*, 275–288.
(16) Azevedo, A. M., Rosa, P. A. ., Ferreira, I. . F., and Aires-Barros, M. R. (2007) Optimisation of aqueous two-phase extraction of human antibodies. *J. Biotechnol. 132*, 209–17.
(17) Pei, Y., Wang, J., Wu, K., Xuan, X., and Lu, X. (2009) Ionic liquid-based aqueous two-phase extraction of selected proteins. *Sep. Purif. Technol. 64*, 288–295.
(18) Liu, J., Yang, J., Xu, H., Zhu, H., Qu, J., Lu, J., and Cui, Z. (2011) Isolation of Immunoglobulin from Chicken Egg Yolk using Single-Stage Ultrafiltration with 100-kDa Regenerated Cellulose Membranes. *Int. J. Food Eng. 7*, 1556–3758.
(19) Freire, M. G., Cláudio, A. F. M., Araújo, J. M. M., Coutinho, J. a. P., Marrucho, I. M., Canongia Lopes, J. N., Rebelo, L. P. N., Lopes, J. N. C., and Rebelo, L. P. N. (2012) Aqueous biphasic systems: a boost brought about by using ionic liquids. *Chem. Soc. Rev. 41*, 4966–95.
(20) Stålberg, J., and Larsson, A. (2001) Extraction of IgY from egg yolk using a novel aqueous two-phase system and comparison with other extraction methods. *J. Med. Sci. 106*, 99–110.
(21) Azevedo, A. M., Rosa, P. A. J., Ferreira, I. F., and Aires-Barros, M. R. (2008) Integrated process for the purification of antibodies combining aqueous two-phase extraction, hydrophobic interaction chromatography and size-exclusion chromatography. *J. Chromatogr. A 1213*, 154–61.
(22) Azevedo, A. M., Gomes, a. G., Rosa, P. a. J., Ferreira, I. F., Pisco, A. M. M. O., and Aires-Barros, M. R. (2009) Partitioning of human antibodies in polyethylene glycol–sodium citrate aqueous two-phase systems. *Sep. Purif. Technol. 65*, 14–21.
(23) Rosa, P. A. J., Azevedo, A. M., Ferreira, I. F., de Vries, J., Korporaal, R., Verhoef, H. J., Visser, T. J., and Aires-Barros, M. R. (2007) Affinity partitioning of human antibodies in aqueous two-phase systems. *J. Chromatogr. A 1162*, 103–13.

(24) Ferreira, I. . F., Azevedo, A. M., Rosa, P. A. J., and Aires-Barros, M. R. (2008) Purification of human immunoglobulin G by thermoseparating aqueous two-phase systems. *J. Chromatogr. A 1195*, 94–100.
(25) Taha, M., e Silva, F. a., Quental, M. V., Ventura, S. P. M., Freire, M. G., and Coutinho, J. a. P. (2014) Good's buffers as a basis for developing self-buffering and biocompatible ionic liquids for biological research. *Green Chem. 16*, 3149.
(26) Gutowski, K., Broker, G., Willauer, H., Huddleston, J., Swatloski, R., Holbrey, J., and Rogers, R. (2003) Controlling the aqueous miscibility of ionic liquids: aqueous biphasic systems of water-miscible ionic liquids and water-structuring salts for recycle, metathesis, and separations. *J. Am. Chem. Soc. 125*, 6632–6633.
(27) Will, M. a, Clark, N. a, and Swain, J. E. (2011) Biological pH buffers in IVF: help or hindrance to success. *J. Assist. Reprod. Genet. 28*, 711–24.
(28) Roy, R. N., Roy, L. N., Bodendorfer, B. M., Downs, Z. M., Rocchio, S. D., Wollen, J. T., Stegner, J. M., Henson, I. B., Grove, N. W., and Dieterman, L. A. (2012) Buffer Standards for the Biochemical pH of the Zwitterionic Buffer N -Tris- (Hydroxymethyl) Methyl-2-aminoethanesulfonic Acid (TES) from 5 ˚ C to 55 ˚ C. *Open J. Phys. Chem. 2*, 41–46.
(29) Parham, P. (2009) The Immune System Third Edit. Taylor & Francis Group, 2009.
(30) Hanly, W., Artwohl, J., and Bennett, B. (1995) Review of polyclonal antibody production procedures in mammals and poultry. *ILAR J. 37*, 93–118.
(31) Aragón, M. i, and Mart, M. (2008) Extraction of Immunoglobulin G. Study of Host-Guest mechanisms.
(32) Newcombe, C., and Newcombe, A. R. (2007) Antibody production: Polyclonal-derived biotherapeutics. *J. Chromatogr. B Anal. Technol. Biomed. Life Sci. 848*, 2–7.
(33) Hodek, P., and Stiborová, M. (2003) Chicken Antibodies – Superior Alternative for Conventional Immunoglobulins. *Proc. Indian Natl. Sci. Acad. 468*, 461–468.
(34) Tokunaga, T., Chiba, J., and Ohnishi, K. (1987) Attempts to improve hybridoma technology for the production of human monoclonal antibodies. *Gan To Kagaku Ryoho. 14*, 2198–2204.
(35) Ayyar, B. V., Arora, S., Murphy, C., and O'Kennedy, R. (2012) Affinity chromatography as a tool for antibody purification. *Methods 56*, 116–29.
(36) Baxter, D. (2007) Active and passive immunity, vaccine types, excipients and licensing. *Occup. Med. (Chic. Ill). 57*, 552–556.
(37) Kovacs-Nolan, J., and Mine, Y. (2012) Egg yolk antibodies for passive immunity. *Annu. Rev. Food Sci. Technol. 3*, 163–82.
(38) Van De Perre, P. (2003) Transfer of antibody via mother's milk. *Vaccine 21*, 3374–3376.
(39) Chucri, T. M., Monteiro, J. M., Lima, a. R., Salvadori, M. L. B., Junior, J. R. K., and Miglino, M. a. (2010) A review of immune transfer by the placenta. *J. Reprod. Immunol. 87*, 14–20.
(40) Brambell, F. (1958) The passive immunity of the young mammal. *Biol. Rev.* 488–531.
(41) Lilius, E.-M., and Marnila, P. (2001) The role of colostral antibodies in prevention of microbial infection. *Curret Opin. Infecious Dis. 14*, 295–300.
(42) Garvey, J. S., Cremer, N. E., and Sussdorf, D. H. (1977) Methods in Immunology 3rd editio. W. A. Benjamin, INC.
(43) Schade, R. R., Staak, C., Hendriksen, C., Erhard, M., Hugl, H., Koch, G., Larsson, A., Pollmann, W., Van Regenmortel, M., Rijke, E., Spielmann, H., Steinbusch, H., Straughan, D., Regenmortel, M. van, Rijke, E., Spielmann, H., Steinbush, H., Straughan, D., and Christian, S. (1996) The production of avian (egg yolk) antibodies: IgY. *ATLA Altern. to Lab. Anim. 24*, 925–934.
(44) Borrebaeck, C. A. K. C. (2000) Antibodies in diagnostics–from immunoassays to protein chips. *Immunol. Today 5699*, 379–382.
(45) Kohler, G., and Milstein, C. (1975) Continuos cultures of fused cells secreting antibody of predefined specificity. *Nature 254*, 495–497.
(46) Goldring, J. P. D., and Coetzer, T. H. T. (2003) Isolation of chicken immunoglobulins (IgY) from egg yolk. *Biochem. Mol. Biol. Educ. 31*, 185–187.

(47) Tan, S. H., Mohamedali, A., Kapur, A., Lukjanenko, L., and Baker, M. S. (2012) A novel, cost-effective and efficient chicken egg IgY purification procedure. *J. Immunol. Methods 380*, 73–76.
(48) Ko, K. Y., and Ahn, D. U. (2007) Preparation of immunoglobulin Y from egg yolk using ammonium sulfate precipitation and ion exchange chromatography. *Poult. Sci. 86*, 400–7.
(49) Narat, M. (2003) Production of antibodies in chickens. *Food Technol. Biotechnol. 41*, 259–267.
(50) Leslie, B. Y. G. A., Ph, D., and Clem, L. W. (1969) Phylogeny of immunoglobulin structure and function. *J. Exp. Med. 130*, 1337–1352.
(51) Phyiol, A. J., and Thomas, C. C. (1961) Serum Proteins and the Livetins of Hen's - Egg Yolk. *Biochem. J. 83*, 346–355.
(52) Marcet, I., Laca, A., Paredes, B., and Díaz, M. (2011) IgY isolation from a watery by-product obtained from an egg yolk fractionation process. *Food Bioprod. Process. 89*, 87–91.
(53) Chalghoumi, R., Beckers, Y., Portetelle, D., and Théwis, A. (2009) Hen egg yolk antibodies (IgY), production and use for passive immunization against bacterial enteric infections in chicken : a review. *Biotechnol. Agron. Soc. Environ. 13*, 295–308.
(54) Schade, R., Calzado, E. G., Sarmiento, R., Chacana, P. A., Porankiewicz-Asplund, J., and Terzolo, H. R. (2005) Chicken egg yolk antibodies (IgY-technology): a review of progress in production and use in research and human and veterinary medicine. *Altern. Lab. Anim. 33*, 129–54.
(55) Sh, Shimizu, M., Nagashima, H., Sano, K., Hashimoto, K., Ozeki, M., Tsuda, M., and Hatta, H. (1992) Molecular stability of chicken and rabbit immunoglobulin G. *Biosci. Biotechnol. Biochem. 56*, 270–274.
(56) Hatta, H., Tsuda, K., Akachi, S., Kim, M., Yamamoto, T., and Ebina, T. (1993) Oral Passive Immunization Effect of Anti-Human Rotavirus IgY and Its Behavior against Proteolytic Enzymes. *Biosci. Biotechnol. Biochem. 57*, 1077–1081.
(57) Shimizu, M., Fitzsimmons, R. R. C., and Nakai, S. (1988) Anti-E. coli Immunoglobulin Y Isolated from Egg Yolk of Immunized Chickens as a Potential Food Ingredient. *J. Food Sci. 53*, 1360–1368.
(58) Chang, H. M. H., Ou-Yang, R. F. R., Chen, Y. T., and Chen, C. C. (1999) Productivity and Some Properties of Immunoglobulin Specific against Streptococcus mutans Serotype c in Chicken Egg Yolk (IgY). *J. Agric. Food Chem. 47*, 61–66.
(59) Carlander, D., Kollberg, H., Wejåker, P., and Larsson, A. (2000) Peroral immunotheraphy with yolk antibodies for the prevention and treatment of enteric infections. *Immunol. Res. 21*, 1–6.
(60) Juliarena, M., Gutierrez, S., and Ceriani, C. (2007) Chicken antibodies: a useful tool for antigen capture ELISA to detect bovine leukaemia virus without cross-reaction with other mammalian antibodies. *Vet. Res. Commun. 31*, 43–51.
(61) Tini, M., Jewell, U. R., and Camenisch, G. (2002) Generation and application of chicken egg-yolk antibodies. *Comp. Biochem. Physiol. Part A 131*, 569–574.
(62) Larsson, A., Carlander, D., and Wilhelmsson, M. (1998) Antibody response in laying hens with small amounts of antigen. *Food Agric. Immunol. 10*, 29–36.
(63) Kim, H. O., Durance, T. D., and Li-Chan, E. C. (1999) Reusability of avidin-biotinylated immunoglobulin Y columns in immunoaffinity chromatography. *Anal. Biochem. 268*, 383–397.
(64) Ruiz, E., and Ruffner, H. P. (2002) Immunodetection of Botrytis-specific invertase in infected grapes. *J. Phytopathol. 150*, 76–85.
(65) Altschuh, D., Hennache, G., and Van Regenmortel, M. H. (1984) Determination of IgG and IgM levels in serum by rocket immunoelectrophoresis using yolk antibodies from immunized chickens. *J. Immunol. Methods 69*, 1–7.
(66) Bizhanov, G., and Vyshniauskis, G. (2000) A comparison of three methods for extracting IgY from the egg yolk of hens immunized with Sendai virus. *Vet. Res. Commun. 24*, 103–13.
(67) Peralta, R., and Yokoyama, H. (1994) Passive immunisation against experimental salmonellosis in mice by orally administered hen egg-yolk antibodies specific for 14-kDa fimbriae of Salmonella enteritidis. *J. Med. Microbiol. 41*, 29–35.

(68) Yokoyama, H., Umeda, K., Peralta, R. R. C., Hashi, T., Jr, F. C. I., Kuroki, M., and Ikemori, Y. (1998) Oral passive immunization against experimental salmonellosis in mice using chicken egg yolk antibodies specific for Salmonella enteritidis and S. *Vaccine 16*, 388–393.
(69) Yokoyama, H., Peralta, R. C., Umeda, K., Hashi, T., Icatlo, F. C., Kuroki, M., Ikemori, Y., and Kodama, Y. (1998) Prevention of fatal salmonellosis in neonatal calves, using orally administered chicken egg yolk Salmonella-specific antibodies. *Am. J. Vet. Res. 59*, 416–20.
(70) Methner, U., Kobilke, H., and Fehlhaber, K. (2004) Effect of Orally Administered Egg Yolk Antibodies on Salmonella enteritidis Contamination of Hen ' s Eggs. *J. Vet. Med. Ser. B 134*, 129–134.
(71) Kassaify, Z. G., and Mine, Y. (2004) Effect of Food Protein Supplements on Salmonella enteritidis Infection. *Poult. Sci. 83*, 753–760.
(72) Rahimi, S., Shiraz, Z. M., and Salehi, T. Z. (2007) Prevention of Salmonella Infection in Poultry by Specific Egg-Derived Antibody. *Int. J. Poult. Sci. 6 6*, 230–235.
(73) Tsubokura, K., Berndtson, E., Bogstedt, A., Kaijser, B., Kim, M., and Ozeki, M. (1997) Oral administration of antibodies as prophylaxis and therapy in Campylobacter jejuni -infected chickens. *Clin. Exp. Immunol. 108*, 451–455.
(74) Yokoyama, H., Peralta, R. R. C., Diaz, R., and Sendo, S. (1992) Passive protective effect of chicken egg yolk immunoglobulins against experimental enterotoxigenic Escherichia coli infection in neonatal piglets. *Infect. Immun. 60*, 998–1007.
(75) Imberechts, I., Deprez, P., Van Driessche, E., and Pohl, P. (1997) Chicken egg yolk antibodies against F18ab fimbriae of Escherichia coli inhibit shedding of F18 positive E . coli by experimentally infected pigs. *Vet. Microbiol. 54*, 329–341.
(76) Zuniga, A., Yokoyama, H., Albicker-Rippinger, P., Eggenberger, E., and Bertschinger, H. U. (1997) Reduced intestinal colonisation with F18-positive enterotoxigenic Escherichia coli in weaned pigs fed chicken egg antibody against the fimbriae. *FEMS Immunol. Med. Microbiol. 18*, 153–161.
(77) Erhard, M. H., Aytug, N., Baklaci, C., Karamiiptioglu, S., Hofmann, A., and Lsch, U. (1996) Dose-dependent effects of specific egg-yolk antibodies on diarrhea of newborn calves. *Prev. Vet. Med. 5877*, 67–73.
(78) Farrelly, C. O., Branton, D., Wanke, C. A., O'farrelly, C., Branton, D., and Wanke, C. A. (1992) Oral ingestion of egg yolk immunoglobulin from hens immunized with an enterotoxigenic Escherichia coli strain prevents diarrhea in rabbits challenged with the same. *Infect. Immun. 60*, 2593–2597.
(79) Yolken, R. R. H. R., Leister, F., Wee, S. S., and Miskuff, R. (1988) Antibodies to rotaviruses in chickens' eggs: a potential source of antiviral immunoglobulins suitable for human consumption. *Pediatrics 81*, 291–5.
(80) Hatta, H., Tsuda, K., Akachi, S., Kim, M., and Yamamoto, T. (1993) Productivity and some properties of egg yolk antibody (IgY) against human rotavirus compared with rabbit IgG. *Biosci Biotechnol Biochem 57*, 450–454.
(81) Ikemori, Y., Ohta, M., Umeda, K., and Jr, F. I. (1997) Passive protection of neonatal calves against bovine coronavirus-induced diarrhea by administration of egg yolk or colostrum antibody powder. *Vet. Microbiol. 58*, 105–111.
(82) Azevedo, A. M., Rosa, P. aaJ., Ferreira, I. F., Pisco, A. M. M. O., de Vries, J., Korporaal, R., Visser, T. J., and Aires-Barros, M. R. (2009) Affinity-enhanced purification of human antibodies by aqueous two-phase extraction. *Sep. Purif. Technol. 65*, 31–39.
(83) Bischof Delaloye, A., and Delaloye, B. (1995) Tumor imaging with monoclonal antibodies. *Semin. Nucl. Med. 25*, 144–164.
(84) Jong, J. R. De, Vries, E. G. E. De, and Hooge, M. N. L. (2015) Development and Characterization of HER2 / neu ImmunoPET Imaging *50*, 974–982.
(85) Saleem, M., and Kamal, M. (2008) Monoclonal antibodies in clinical diagnosis : A brief review application *7*, 923–925.
(86) Hober, S., Nord, K., and Linhult, M. (2007) Protein A chromatography for antibody purification. *J. Chromatogr. B Anal. Technol. Biomed. Life Sci. 848*, 40–47.

(87) Cuatrecasas, P., Wilchek, M., and Anfinsen, C. B. (1968) Selective enzyme purification by affinity chromatography. *Proc. Natl. Acad. Sci. U. S. A. 61*, 636–643.
(88) Starovasnik, M. . A., O'Connell, M. P., Fairbrother, W. J., and Kelley, R. F. (1999) Antibody variable region binding by Staphylococcal protein A: thermodynamic analysis and location of the Fv binding site on E-domain. *Protein Sci. 8*, 1423–1431.
(89) Boyle, M. D. P. (1990) Bacterial Immunoglobulin–Binding Proteins: Applications in Immunotechnology. Elsevier Science.
(90) Boschetti, E., Judd, D., Schwartz, W. E., and Tunon, P. (2000) Hydrophobic Charge-Induction Chromatography. *Genet. Eng. News 20*, 211–221.
(91) Finger, U. B., Brümmer, W., Knieps, E., Thömmes, J., and Kula, M. R. (1996) Investigations on the specificity of thiophilic interaction for monoclonal antibodies of different subclasses. *J. Chromatogr. B. Biomed. Appl. 675*, 197–204.
(92) Konecny, P., Brown, R. J., and Scouten, W. H. (1994) Chromatographic purification of immunoglobulin G from bovine milk whey. *J. Chromatogr. A 673*, 45–53.
(93) Vançan, S., Miranda, E. A., Bueno, S. M. A., Vanc, S., Alves, E., Maria, S., Bueno, A., Vançan, S., Miranda, E. A., and Bueno, S. M. A. (2002) IMAC of human IgG: Studies with IDA-immobilized copper, nickel, zinc, and cobalt ions and different buffer systems. *Process Biochem. 37*, 573–579.
(94) Raja, S., Murty, V. R., Thivaharan, V., Rajasekar, V., and Ramesh, V. (2012) Aqueous Two Phase Systems for the Recovery of Biomolecules – A Review. *Sci. Technol. 1*, 7–16.
(95) Losch, U., Schranner, I., and Wanke, R. (1986) The Chicken Egg, an Antibody Source. *J. Vet. Med. 619*, 609–619.
(96) Hernández-Campos, F. . J., Brito-De la Fuente, E., and Torrestiana-Sánchez, B. (2010) Purification of egg yolk immunoglobulin (IgY) by ultrafiltration: effect of pH, ionic strength, and membrane properties. *J. Agric. Food Chem. 58*, 187–93.
(97) Verdoliva, A., Basile, G., and Fassina, G. (2000) Affinity purification of immunoglobulins from chicken egg yolk using a new synthetic ligand. *J. Chromatogr. B 749*, 233–242.
(98) Hodek, P., Trefil, P., and Simunek, J. (2013) Optimized protocol of chicken antibody (IgY) purification providing electrophoretically homogenous preparations. *Int. J. Electrochem 8*, 113–124.
(99) Bižanov, G., and Jonauskien, I. (2003) Production and Purification of IgY from egg yolk immunization of hens with Pig IgG. *Bull. Vet. Inst. Pulawy 47*, 403–410.
(100) Khil'ko, S. N., Kirasova, M. A., Piker, S. D., Osidze, S. D., Fomina, N. V, Burgasova, M. P., and Tikhonenko, T. I. (1989) Immunoenzyme analysis of adenovirus hexon. Determination of antibodies from hyperimmunized chickens. *Mol. Gen. Mikrobiol. Virusol.* 43–8.
(101) Kwan, L., Helbig, N., and Nakai, S. (1988) Fractionation of Water-Soluble and -Insoluble Components from Egg Yolk with Minimum Use of Organic Solvents. *J. Food Sci. 56*, 1537–1541.
(102) Akita, E. M., and Nakai, S. (1992) lmmunoglobulins from Egg Yolk : Isolation and Purification. *J. Food Sci. 57*, 629–653.
(103) Polson, A., and Barbara von Wechmar, M. (1980) Isolation of viral IgY antibodies from yolks of immunized hens. *Immunol. Commun. 9*, 475–493.
(104) Hansen, P., Scoble, J. a., Hanson, B., and Hoogenraad, N. J. (1998) Isolation and purification of immunoglobulins from chicken eggs using thiophilic interaction chromatography. *J. Immunol. Methods 215*, 1–7.
(105) Jensenius, J. C. H. R. J. C., Andersen, I., Hau, J., Koch, C., and Crone, M. (1981) Eggs: conveniently packeged antibodies. Methods for purification of yolk IgG. *J. Immunol. Methods 46*, 63–68.
(106) Hatta, H., Kim, M., and Yamamoto, T. (1990) A noval isolation method for Hen Egg Yolk Antibody, IgY. *Agric. Biol. Chem. 54*, 2531–2535.
(107) Chang, H.-M., Lu, T.-C., Chen, C.-C., Tu, Y.-Y., and Hwang, J.-Y. (2000) Isolation of immunoglobulin from egg yolk by anionic polysaccharides. *J. Agric. Food Chem. 48*, 995–9.

(108) Pauly, D., Chacana, P. a, Calzado, E. G., Brembs, B., and Schade, R. (2011) IgY technology: extraction of chicken antibodies from egg yolk by polyethylene glycol (PEG) precipitation. *J. Vis. Exp.* 3–7.
(109) Rosa, P. A. J., Azevedo, A. M., Sommerfeld, S., Bäcker, W., and Aires-Barros, M. . (2012) Continuous aqueous two-phase extraction of human antibodies using a packed column. *J. Chromatogr. B. Analyt. Technol. Biomed. Life Sci. 880*, 148–56.
(110) Schluederberg, A. (1973, June 1) Partition of Cell Particles and Macromolecules. *Yale J. Biol. Med.* Yale Journal of Biology and Medicine.
(111) Tjerneld, F., Persson, I., and Albertsson, P. (1985) Enzymatic Hydrolysis of Cellulose in of Cellulases from Trichoderma reesei. *Biotechnol. Bioeng. XXVII*, 1036–1043.
(112) Rito-Palomares, M. (2004) Practical application of aqueous two-phase partition to process development for the recovery of biological products. *J. Chromatogr. B 807*, 3–11.
(113) Benavides, J., and Rito-palomares, M. (2008) Practical experiences from the development of aqueous two-phase processes for the recovery of high value biological products. *J. Chem. Technol. Biotechnol. 142*, 133–142.
(114) Zijlstra, G. M., Michielsen, M. J., de Gooijer, C. D., van der Pol, L. A., and Tramper, J. (1996) Separation of hybridoma cells from their IgG product using aqueous two-phase systems. *Bioseparation 6*, 201–10.
(115) Andrews, B. A., Nielsen, S., and Asenjo, J. A. (1996) Partitioning and purification of monoclonal antibodies in aqueous two-phase systems. *Bioseparation 6*, 303–13.
(116) Rosa, P. A. J., Azevedo, A. M., and Aires-Barros, M. R. (2007) Application of central composite design to the optimisation of aqueous two-phase extraction of human antibodies. *J. Chromatogr. A 1141*, 50–60.
(117) Azevedo, A. M., Rosa, P. A. J., Ferreira, I. F., de Vries, J., Visser, T. J., and Aires-Barros, M. R. (2009) Downstream processing of human antibodies integrating an extraction capture step and cation exchange chromatography. *J. Chromatogr. B 877*, 50–8.
(118) Kornmann, I. H., and Ch, V. (2008) United States Patent 7 439 336.
(119) Platis, D., and Labrou, N. E. (2006) Development of an aqueous two-phase partitioning system for fractionating therapeutic proteins from tobacco extract. *J. Chromatogr. A 1128*, 114–24.
(120) Persson, J., Andersen, D. C., and Lester, P. M. (2005) Evaluation of different primary recovery methods for E. coli-derived recombinant human growth hormone and compatibility with further down-stream purification. *Biotechnol. Bioeng. 90*, 442–51.
(121) Cited, R., Zaslavsky, B. Y., Chemistry, P., Applications, B., and Dek, M. (2002) United States Patent 6 437 101 B1.
(122) Hart, R. A., Lester, P. M., Reifsnyder, D. H., Ogez, J. . R., and Builder, S. E. (1994) Large scale, in situ isolation of periplasmic IGF-I from E. coli. *Biotechnology. (N. Y). 12*, 1113–7.
(123) Sulk, B., Birkenmeier, G., and Kopperschläger, G. (1992) Application of phase partitioning and thiophilic adsorption chromatography to the purification of monoclonal antibodies from cell culture fluid. *J. Immunol. Methods 149*, 165–171.
(124) Wijnendaele, V., Gilles, D., Simonet, G., Smith, A., and Rit, K. (1987) United States Patent 4 683 294.
(125) Jiang, Y., Xia, H., Yu, J., Guo, C., and Liu, H. (2009) Hydrophobic ionic liquids-assisted polymer recovery during penicillin extraction in aqueous two-phase system. *Chem. Eng. J. 147*, 22–26.
(126) Pereira, J. F. B., Lima, Á. S., Freire, M. G., and Coutinho, J. A. P. (2010) Ionic liquids as adjuvants for the tailored extraction of biomolecules in aqueous biphasic systems †. *Green Chem 12*, 1661–1669.
(127) Freire, M. G., Louros, C. L. S., Rebelo, L. P. N., and Coutinho, J. A. P. (2011) Aqueous biphasic systems composed of a water-stable ionic liquid + carbohydrates and their applications. *Green Chem. 13*, 1536.
(128) Ventura, S. P. M., Sousa, S. G., Freire, M. G., Serafim, L. S., Lima, Á. S., and Coutinho, J. A. P. (2011) Design of ionic liquids for lipase purification. *J. Chromatogr. B 879*, 2679–2687.

(129) Freire, M. G., Neves, C. M. . . . S., Marrucho, I. M., Rebelo, N., and Coutinho, J. A. P. (2010) High-performance extraction of alkaloids using aqueous two-phase systems with ionic liquids †. *Green Chem. 12*, 1715–1718.
(130) Cláudio, A. F. M., Freire, M. G., Freire, C. S. R., Silvestre, A. J. D., and Coutinho, J. A. P. (2010) Extraction of vanillin using ionic-liquid-based aqueous two-phase systems. *Sep. Purif. Technol. 75*, 39–47.
(131) Cláudio, A. F. M., Ferreira, A. M., Freire, C. S. R., Silvestre, A. J. . D., Freire, M. G., and Coutinho, J. A. P. (2012) Optimization of the gallic acid extraction using ionic-liquid-based aqueous two-phase systems. *Sep. Purif. Technol. 97*, 142–149.
(132) Deive, F. J., Rodríguez, A., Pereiro, A. B., Araújo, J. M. M., Longo, M. A., Coelho, M. A. Z., Lopes, J. N. C., Esperança, J. M. S. S., Rebelo, L. P. N., and Marrucho, I. M. (2011) Ionic liquid-based aqueous biphasic system for lipase extraction. *Green Chem. 13*, 390.
(133) Dreyer, S., Salim, P., and Kragl, U. (2009) Driving forces of protein partitioning in an ionic liquid-based aqueous two-phase system. *Biochem. Eng. J. 46*, 176–185.
(134) Cao, Q., Quan, L., He, C., Li, N., Li, K., and Liu, F. (2008) Partition of horseradish peroxidase with maintained activity in aqueous biphasic system based on ionic liquid. *Talanta 77*, 160–5.
(135) Ruiz-Angel, M. J., Pino, V., Carda-Broch, S., and Berthod, A. (2007) Solvent systems for countercurrent chromatography: an aqueous two phase liquid system based on a room temperature ionic liquid. *J. Chromatogr. A 1151*, 65–73.
(136) Gupta, B. S., and Lee, M. (2014) Buffers more than buffering agent: introducing a new class of stabilizers for the protein BSA †. *Phys. Chem. Chem. Phys. 17*, 1114–1133.
(137) Okur, H. I., Kherb, J., and Cremer, P. S. (2013) Cations bind only weakly to amides in aqueous solutions. *J. Am. Chem. Soc. 135*, 5062–7.
(138) Ferguson, W. J., Braunschweiger, K. I., Braunschweiger, W. R., Smith, J. R., McCormick, J. J., Wasmann, C. C., Jarvis, N. P., Bell, D. H., and Good, N. E. (1980) Hydrogen ion buffers for biological research. *Anal. Biochem. 104*, 300–310.
(139) Taha, M., Almeida, M. R., Silva, F. A. e. S., Domingues, P., Ventura, S. P. M., Coutinho, J. A. P., Freire, M. G., (2015) Novel Biocompatible and Self-buffering Ionic Liquids for Biopharmaceutical Applications. *Chem. - A Eur. J. 21*, 4781–4788.
(140) Neves, C. M. S. S., Ventura, P. M., Freire, M. G., and Marrucho, I. M. (2009) Evaluation of Cation Influence on the Formation and Extraction Capability of Ionic-Liquid-Based Aqueous Biphasic Systems. *J. Phys. Chem. B 113*, 5194–5199.
(141) Zaslavsky, B. Y. (1994) Aqueous Two-Phase Partitioning: Physical Chemistry and Bioanalytical Applications. CRC Press.
(142) Merchuk, J. C., Andrews, B. a, and Asenjo, J. a. (1998) Aqueous two-phase systems for protein separation: Studies on phase inversion. *J. Chromatogr. B Biomed. Sci. Appl. 711*, 285–293.
(143) Liu, J., Yang, J., Xu, H., Lu, J., and Cui, Z. (2010) A new membrane based process to isolate immunoglobulin from chicken egg yolk. *Food Chem. 122*, 747–752.
(144) Trott, O., and Olson, A. (2010) AutoDock Vina: improving the speed and accuracy of docking with a new scoring function, efficient optimization and multithreading. *J. Comput. Chem. 31*, 455–461.
(145) Taylor, A. I., Fabiane, S. M., Sutton, B. J., and Calvert, R. A. (2009) The crystal structure of an avian IgY-Fc fragment reveals conservation with both mammalian IgG and IgE. *Biochemistry 48*, 558–562.
(146) Marques, C. F. C., Mourão, T., Neves, C. M. S. S., Lima, Á. S., Boal-Palheiros, I., Coutinho, J. a P., and Freire, M. G. (2013) Aqueous biphasic systems composed of ionic liquids and sodium carbonate as enhanced routes for the extraction of tetracycline. *Biotechnol. Prog. 29*, 645–654.
(147) Mourão, T., Cláudio, A. F. M., Boal-Palheiros, I., Freire, M. G., and Coutinho, J. a P. (2012) Evaluation of the impact of phosphate salts on the formation of ionic-liquid-based aqueous biphasic systems. *J. Chem. Thermodyn. 54*, 398–405.

(148) Pegram, L. M., and Record, M. T. (2007) Hofmeister salt effects on surface tension arise from partitioning of anions and cations between bulk water and the air-water interface. *J. Phys. Chem. B 111*, 5411–5417.
(149) Quental, M. V. (2012) Application of ionic liquids in the concentration of cancer biomarkers. Universidade de Aveiro.
(150) Passos, H., Ferreira, A. R., Cláudio, A. F. M., Coutinho, J. A. P., and Freire, M. G. (2012) Characterization of aqueous biphasic systems composed of ionic liquids and a citrate-based biodegradable salt. *Biochem. Eng. J. 67*, 68–76.
(151) Louros, C. L. S., Cláudio, A. F. M., Neves, C. M. S. S., Freire, M. G., Marrucho, I. M., Pauly, J., and Coutinho, J. A. P. (2010) Extraction of biomolecules using phosphonium-based ionic liquids + K3PO4 aqueoUs biphasic systems. *Int. J. Mol. Sci. 11*, 1777–1791.
(152) Ventura, P. M., Ventura, P. M., Freire, M. G., Freire, M. G., Marrucho, I. M., and Marrucho, I. M. (2009) Evaluation of Anion Influence on the Formation and Extraction Capacity of Ionic-Liquid-Based Aqueous Biphasic Systems. *J. Phys. Chem. B 113*, 9304–9310.
(153) Franco, T. T., Andrews, A. T., and Asenjo, J. A. (1996) Use of chemically modified proteins to study the effect of a single protein property on partitioning in aqueous two-phase systems: Effect of surface hydrophobicity. *Biotechnol. Bioeng. 49*, 300–308.
(154) Lu, R., Li, W.-W., Katzir, A., Raichlin, Y., Yu, H.-Q., and Mizaikoff, B. (2015) Probing the secondary structure of bovine serum albumin during heat-induced denaturation using mid-infrared fiberoptic sensors. *Analyst 140*, 765–770.
(155) Pereira, M. M., Pedro, S. N., Quental, M. V., Lima, Á. S., Coutinho, J. A. P., and Freire, M. G. (2015) Enhanced extraction of bovine serum albumin with aqueous biphasic systems of phosphonium- and ammonium-based ionic liquids. *J. Biotechnol. 206*, 17–25.
(156) Pelton, J. T., and McLean, L. R. (2000) Spectroscopic methods for analysis of protein secondary structure. *Anal. Biochem. 277*, 167–176.
(157) Matheus, S., Friess, W., and Mahler, H. C. (2006) FTIR and nDSC as analytical tools for high-concentration protein formulations. *Pharm. Res. 23*, 1350–1363.
(158) Kong, J., and Yu, S. (2007) Fourier Transform Infrared Spectroscopic Analysis of Protein Secondary Structures Protein FTIR Data Analysis and Band Assign- ment. *Acta Biochim. Biophys. Sin. (Shanghai). 39*, 549–559.
(159) Lilienthal, S., Drotleff, A. M., and Ternes, W. (2008) Changes in the protein secondary structure of hen's egg yolk determined by Fourier transform infrared spectroscopy during the first eight days of incubation 68–79.
(160) Patel, R., Kumari, M., and Khan, A. B. (2014) Recent advances in the applications of ionic liquids in protein stability and activity: A review. *Appl. Biochem. Biotechnol. 172*, 3701–3720.
(161) Gao, F., Wang, Y., Qiu, Y., Li, Y., Sha, Y., Lai, L., and Wu, H. (2002) Beta-turn formation by a six-residue linear peptide in solution. *J. Pept. Res. 60*, 75–80.
(162) Schüle, S., Frieß, W., Bechtold-Peters, K., Garidel, P., Schu, S., Frieß, W., Bechtold-Peters, K., and Garidel, P. (2007) Conformational analysis of protein secondary structure during spray-drying of antibody/mannitol formulations. *Eur. J. Pharm. Biopharm. 65*, 1–9.
(163) Yang, Z., and Pan, W. (2005) Ionic liquids: Green solvents for nonaqueous biocatalysis. *Enzyme Microb. Technol. 37*, 19–28.
(164) Laszlo, J. a, and Compton, D. L. (2001) Alpha-chymotrypsin catalysis in imidazolium-based ionic liquids. *Biotechnol. Bioeng. 75*, 181–186.
(165) Burgess, R. R. (2009) Protein Precipitation Techniques, in *Methods in Enzymology* 1st ed., pp 331–342. Elsevier Inc.
(166) Polson, C., Sarkar, P., Incledon, B., Raguvaran, V., and Grant, R. (2003) Optimization of protein precipitation based upon effectiveness of protein removal and ionization effect in liquid chromatography-tandem mass spectrometry. *J. Chromatogr. B Anal. Technol. Biomed. Life Sci. 785*, 263–275.
(167) Englard, S., and Seifter, S. (1990) Precipitation Techniques, in *Purification Procedures: Bulk Methods*, pp 285–300.
(168) Hundred, V. F. (2009) Guide to Protein Purification (Abelson, J., and Simon, M., Eds.) 2nd editio. ELSEVIER.

(169) Ghosh, R., and Cui, Z. F. (1998) Fractionation of BSA and lysozyme using ultrafiltration: Effect of pH and membrane pretreatment. *J. Memb. Sci. 139*, 17–28.
(170) Khan, J. M., Qadeer, A., Chaturvedi, S. K., Ahmad, E., Rehman, S. A., Gourinath, S., and Khan, R. H. (2012) SDS can be utilized as an amyloid inducer: A case study on diverse proteins. *PLoS One 7*.
(171) Crowell, A. M. J., Wall, M. J., and Doucette, A. a. (2013) Maximizing recovery of water-soluble proteins through acetone precipitation. *Anal. Chim. Acta 796*, 48–54.

Appendix A: Experimental binodal data for the system composed of K_3PO_4 + $[C_4mim]Cl$ + H_2O

A.1. Phase diagrams of the ternary systems composed of K_3PO_4 + $[C_4mim]Cl$ + H_2O

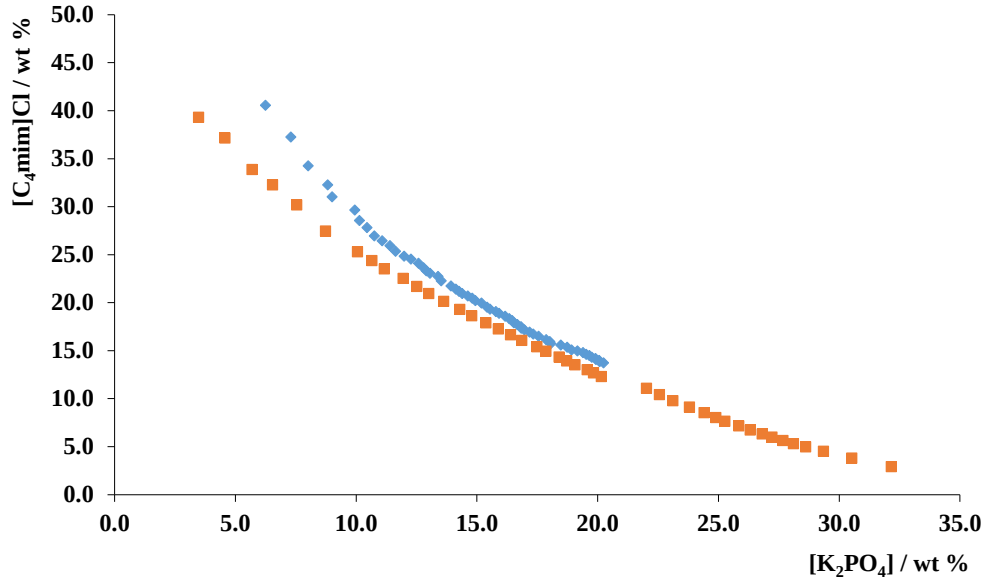

Figure A. 1 – Phase diagram for the ternary system composed of K_3PO_4 + $[C_4mim]Cl$ + H_2O at (25 ± 1) °C: this work (♦), literature data (■) *(140)*.

Appendix B: HPLC calibration curve

B.1. HPLC Calibration curve for IgY

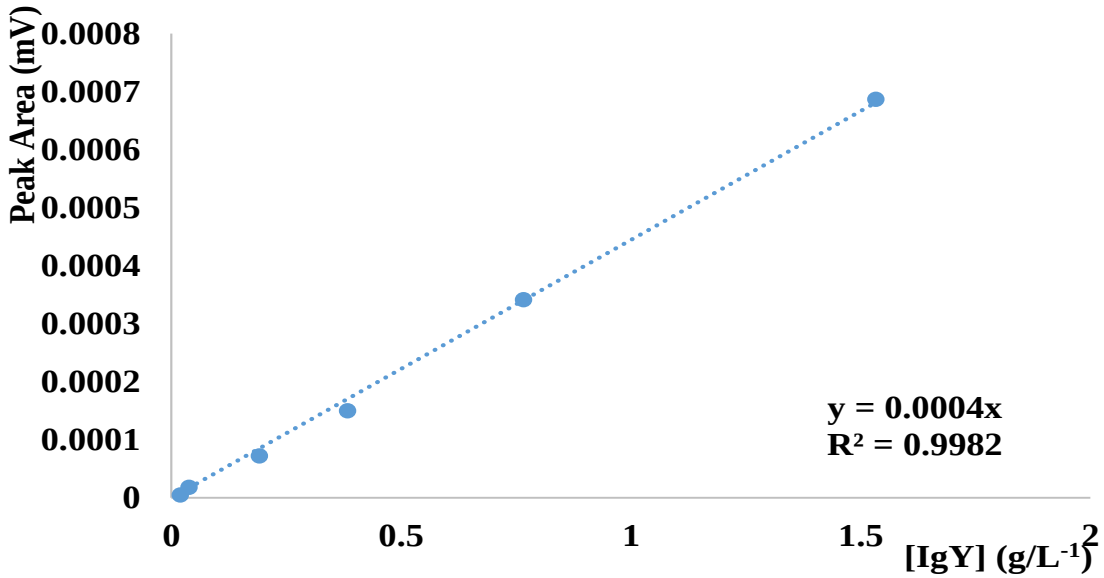

Figure B. 1 – HPLC calibration curve for IgY (purified using the EggsPure IgY commercial kit).

Appendix C: SDS-PAGE calibration curve

C.1. – SDS-PAGE of a gel load with 10 µg of pure IgY, at different concentrations, stained with Coomassie blue

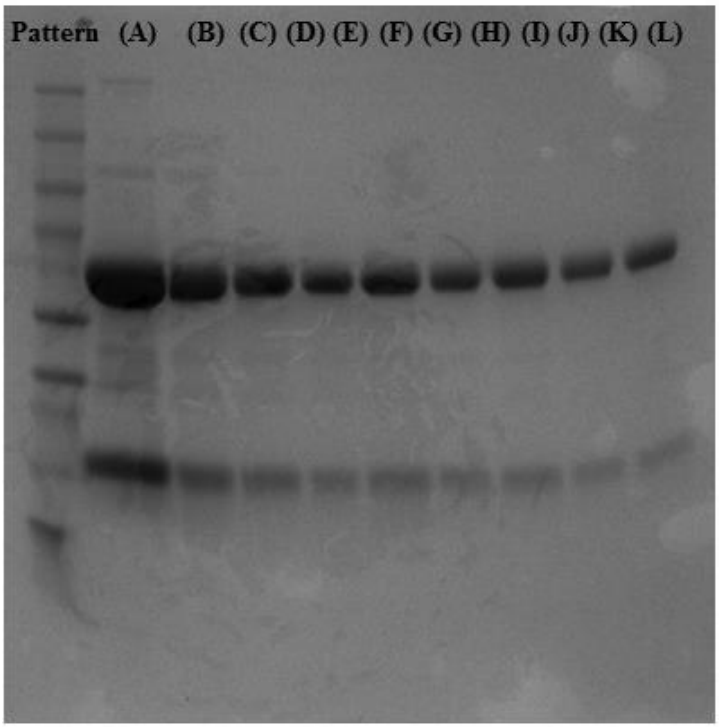

Figure C. 1 – SDS PAGE gel – calibration curve.

C.2 – SDS-PAGE calibration curve obtained through the analysis of the intensity of the IgY light chain bands, using the GenoSoft software, from VWR

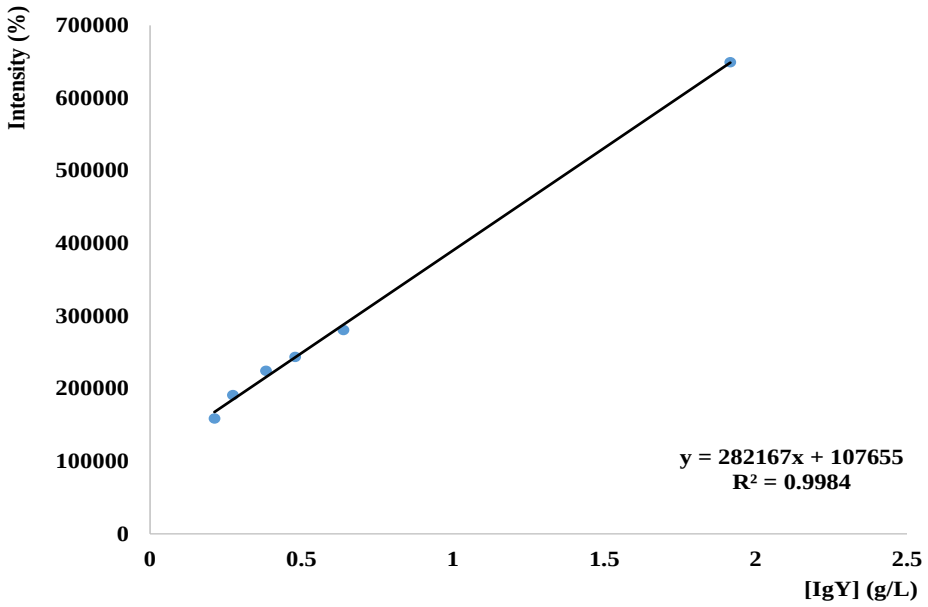

Figure C. 2 – SDS-PAGE calibration curve.

Appendix D: Experimental binodal data for the system composed of $[N_{4444}][CHES] + C_6H_5K_3O_7 + H_2O$

D.1. Phase diagrams of the ternary systems composed of $[N_{4444}][CHES] + C_6H_5K_3O_7 + H_2O$

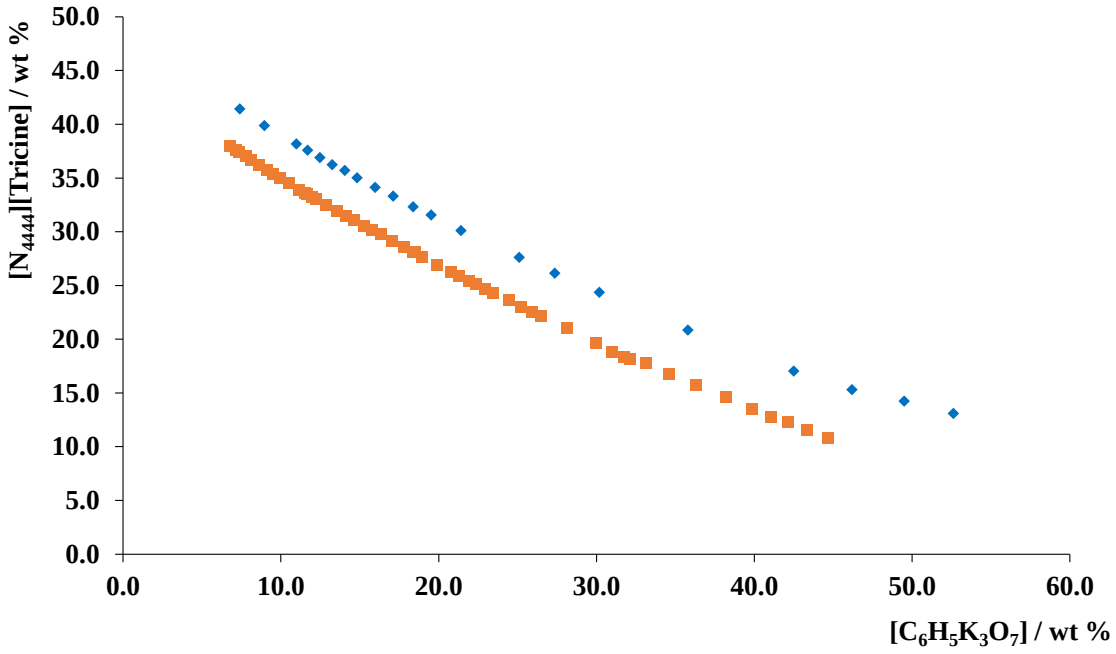

Figure D. 1 – Phase diagram for the ternary system composed of $[N_{4444}][CHES] + C_6H_5K_3O_7 + H_2O$ this work (♦), literature data (■) *(25)*.

Appendix E: Experimental binodal data

E.1. Experimental binodal data for systems composed of GB-IL + salt + H_2O

Table E. 1- Experimental weight fraction data for the binodal curve of the systems composed of of $[P_{4444}][GB]$ (1) + $C_6H_5K_3O_7$ (2) at (25 ± 1) °C.

$[P_{4444}][CHES]$		**$[P_{4444}][HEPES]$**			
***Mw* = 465.71 g.mol^{-1}**		***Mw* = 496.72 g.mol^{-1}**			
100 w_1	***100* w_2**	**100 w_1**	***100* w_2**	**100 w_1**	***100* w_2**
45.8725	5.1594	52.4356	3.3809	19.9875	20.6444
33.0703	7.9812	50.8571	3.7208	19.7789	20.7202
31.4785	8.3151	48.7809	4.0110	19.1789	21.1907
30.7663	8.8449	47.0015	4.6767	18.9802	21.2130
29.4375	9.3324	45.9192	5.3926	18.5920	21.5111
28.3701	9.5904	44.5339	5.6672	18.3375	21.7429
27.4919	9.7877	43.2175	6.4013	17.9787	22.0167
26.5363	10.3651	41.7748	7.2840	17.5852	22.2453
25.3700	10.5256	40.9755	7.5740	17.0421	22.8133
24.6482	10.8738	40.0870	8.0190	16.7673	22.9471
23.8099	11.1523	38.5449	8.8895	16.3891	23.2295
23.4740	11.3404	36.7448	9.5462	15.8899	23.6604
22.5056	11.5514	35.8968	10.0308	15.5849	23.7256
21.7753	11.7923	35.1236	10.5409	15.3261	23.9031
20.9845	12.1692	34.3325	11.0165	15.0627	24.1947
20.4830	12.3391	32.9362	11.8402		
19.7301	12.8603	31.8346	12.5471		
19.2710	12.8446	31.0433	12.8594		
19.0036	12.8981	30.2768	13.4966		
18.7101	13.0962	29.7060	13.8282		
18.1123	13.3936	29.2446	13.9475		
17.5929	13.5070	28.1301	14.9854		
17.2801	13.6192	27.2980	15.4338		
16.7026	13.8189	26.4976	15.8693		
16.0024	14.2690	26.2008	15.9438		
15.6821	14.4136	25.8698	16.2748		
43.4923	5.5777	25.2302	16.7156		
41.4743	5.9829	24.9559	16.7906		
37.6457	7.0174	23.9968	17.4865		
35.4748	7.5777	23.5426	17.7956		
		22.9207	18.2905		
		22.6492	18.3176		
		22.2784	18.5603		
		21.2308	19.6799		
		20.8939	19.9928		
		20.4733	20.1856		

$[P_{4444}][MES]$				$[P_{4444}][TES]$			
Mw = 453.66 g.mol^{-1}				Mw = 487.67 g.mol^{-1}			
100 w_1	***100*** w_2	**100** w_1	***100*** w_2	**100** w_1	***100*** w_2	**100** w_1	***100*** w_2
56.0860	3.7199	10.0759	26.2305	49.3274	11.0418	10.4352	33.0947
49.2000	5.8793	9.8190	26.4062	46.6779	12.5385	10.0084	33.4136
39.9060	9.0502	9.5313	26.6884	44.0800	13.7779	9.1108	34.1036
35.6838	10.7092	9.2917	26.8819	41.9299	14.6122	8.7044	34.5777
32.2299	12.4537	8.7880	27.1615	40.1138	15.3985	8.3336	34.7034
30.4517	13.5385	8.5138	27.3950	37.3418	16.5271		
28.0286	14.6491	7.5849	28.3888	34.7350	17.8627		
26.5401	15.3376	7.2616	28.6334	32.6036	19.2519		
25.6381	15.9660	7.1183	28.7600	31.2374	19.9006		
20.3539	19.6793			28.1143	22.0356		
19.8426	20.0167			26.3828	22.8026		
19.1169	20.4386			25.1128	23.4566		
18.7675	20.6581			24.5141	23.8630		
18.2459	20.8573			23.6911	24.3018		
17.9733	20.9879			22.7221	25.0937		
17.4030	21.4728			22.0661	25.4115		
16.9966	21.6709			21.5211	25.6630		
16.8141	21.7022			20.9795	25.8474		
16.5786	21.8329			20.2755	26.2981		
16.3307	22.0440			19.6014	26.7392		
16.0450	22.1776			18.3204	27.4774		
15.5163	22.6462			17.7554	27.8490		
15.1383	22.8364			17.3485	28.0255		
14.7511	22.9795			16.8705	28.3363		
14.2062	23.4197			16.1936	28.8914		
13.0638	24.1036			15.7599	29.0546		
12.9685	24.1744			15.3022	29.3814		
12.8049	24.2182			14.8725	29.6818		
12.5917	24.4750			14.5128	29.9909		
12.4553	24.5281			14.1003	30.3482		
12.3524	24.5791			13.8150	30.4762		
12.0765	24.8012			13.1270	30.9739		
11.7216	25.1559			12.5738	31.3816		
10.9443	25.6166			11.9999	31.7973		
10.6865	25.7738			11.4861	32.2455		
10.3012	26.0616			10.8326	32.6925		

$[P_{4444}][Tricine]$					
Mw = 437.59 g.mol^{-1}					
100 w_1	***100*** w_2	**100** w_1	***100*** w_2	**100** w_1	***100*** w_2
42.1255	12.6009	20.2641	27.4060	12.0250	34.0183
40.3602	13.4219	20.0440	27.4713	11.8725	34.1810
38.4601	14.4712	19.6646	27.8548	11.7110	34.3599
37.2505	15.2329	19.4356	28.0177	11.5823	34.4851
35.3379	16.3926	19.2146	28.1671	11.4282	34.6641
32.6121	18.6625	18.8964	28.4463	11.3124	34.7944
31.5688	19.2229	18.6063	28.7423	11.1593	34.8316
30.1933	20.2199	18.3036	29.0215	11.0294	35.0037
28.0745	21.6510	18.1074	29.1358	10.8889	35.1658
27.1834	22.1727	17.7775	29.4780	10.8121	35.1672
26.4801	22.6583	17.5843	29.5748	10.7023	35.3094
32.2737	18.5240	17.4062	29.7475	10.4568	35.5745
31.5877	18.9671	17.1936	29.8764		
30.9769	19.3892	16.9327	30.1473		
30.4459	19.6828	16.6746	30.3763		
29.8602	20.0574	16.5059	30.5192		
29.3288	20.4102	16.2517	30.7703		
28.7964	20.7798	16.0879	30.8671		
27.9689	21.6115	15.8639	31.0559		
27.5021	21.9881	15.6137	31.2773		
27.0526	22.2898	15.3613	31.5346		
26.6139	22.5766	15.2180	31.5846		
26.1790	22.8039	14.9933	31.7975		
25.5152	23.4747	14.7745	31.9996		
25.1113	23.7524	14.5414	32.2434		
24.7146	23.9830	14.2661	32.4125		
24.2941	24.1475	14.0897	32.6000		
23.9505	24.3704	13.9659	32.6448		
23.4108	24.9376	13.7769	32.8457		
23.0802	25.1276	13.6422	32.9745		
22.7777	25.3079	13.4665	33.1494		
21.9759	25.9534	13.2741	33.2291		
21.6897	26.1745	13.0964	33.4211		
21.2422	26.6289	12.8799	33.7079		
20.9856	26.7786	12.7729	33.7572		
20.7143	26.9484	12.4852	33.9822		

Table E. 2 - Experimental weight fraction data for the binodal curve of the systems composed of $[N_{4444}][GB]$ (1) + $C_6H_5K_3O_7$ (2) at (25 ± 1) °C.

$[N_{4444}][CHES]$				**$[N_{4444}][HEPES]$**		**$[N_{4444}][MES]$**	
***Mw* = 448.74 g.mol^{-1}**				***Mw* = 479.75 g.mol^{-1}**		***Mw* = 436.69 g.mol^{-1}**	
100 w_1	***100* w_2**	**100 w_1**	***100* w_2**	**100 w_1**	***100* w_2**	**100 w_1**	***100* w_2**
57.5741	4.3595	6.0328	23.0630	34.9668	7.8678	42.2318	6.3505
49.7951	5.4885			26.5656	14.0779	34.4280	10.1559
45.0789	6.4316			20.5902	19.8164	25.2272	17.3299
42.4844	7.3569			15.6250	26.0832	15.5028	23.0078
40.4427	8.2403			9.5904	31.9512	6.7431	33.2543
37.8860	8.7157			5.6848	38.1506	3.4741	38.0405
35.7309	9.3461						
34.6828	9.9063						
32.7218	10.8505						
29.9862	11.6212						
25.5988	13.5087						
24.1441	13.9681						
23.1690	14.3891						
20.0463	14.9631						
19.2217	15.2093						
16.0534	16.6588						
14.9346	17.0590						
13.8988	17.6751						
13.3392	17.7773						
12.1397	18.4118						
11.2020	18.9461						
10.3645	19.5405						
10.0122	19.6938						
9.4483	19.8957						
9.1472	19.9609						
8.7535	20.7380						
8.4425	20.6750						
7.8725	21.1431						
7.6509	21.2652						
7.4447	21.5299						
7.2393	21.5823						
7.0532	21.6714						
6.9287	22.1551						
6.7150	22.5621						
6.4749	22.6996						
6.2308	22.8082						

$[P_{4444}][TES]$		$[P_{4444}][Tricine]$			
Mw = 470.70 g.mol^{-1}		Mw = 420.62 g.mol^{-1}			
100 w_1	***100*** w_2	**100** w_1	***100*** w_2	**100** w_1	***100*** w_2
60.0979	7.1499	44.6489	10.7724	12.8619	32.5152
38.1764	14.0610	43.3425	11.5793	12.2324	33.0209
31.6561	17.2741	42.1253	12.2497	12.0106	33.1806
21.8117	24.9401	41.0591	12.7489	11.6513	33.4869
17.4213	29.3787	39.8372	13.5505	11.4962	33.6289
10.4669	35.3515	38.1933	14.6085	11.1564	33.8981
4.4736	41.3063	36.2742	15.7678	10.4995	34.4976
32.6036	19.2519	34.6087	16.7694	9.9389	35.0097
		33.1372	17.7943	9.4991	35.3803
		32.1573	18.1785	9.1337	35.7540
		31.7469	18.3389	8.6148	36.2365
		31.0114	18.8360	8.0910	36.6959
		29.9834	19.6339	7.7570	36.9904
		28.1113	20.9998	7.3539	37.3906
		26.4768	22.2000	7.1370	37.6344
		25.9227	22.5364	6.7822	37.9600
		25.2101	23.0306	6.4953	38.2110
		24.4242	23.6589		
		23.4762	24.3404		
		22.9368	24.7026		
		22.3403	25.1777		
		21.8922	25.4478		
		21.3077	25.9037		
		20.7949	26.2962		
		19.8940	26.9181		
		18.9674	27.6444		
		18.5053	28.0635		
		18.3376	28.1522		
		17.7885	28.5883		
		17.0513	29.1451		
		16.3110	29.7432		
		15.7645	30.1447		
		15.2459	30.5384		
		14.6169	31.0718		
		14.1015	31.4787		
		13.5202	31.9596		

Appendix F: Phase diagrams and TLs

F.1 – Phase diagrams and TLs for the ternary systems composed of GB-ILs + $C_6H_5K_3O_7$ + water

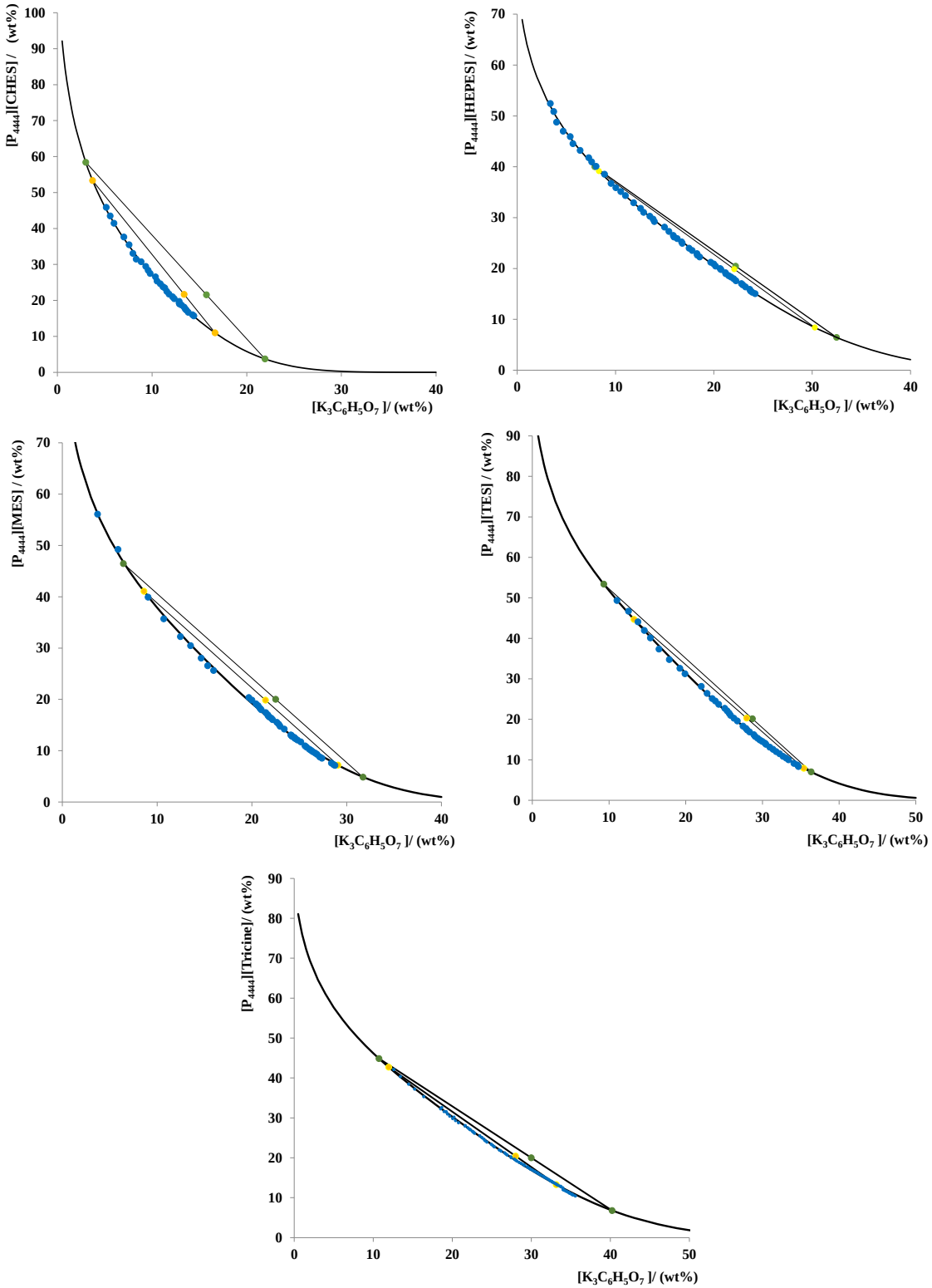

Figure F. 1 - Phase diagrams and TLs for the ternary systems composed of $[P_{4444}][GB]$ + $C_6H_5K_3O_7$ + water, at (25 ± 1) °C and atmospheric pressure: binodal data (●), TL1 data (●), TL2 data (●), adjusted binodal data using Equation 1 (-).

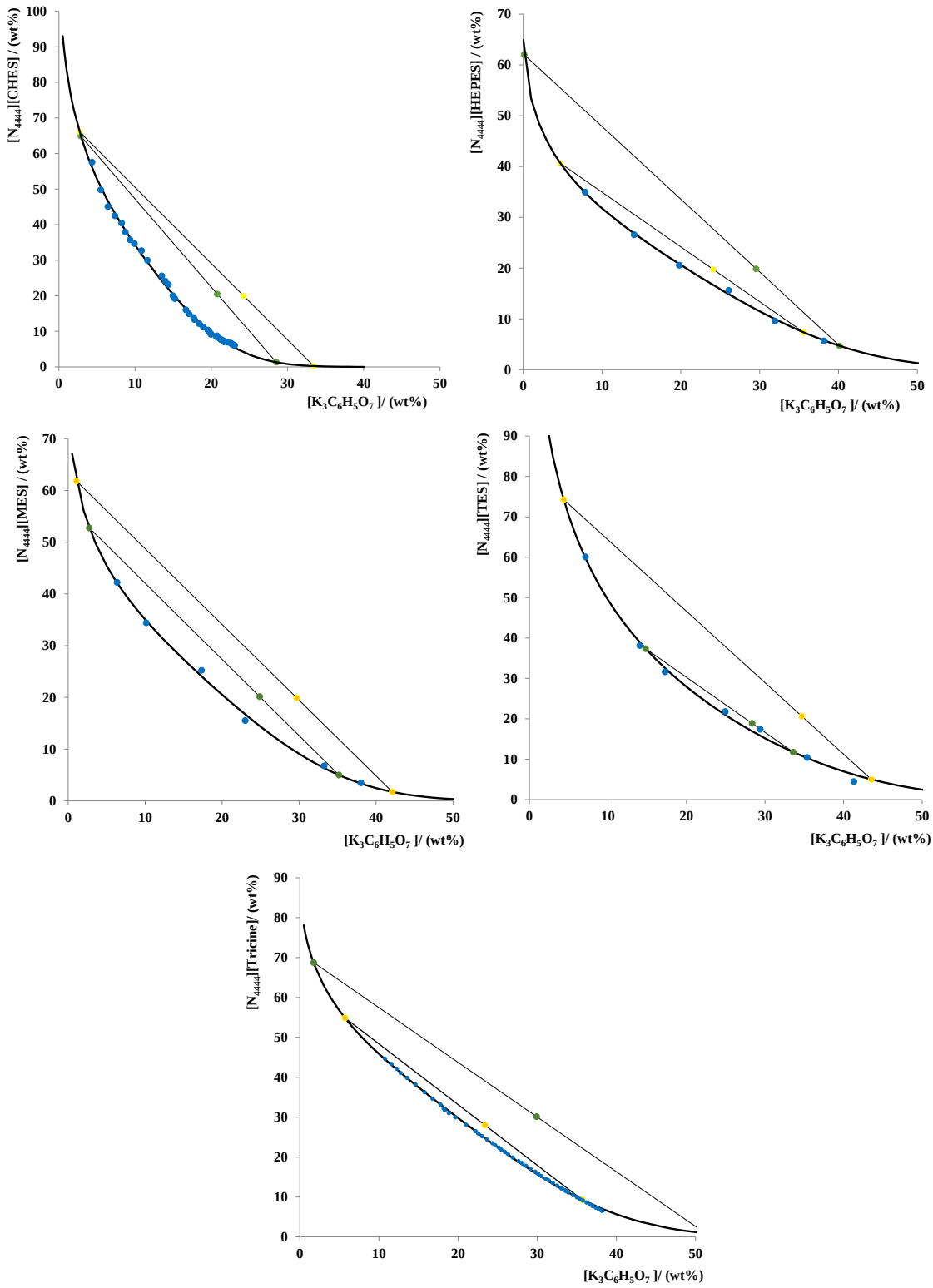

Figure F. 2 - Phase diagrams and TLs for the ternary systems composed of $[P_{4444}][GB]$ + $C_6H_5K_3O_7$ + water, at (25 ± 1) °C and atmospheric pressure: binodal data (●), TL1 data (●), TL2 data (●), adjusted binodal data using Equation 1 (-).

Appendix G: HPLC chromatograms

G.1. HPLC chromatograms from the systems composed of $[P_{4444}][GB]$ + $C_6H_5K_3O_7$ + WSPF

Table G. 1 – HPLC chromatograms from the WSPF (–), top phase (–) and bottom phase (–) of the systems composed of $[P_{4444}][GB]$ + $C_6H_5K_3O_7$ + WSPF.

ABS				**Chromatograms**
[GB-IL]	[IL] (wt %)	[$C_6H_5K_3O_7$] (wt %)	[WSPF] (wt %)	
$[P_{4444}][CHES]$	20	13.5	66.5	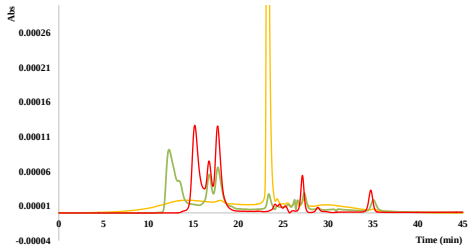
$[P_{4444}][HEPES]$	20	22	48	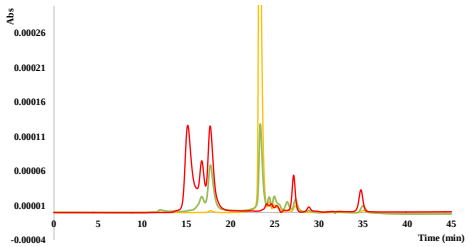
$[P_{4444}][MES]$	20	21	49	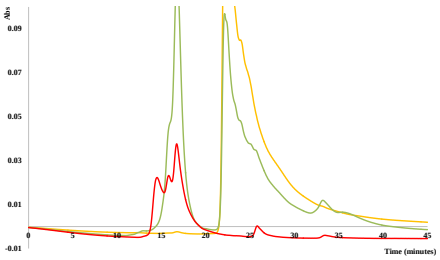
$[P_{4444}][TES]$	20	28	52	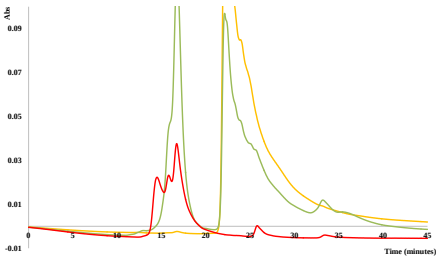
$[P_{4444}][Tricine]$	20	29	51	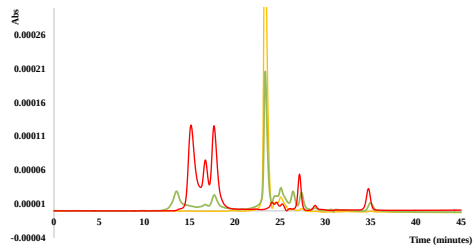

G.2. HPLC chromatograms from the systems composed of $[N_{4444}][GB]$ + $C_6H_5K_3O_7$ + WSPF

Table G. 2 - HPLC chromatograms from the WSPF (–), top phase (–) and bottom phase (–) of the systems composed of $[N_{4444}][GB]$ + $C_6H_5K_3O_7$ + WSPF.

ABS				Chromatograms
[GB-IL]	[IL] (wt %)	[$C_6H_5K_3O_7$] (wt %)	[WSPF] (wt %)	
$[N_{4444}][CHES]$	20	17	63	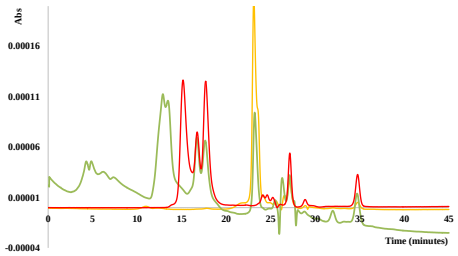
$[N_{4444}][HEPES]$	20	23	47	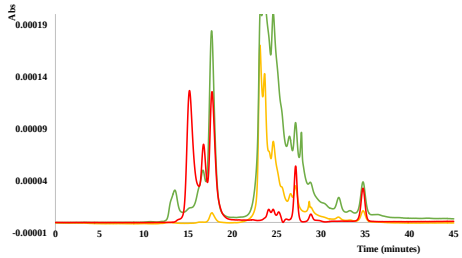
$[N_{4444}][MES]$	20	22	48	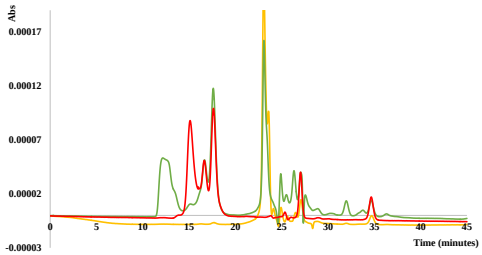
$[N_{4444}][TES]$	20	28.5	51.5	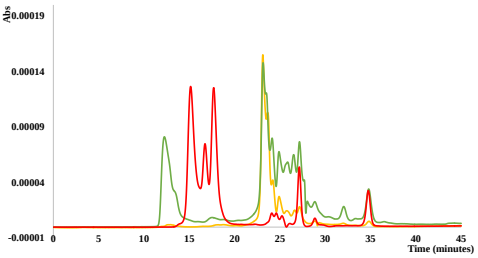
$[N_{4444}][Tricine]$	25	30	45	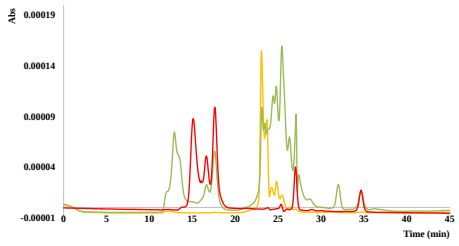

Appendix H: FT-IR data

H.1. – FT-IR spectra of the ABS composed of $[P_{4444}][GB] + C_6H_5K_3O_7$ + WSPF

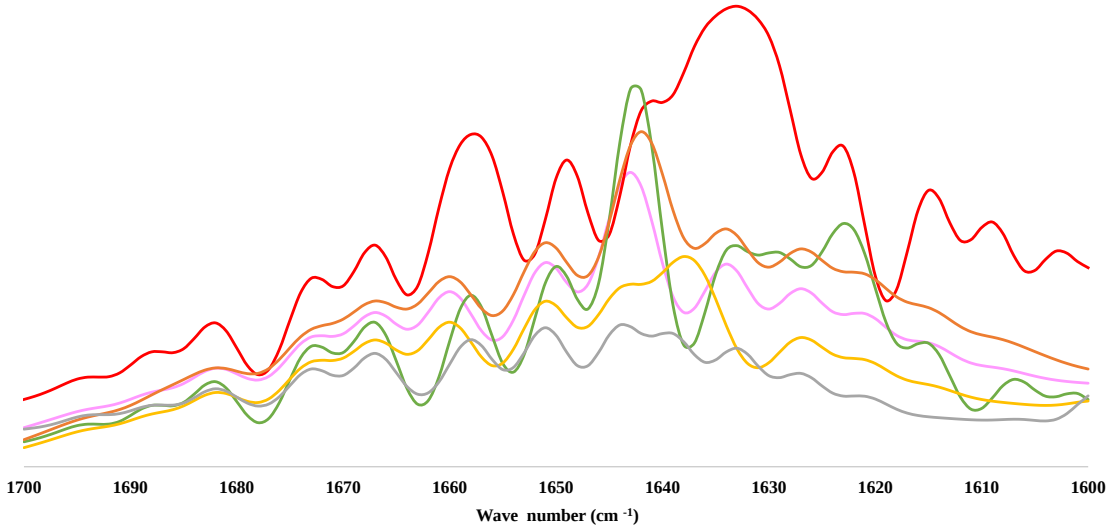

Figure H. 1 – FT-IR spectra from the top phase of the ABS composed of: (–) $[P_{4444}][CHES]$, (–) $[P_{4444}][HEPES]$, (–) $[P_{4444}][MES]$, (–) $[P_{4444}][TES]$ and (–) $[P_{4444}][Tricine]$ and (–) WSPF.

H.12 – FT-IR spectra of the ABS composed of $[N_{4444}][GB] + C_6H_5K_3O_7$ + WSPF

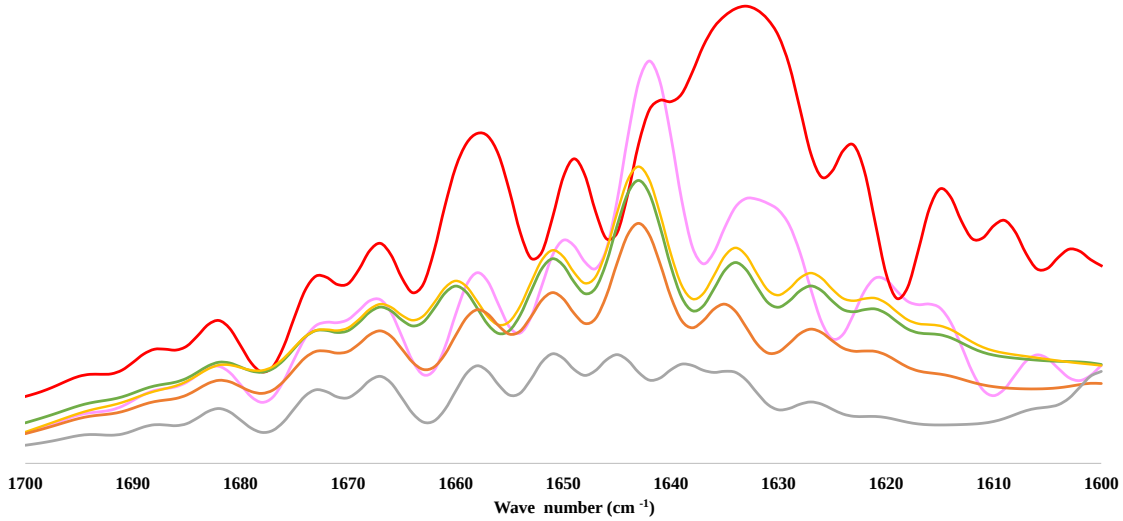

Figure H. 2 - FT-IR spectra from the top phase of the ABS composed of: (–) $[N_{4444}][CHES]$, (–) $[N_{4444}][HEPES]$, (–) $[N_{4444}][MES]$, (–) $[N_{4444}][TES]$ and (–) $[N_{4444}][Tricine]$ and (–) WSP

Table H. 1 – Comparison of the second derivative peak values from the top phase of the systems composed of $[P_{4444}][GB]$-IL and the WSPF, with the literature data.

	Wave length (cm^{-1})								
	(158)	*(157)*	*(162)*	**WSPF**	**$[P_{4444}][CHES]$**	**$[P_{4444}][HEPES]$**	**$[P_{4444}][MES]$**	**$[P_{4444}][TES]$**	**$[P_{4444}][Tricine]$**
β–turn	1667±1.0	1655-1675	1660-1667	1660	1660	1656	1660	1660	1658
	1675±1.0	1680-1696	1676-1680	1667	1667	1667	1667	1667	1667
	1680±2.0			1673	1673	1673	1673	1673	1673
	1685±2.0			1682	1682	1682	1682	1682	1682
				1688	1688	1687	1688	1687	1688
				1694	1694	1694	1694	1694	1694
						1697			
α–helix	1656±2.0	1650-1657	1650-1658	1656	1651	1651	1651	1651	1651
						1656			
Random coil	1648±2.0	1640-1651	1640-1650	1642	1642	1642	1644	1641	1644
				1649	1644			1643	
β-sheet	1624±1.0	1626-1640	1615-1620	1615	1615	1615	1615	1615	
	1627±2.0	1612-1642	1628-1645	1623	1621	1623	1621	1621	1621
	1633±2.0	1670-1690	1686-1697	1629	1627	1626	1627	1627	1627
	1638±2.0			1633	1634	1628	1636	1634	1633
	1642±1.0			1637	1642	1633	1639	1641	1639
	1691±2.0			1642	1644	1638	1644	1643	1644
	1696±2.0			1673	1673	1642	1673	1673	1673
				1682	1682	1673	1682	1682	1682
				1688	1688	1682	1688	1687	1688
				1694	1694	1687	1694	1694	1694
						1694			
						1697			

Table H. 2 – Comparison of the second derivative peak values from the top phase of the systems composed of [N_{4444}][GB]-IL and the WSPF, with the literature data.

	Wave length (cm^{-1})								
	(158)	*(157)*	*(162)*	**WSPF**	**[N_{4444}][CHES]**	**[N_{4444}][HEPES]**	**[N_{4444}][MES]**	**[N_{4444}][TES]**	**[N_{4444}][Tricine]**
β–turn	1667±1.0	1655-1675	1660-1667	1660	1658	1656	1660	1658	1658
	1675±1.0	1680-1696	1676-1680	1667	1667	1667	1667	1667	1667
	1680±2.0			1673	1673	1673	1673	1673	1673
	1685±2.0			1682	1682	1682	1682	1682	1682
				1688	1688	1687	1688	1688	1688
				1694	1694	1694	1694	1694	1694
						1697			
α–helix	1656±2.0	1650-1657	1650-1658	1656	1650	1651	1651	1651	1651
					1658	1656		1658	1658
Random coil	1648±2.0	1640-1651	1640-1650	1642	1641	1642	1642	1642	1645
				1649	1643		1644	1644	
β-sheet	1624±1.0	1626-1640	1615-1620	1615	1650				
	1627±2.0	1612-1642	1628-1645	1623	1615	1615	1615	1615	
	1633±2.0	1670-1690	1686-1697	1629	1621	1623	1621	1621	1621
	1638±2.0			1633	1629	1626	1627	1627	1627
	1642±1.0			1637	1634	1628	1634	1635	1634
	1691±2.0			1642	1641	1633	1642	1642	1639
	1696±2.0			1673	1643	1638	1644	1644	1645
				1682	1673	1642	1673	1673	1673
				1688	1682	1673	1682	1682	1682
				1694	1688	1682	1688	1688	1688
					1694	1687	1694	1694	1694
					1697	1694			